



FRIEDRICH-SCHILLER-
UNIVERSITÄT
JENA



The functions of miR-193b-3p in trophoblast cells and its possible association to placenta disorders associated with abnormal invasion

Dissertation

in partial fulfilment of the requirements for the degree of
doctor rerum naturalium (Dr. rer. nat.)

**Submitted to the Faculty of Medicine,
Friedrich Schiller University, Jena**

By

M.Sc., Heba M. A. Skaik (El-Shorafa),

born on 05. 09. 1987 in Abu Dhabi, UAE,
from Gaza strip, Palestine

Reviewers

Prof. Dr. Aria Baniahmad

Institute for Human Genetics, Jena University clinic, Jena, Germany.

Prof. Dr. Tanja Groten

Gynecology and Obstetrics, Jena University Clinic, Jena, Germany.

Prof. Dr. Frauke von Versen-Höynck

Hannover Medical School, Hannover, Germany.

Public Defense Day: 18.06.2024

TABLE OF CONTENTS

List of Abbreviations	VI
Summary	IX
Zusammenfassung.....	XI
INTRODUCTION	1
1.1. Development of the placenta	1
1.2. Pathways of human placental trophoblast cell differentiation	3
1.2.1. Villous trophoblasts	3
1.2.2. Invasive EVT.....	5
1.3. Trophoblasts markers.....	7
1.4. Placenta accreta spectrum	9
1.4.1. Definition and epidemiology	9
1.4.2. Pathophysiology.....	9
1.4.3. Risk factors	10
1.4.4. Diagnosis and clinical complications.....	11
1.5. miRNAs and control of gene expression	11
1.5.1. miRNA.....	11
1.5.2. miRNA clusters and families	12
1.5.3. Biogenesis pathways.....	12
1.5.4. Experimental strategies to modulate miRNA levels	13
1.6. miRNA in pregnancy	15
1.6.1. miRNAs and PAS	17
1.6.2. miR-193b-3p.....	20
1.7. Extracellular Vesicles	22
1.7.1. Extracellular vesicles classification	23
1.7.2. Mechanisms of extracellular vesicles uptake.....	24
2. HYPOTHESIS AND OBJECTIVES.....	27
2.1. Hypothesis	27
2.2. Objectives	27
2.2.1. General.....	27
2.2.2. Specific objectives	27
3. MATERIAL AND METHODS.....	28
3.1. Materials	28
3.2. Methods	38
3.2.1. Human placenta samples collection.....	38

3.2.2.	RNA Extraction	38
3.2.3.	cDNA Synthesis, and Quantitative real time PCR (qPCR)	38
3.2.4.	miRNA in situ hybridization (miRNA-ISH).....	39
3.2.5.	Immune staining of Cytokeratin-7	40
3.2.6.	Isolation of primary trophoblast cells (PTC)	41
3.2.7.	Cell culture.....	41
3.2.8.	Western Blot	41
3.2.9.	Cell transfection.....	42
3.2.10.	BeWo syncytialization	42
3.2.11.	Wound Healing assay (cell migration)	43
3.2.12.	Cell proliferation.....	44
3.2.13.	Apoptosis assay.....	45
3.2.14.	EVs isolation.....	45
3.2.15.	Nanoparticle Tracking Analysis	46
3.2.16.	Transmission Electron Microscopy	47
3.2.17.	JEG-3 cell-derived EVs uptake.....	47
3.2.18.	LC-MS/MS Proteomic analysis	48
	Cells preparation.....	48
	FASP sample preparation	48
3.2.19.	Bioinformatic Prediction of miR-193b-3p Target Gene	49
3.2.20.	Statistical Analysis and figures.....	50
4.	RESULTS.....	51
4.1.	miR-193b-3p localization and expression in human placenta	51
4.2.	miR-193b-3p expression in cells	52
4.3.	The role of miR-193b-3p in BeWo cells syncytialization	54
4.4.	Cell migration	57
4.5.	Cell proliferation.....	57
4.6.	Cell apoptosis.....	58
4.7.	Characterization of isolated EVs	58
4.8.	The effect of miR-193b-3p-enriched trophoblast EVs on Jurkat T cells uptake and proliferation	60
4.9.	Effects of miR-193b-3p on JEG-3 cells proteome.....	66
4.10.	Gene and protein expression in transfected JEG-3 cell	68
5.	DISCUSSION.....	73
5.1.1.	miR-193b-3p expression and localization in human placentas.....	73
5.1.2.	Syncytialization	75
5.1.3.	Cell migration	77

5.1.4.	Proliferation and apoptosis	78
5.1.5.	The effect of miR-193b-3p-containing EV on Jurkat T cells proliferation	79
5.1.6.	Influence of miR-193b-3p downregulation on trophoblast cell proteome.....	81
6.	CONCLUSIONS	89
	REFERENCES	91
	APPENDIX.....	112
	List of figures.....	117
	List of tables.....	118
	ACKNOWLEDGEMENT	119

List of Abbreviations

AAV	Adenovirus-associated virus
ABI2	abl-interactor 2
AGC	Automatic gain control
AGGF1	Angiogenic factor with G-patch and FHA domains 1
AGO	Argonaute
AKT1	AKT serine/threonine kinase 1
AML	Acute Myeloid Leukemia
AMOs	Anti-microRNA oligonucleotides
AP	Alkaline phosphatase
ARDS	Acute Respiratory Distress Syndrome
ARPC5	Actin-related protein 2/3 complex subunit 5
C14MC	Chromosome 14 miRNA cluster
C19MC	Chromosome 19 miRNA cluster
CALM1	Calmodulin 1
CI	Cell Index
CS	Cesarean section
CTBs	Cytotrophoblasts
DIG	Double-labelled digoxigenin
DTT	Dithiothreitol
ECM	Extracellular matrix
ED-FBS	Exosomes depleted FBS
egEVTs	Endoglandular EVTs
EGFR	Epidermal growth factor receptor
EMT	Epithelial-mesenchymal transition
enEVTs	Endovascular EVTs
ERR γ	Estrogen-related receptor γ
ERV	Endogenous retroviruses
ERVFRD-1	Endogenous retrovirus group FRD member 1

ERVW-1	Endogenous retrovirus group W member 1
EVs	Extracellular vesicles
EVTs	Extravillous trophoblasts
FAK	Focal adhesion kinase
FGR	Fetal growth restriction
GAPDH	Glyceraldehyde 3-phosphate dehydrogenase
GCM-1	Glial cells missing-1
HCC	Hepatocellular carcinoma
HERVs	Endogenous retroviral genes
HLA	Human leukocyte antigens
HMs	Hydatidiform moles
hPL	Human placental lactogen
HSD17B1	Hydroxysteroid 17-beta dehydrogenase 1
HUVEC	Human Umbilical Vein Endothelial Cells
ICM	Inner cell mass
iEVTs	Interstitial EVT's
IGFBP-1	Insulin growth factor binding protein-1
IUGR	Intrauterine growth restriction
K-Ras	KRAS proto-oncogene, GTPase
IEV	Microvesicles-enriched large vesicles
MCL1	Myloid cell leukemia 1
MDD	Major Depressive Disorder
miRISC	miRNA-containing RNA-induced silencing complex
miRNAs	microRNAs
MMP	Matrix metalloproteinases
MVBs	Multivesicular bodies
NF1	Neurofibromin 1
NK	Natural killer
NP	Normal pregnancy
NTC	Non-transfected cells

OPN	Osteopontin
PAS	Placenta accreta spectrum
PBS	Phosphate buffer saline
PKA	Protein kinase A
pol II	RNA polymerase II
PTC	Primary trophoblast
PTK2	Protein tyrosine kinase 2
RT	Room temperature
sEV	Exosome-enriched small vesicles
SHMT2	Mitochondrial serine hydroxymethyltransferase
shRNAmir	Small-hairpin miRNA
STBs	Syncytiotrophoblasts
T-ALL	Acute lymphoblastic leukaemia
TE	Trophectoderm
TEM	Transmission Electron Microscopy
TGF- β 2	Transforming growth factor- β 2
TIMP	Tissue inhibitors of metalloproteinases
TMPPE	Transmembrane Protein with Metallophosphoesterase
TU	Transcription unit
uPA	urokinase-type plasminogen activator
UTR	Untranslated regions
VEGF	Vascular endothelial growth factor
YWHAZ	Tyrosine 3-monooxygenase/tryptophan 5-monooxygenase activation protein zeta
β hCG	Human chorionic gonadotropin

Summary

Background: microRNAs (miRNAs) regulate trophoblast cell functions and are packed into extracellular vesicles (EVs) to mediate intercellular communication. miR-193b-3p is expressed by the human placenta and dysregulated in different placental pathologies. Nevertheless, the role of miR-193b-3p in trophoblast cells has been poorly characterized. Therefore, this study aimed to evaluate miR-193b-3p expression and localization in human placenta, examine its potential targets, and investigate whether this miRNA influences trophoblast cell responses as well as trophoblast-immune cell interactions.

Methodology: Expression and localization of miR-193b-3p was investigated in human term placentas by miRNA in situ hybridization (miRNA-ISH). To examine the effects of miR-193b-3p on trophoblastic cell functions, trophoblastic cells (BeWo and JEG-3) were transfected with miR-193b-3p-mimic or -inhibitor. BeWo cells were additionally treated with forskolin to induce syncytialization (cell fusion). Cells and their media were collected to analyze the expression of syncytialization markers. To calculate the cell fusion ratio, BeWo cells were processed for E-cadherin immunofluorescence. The migration of transfected JEG-3 cells was monitored by real-time wound healing assay and the proliferation was assessed with an xCELLigence real-time cell analyzer. Early and late apoptosis were determined by flow cytometry after staining with Annexin V and 7-AAD. EVs were collected from miR-193b-3p-mimic transfected JEG-3 cells (EV_{miR-193b-3p}) and isolated by ultracentrifugation to yield small EVs (sEVs) and large EVs (lEVs) fractions. EVs fractions were characterized regarding their size, concentration, and marker expression. EVs uptake by Jurkat T cells was evaluated via flow cytometry and confocal microscopy. miR-193b-3p levels in Jurkat T cells treated with EV_{miR-193b-3p} were examined by qPCR over a period of 10 days. The proliferation of Jurkat T cells treated with EV_{miR-193b-3p} was assessed with xCELLigence real-time cell analyzer and colourimetric BrdU assay. miR-193b-3p-inhibitor transfected JEG-3 cells were processed for label-free LC-MS/MS quantitative proteomics. Proteomics results were additionally verified in transfected JEG-3 cells at mRNA and protein levels using qPCR and Western blot, respectively.

Results: In the placental villous, miR-193b-3p was present in the syncytiotrophoblasts and endothelial cells. In the decidual layer, miR-193b-3p was detected in endovascular trophoblasts and interstitial trophoblasts. Although its levels did not change during BeWo syncytialization, overexpression of miR-193b-3p reduced the cell fusion ratio, *syncytin-1*, and *syncytin-2* expression, and beta-human chorionic gonadotropin (β hCG) production.

Accordingly, the miR-193b-3p-inhibitor had the opposite effects. Overexpression of this miRNA reduced JEG-3 cell migration, while on the other hand it was increased after treatment with the miRNA inhibitor. miR-193b-3p-mimic transfected cells had increased cell proliferation and decreased late apoptosis, whereas miR-193b-3p-inhibitor transfected cells showed a decreased proliferation rate and an increased number of cells that undergo early and late apoptosis. CD63 and ALIX were enriched in sEVs and barely detected in IEVs fractions. GAPDH and CD47 were present in sEVs and IEVs fractions from both JEG-3 EVs as well as placental perfusate EVs, used as control. Flow cytometry and confocal microscopy of Jurkat T cells treated with JEG-3 EVs showed a tendency for these cells to take up more IEVs than sEVs. Treatment of Jurkat T cells with EV_{miR-193b-3p} resulted in increased intracellular levels of miR-193b-3p, which persisted for up to 5 days, and decreased their proliferation. Out of the 35 dysregulated proteins detected by proteomics in JEG-3 cells transfected with miR-193b-3p-inhibitor, 11 targets were selected for further qPCR analysis. qPCR revealed 6 targets (*K-Ras*, *AKT1*, *TMPPE*, *PTK2*, *SHMT2*, and *MCL1*) in miR-193b-3p-mimic transfected JEG-3 to be significantly downregulated. Accordingly, protein levels of AKT1 and TMPPE were also decreased. In miR-193b-3p-inhibitor transfected JEG-3, qPCR detected 6 targets (*K-Ras*, *TMPPE*, *PTK2*, *MCL1*, *NF1*, and *ARPC5*) significantly upregulated. Protein levels of AKT1 and TMPPE were increased.

Conclusions: The expression of miR-193b-3p was detected in villous syncytiotrophoblast and interstitial, as well as endovascular trophoblasts present in the decidual compartment of human term placenta. Upregulation of miR-193b-3p reduced trophoblastic cell syncytialization, migration, apoptosis and enhanced their proliferation. Downregulation of this miRNA promoted the opposite effects. EV_{miR-193b-3p} were taken up by Jurkat T cells resulting in reduced proliferation. A total of 35 proteins were significantly changed after miR-193b-3p-inhibitor transfection and indicated *K-Ras*, *TMPPE*, *PTK2*, and *MCL1* as potential primary targets of this miRNA. Taken together, these results demonstrate that miR-193b-3p regulates main trophoblast cell functions. They also indicate that changes in miR-193b-3p levels in placental diseases may influence critical trophoblast cell functions, contributing to the disease progression and patient outcome.

Zusammenfassung

Hintergrund: microRNAs (miRNAs) regulieren die Funktionen der Trophoblastenzellen und sind in extrazelluläre Vesikel (EVs) verpackt, um die interzelluläre Kommunikation zu vermitteln. miR-193b-3p wird von der menschlichen Plazenta exprimiert und ist bei verschiedenen Schwangerschaftspathologien dysreguliert. Die Rolle von miR-193b-3p in Trophoblastenzellen ist bisher nur unzureichend untersucht worden. Ziel dieser Arbeit war es daher, die Expression und Lokalisierung von miR-193b-3p in der Plazenta normaler Schwangerschaften zu bewerten, ihre potenziellen Zielstrukturen zu untersuchen und zu prüfen, ob diese miRNA die Funktionen der Trophoblastenzellen sowie die Interaktionen zwischen Trophoblasten und Immunzellen beeinflusst.

Methodik: Die Expression und Lokalisierung von miR-193b-3p wurde in der menschlichen Plazenta mittels miRNA-in-situ-Hybridisierung (miRNA-ISH) untersucht. Um die Auswirkungen von miR-193b-3p auf die Funktionen von Trophoblastenzellen zu untersuchen, wurden BeWo- und JEG-3-Zellen mit miR-193b-3p-Mimik oder -Inhibitor transfiziert. Die BeWo-Zellen wurden mit Forskolin behandelt, um eine Synzytialisierung (Zellfusion) zu bewirken. Die Zellen und ihre Medien wurden gesammelt, um die Expression von Synzytialisierungsmarkern zu analysieren. Zur Berechnung des Zellfusionsverhältnisses wurden die BeWo-Zellen für die E-Cadherin-Immunfluoreszenz aufbereitet. Die Migration transfizierter JEG-3-Zellen wurde mittels eines Echtzeit-Wundheilungstests überwacht, und die Proliferation wurde mit einem xCELLigence-Echtzeit-Zellanalysator bewertet. Die frühe und späte Apoptose wurde mittels Durchflusszytometrie nach Färbung mit Annexin V und 7-AAD bestimmt. EVs wurden aus miR-193b-3p-mimic transfizierten JEG-3-Zellen (EV_{miR-193b-3p}) gesammelt und durch Ultrazentrifugation isoliert, um kleine EVs- (sEVs) und große EVs- (IEVs) Fraktionen zu erhalten. Die EVs-Fraktionen wurden hinsichtlich ihrer Größe, Konzentration und Markerexpression charakterisiert. Die EVs-Aufnahme durch Jurkat-T-Zellen wurde mittels Durchflusszytometrie und konfokaler Mikroskopie untersucht. Die miR-193b-3p-Konzentration in Jurkat-T-Zellen, die mit EV_{miR-193b-3p} behandelt wurden, wurde über einen Zeitraum von 10 Tagen mittels qPCR untersucht. Die Proliferation der mit EV_{miR-193b-3p} behandelten Jurkat-T-Zellen wurde mit dem xCELLigence-Echtzeit-Zellanalysator und dem kolorimetrischen BrdU-Assay bewertet. Die mit dem miR-193b-3p-Inhibitor transfizierten JEG-3-Zellen wurden für markierungsfreie quantitative LC-MS/MS-Proteomik verarbeitet. Die Proteomik-Ergebnisse wurden zusätzlich durch transfizierte JEG-3-Zellen auf mRNA- und Proteinebene mittels qPCR beziehungsweise Western Blot überprüft.

Ergebnisse: In der Plazentazotte konnte die Expression von miR-193b-3p in den Synzytiotrophoblasten und Endothelzellen gezeigt werden. In der Dezidialschicht wurde miR-193b-3p in endovaskulären Trophoblasten und interstitiellen Trophoblasten nachgewiesen. Obwohl sich die miR-193b-3p Expression, während der BeWo-Synzytialisierung nicht veränderte, reduzierte die Überexpression von miR-193b-3p das Zellfusionsverhältnis, die Expression von *Syncytin-1* und *Syncytin-2* sowie die β hCG-Produktion. Dementsprechend hatte der miR-193b-3p-Inhibitor die gegenteilige Wirkung. Die Überexpression dieser miRNA verringerte die Migration von JEG-3-Zellen, die nach der Behandlung mit dem miRNA-Inhibitor zunahm. miR-193b-3p-mimic-transfizierte Zellen wiesen eine erhöhte Zellproliferation auf, während miR-193b-3p-Inhibitor-transfizierte Zellen eine verringerte Proliferationsrate zeigten. miR-193b-3p-mimic-transfizierte Zellen wiesen eine verringerte späte Apoptose auf, während miR-193b-3p-Inhibitor-transfizierte Zellen eine erhöhte Anzahl von Zellen aufwiesen, die frühe und späte Apoptose durchlaufen. CD63 und ALIX waren in sEVs angereichert und wurden in IEVs-Fractionen kaum nachgewiesen. GAPDH und CD47 waren sowohl in den sEVs- als auch in den IEVs-Fractionen von JEG-3-EVs sowie im Plazenta-Perfusat-EVs vorhanden, welche als Kontrolle dienten. Durchflusszytometrie und konfokale Mikroskopie von Jurkat-T-Zellen, die mit JEG-3 EVs behandelt wurden, zeigten eine Tendenz, dass diese Zellen mehr IEVs als sEVs aufnehmen. Die Behandlung von Jurkat-T-Zellen mit EV_{miR-193b-3p} führte zu einem erhöhten intrazellulärem Nachweis von miR-193b-3p, welcher bis zu 5 Tage lang anhielt und die Proliferation der Zellen verringerte. Von den 35 dysregulierten Proteinen, die durch Proteomik in den mit dem miR-193b-3p-Inhibitor transfizierten JEG-3-Zellen nachgewiesen werden konnten, wurden 11 Ziel-mRNAs für die qPCR-Analyse ausgewählt. Die qPCR Analyse ergab, dass 6 Ziel-mRNAs (*K-Ras*, *AKT1*, *TMPPE*, *SHMT2*, *PTK2* und *MCL1*) in den mit miR-193b-3p-Mimik transfizierten JEG-3 Zellen signifikant herunterreguliert waren. Die Proteinspiegel von AKT1 und TMPPE waren ebenfalls herunterreguliert. Im Vergleich, in miR-193b-3p-Inhibitor-transfiziertem JEG-3 Zellen wurden 6 Ziel-mRNAs (*K-Ras*, *TMPPE*, *PTK2*, *MCL1*, *NF1* und *ARPC5*) signifikant hochreguliert. Die Proteinspiegel von AKT1 und TMPPE waren dabei erhöht.

Schlussfolgerungen: Die Expression von miR-193b-3p konnte in villösen Synzytiotrophoblasten und interstitiellen sowie endovaskulären Trophoblasten im Dezidualkompartiment der menschlichen Term-Plazenta nachgewiesen werden. Die Hochregulierung von miR-193b-3p verringerte die Synzytialisierung, Migration und Apoptose der Trophoblastenzellen und erhöhte ihre Proliferation. Die Herunterregulierung

dieser miRNA bewirkte das Gegenteil. EV_{miR-193b-3p} wurden von Jurkat-T-Zellen aufgenommen, was zu einer verringerten Proliferation führte. Insgesamt 35 Proteine waren nach der Transfektion mit dem miR-193b-3p-Inhibitor signifikant verändert und wiesen auf *K-Ras*, *TMPPE*, *PTK2* und *MCL1* als potenzielle primäre Ziele dieser miRNA hin. Zusammengefasst zeigen diese Ergebnisse, dass miR-193b-3p wichtige zelluläre Funktionen von Trophoblastenzellen reguliert. Sie deuten auch darauf hin, dass Veränderungen des miR-193b-3p-Spiegels bei Krankheiten der Plazenta kritische Funktionen der Trophoblastzellen beeinflussen und so zum Fortschreiten der Erkrankung beitragen können.

INTRODUCTION

1.1. Development of the placenta

Successful human pregnancy relies on fundamental processes such as oocyte fertilization, preimplantation development of the conspectus, and its implantation into the uterine wall (Cha et al. 2012a). Embryo implantation is followed by placental development. The placenta constitutes the maternal-fetal interface that supports fetal growth and development. Particularly in the first stages of pregnancy, the placenta substitutes for fetal organs until they mature (Burton and Jauniaux 2015). It also acts as a physical barrier that separates the fetal and maternal circulations, allowing the controlled exchange of nutrients, gases, and waste products. Importantly, it restricts the entrance of hazardous materials such as pathogens, toxins, and maternal immune cells into the fetus circulation. Additionally, the placenta performs as an endocrine organ, secreting hormones, proteins, and cytokines that are important for maternal adaptation to pregnancy. The main placental cell responsible for these functions is the trophoblast (Gauster et al. 2022). Trophoblasts originate from trophectoderm (TE) and undergo different routes of differentiation towards specialized morphologies and functions (Shao et al. 2022).

Five days after fertilization, the first cells start to differentiate in the embryo to form the TE which is considered the earliest epithelium to appear during embryogenesis. The TE constitutes the outer layer of the preimplantation embryo, which at this stage is called a blastocyst. The blastocyst is divided into the inner cell mass (ICM) and the TE (**Fig. 1A**). Thereafter, the polar TE, which is in contact with the ICM, interacts with the uterine luminal epithelium to initiate the implantation process at day 6-7 post fertilization. This process represents the beginning of placenta development and leads to TE fusion to form the primary syncytium (**Fig. 1B**) (Li and Winuthayanon 2017, Zhu and Zernicka-Goetz 2020).

The implantation process can be divided into 3 sequential stages: i) apposition of the blastocyst to the uterine epithelium; ii) adhesion to the epithelial surface; iii) invasion of trophoblast cells into the endometrium. During implantation and placentation, trophoblast cells displace the luminal epithelial cells and migrate through the endometrium, highlighting the importance of trophoblast migration to build the placenta, a cell process that was investigated in this study (Fitzgerald et al. 2008, Cha et al. 2012b).

The endometrium, which undergoes a series of transformations to generate the decidua, forms the maternal part of the placenta (Crha et al. 2019). Around day 9 after fertilization, the TE generates a primitive syncytium that is characteristic of the syncytiotrophoblasts (STBs) on the placenta villi. The trophoblast cells of primitive syncytium digest the surrounding stroma to enable the invasion of blastocyst, which are considered the first invasive placental cell type (Knofler et al. 2019). Beneath the primitive syncytium, primitive cytotrophoblast (CTB) populations proliferate rapidly and start to produce outward protrusions of the first villi around 12 days after fertilization (James et al. 2022). During this time, the extraembryonic mesoderm that is produced from the hypoblast of inner cell mass expands below the primitive CTBs. Following, it invades the developing villi to form the secondary villi. A heterogeneous population of cells composes the invading extraembryonic mesoderm including the progenitor cells of villous core (Ji et al. 2013, Turco and Moffett 2019, Gauster et al. 2022).

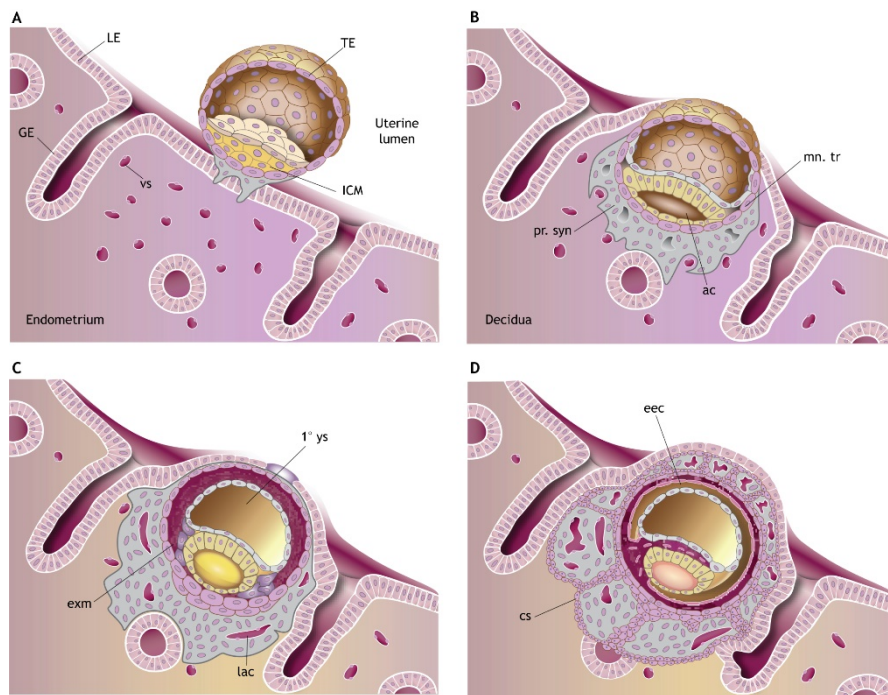


Figure 1. The early phases of human placental development. A scheme illustrating the early steps in placenta formation after blastocyst implantation. **(A, B)** The pre-lacunar stages. **(C)** The lacunar stages. **(D)** The primary villous stage. 1° ys: primary yolk sac; ac: amniotic cavity; cs: cytotrophoblastic shell; eec: extra-embryonic coelom; exm: extra-embryonic mesoderm; GE: glandular epithelium; ICM: inner cell mass; lac: lacunae; LE: luminal epithelium; mn. Tr: mononuclear trophoblast; pr. Syn: primary syncytium; TE: trophoblast; vs: blood vessels. Adjusted from (Turco and Moffett 2019).

Around 14 days after fertilization, the blastocyst is totally embedded in the decidua, heralding the end of the implantation process. Following this, lacunae (fluid-filled spaces) appear within the syncytial mass that expand and fuse, splitting it into a system of trabeculae in what is called the lacunar stage (Turco and Moffett 2019). The trophoblast cells also invade

decidual glands, enabling secretions to bathe the syncytial mass and nourish the conceptus (Hertig et al. 1956, Burton et al. 2020) (**Fig.1C-D**).

Around day 17-18 post-conception, the extraembryonic mesenchymal cells penetrate through the villous core of the secondary villi, which is followed by the appearance of fetal capillaries within the core resulting in tertiary villi development. The villous branches progressively and continuously establish what is known as a villous tree. The CTB shell is in contact with decidua; however, some CTBs leave the shell to invade the decidua as extravillous trophoblasts (EVTs). The EVT's undergo further differentiation (see section 1.2.2) and the placental architecture is fully established by the end of first trimester.

1.2. Pathways of human placental trophoblast cell differentiation

The progenitor cells of human CTBs differentiate into villous trophoblasts and invasive EVT's. An illustration of this process is shown in **Fig. 2**.

1.2.1. Villous trophoblasts

In this differentiation pathway, mononucleated CTBs merge to form multinucleated STBs that develop into the syncytial layer enveloping the placental villous tree. These cells are responsible for the exchange of nutrients, gases, and waste products between maternal and fetal circulations (Kaufmann et al. 2003, Turco and Moffett 2019, Nakashima et al. 2021). This layer presents a high absorptive performance, which is maximized by the existence of microvilli on the surface of STBs. STBs also produce pregnancy-related hormones such as human chorionic gonadotropin (β hCG) and human placental lactogen (hPL) (Lunghi et al. 2007, Velicky et al. 2016). Furthermore, STBs exhibit immune tolerance as they are in direct contact with the maternal blood but are not attacked by the maternal immune system. These cells lack expression of classical class I human leukocyte antigens (HLA) (Nakamura 2009). As the STBs do not proliferate, they are continuously renewed by fusion of the underlying CTBs layer and the shedding of the aged STBs, through syncytial knots (Richart 1961, Kidron et al. 2017).

Although the mechanisms of trophoblast syncytialization or fusion are not fully understood, this requires a tightly controlled orchestration of hormones, growth factors, cytokines, protein kinases, intracellular proteases, transcription factors, and membrane proteins. This involves a signaling cascade that is initiated with increased cAMP levels triggered by adenylyl cyclase, resulting in the activation of protein kinase A (PKA) (Huppertz and Gauster 2011). The downstream activation of transcription factors, such as glial cells missing-1 (GCM-1) and its target genes, code for fusion proteins, including syncytin-1, that induces syncytialization and subsequent increase in β hCG production (Cheong et al. 2016). Syncytins

are encoded by endogenous retroviral genes (HERVs) and are uniquely expressed by the placenta. Syncytin-1 is encoded by *HERV-W* and expressed by STBs during pregnancy. Syncytin-2 is encoded by *ERVFRD1* and is solely expressed in villous CTB cells and gradually decreases throughout pregnancy (Okahara et al. 2004, Durnaoglu et al. 2021).

Syncytin-1 and syncytin-2 are originally produced as precursor polyproteins that are subsequently cleaved into surface and transmembrane domains. The surface domain is required for receptor binding on nearby cells. The transmembrane domain attaches the protein to the plasma membrane (Chen et al. 2008). After binding to their receptors on the target cells, syncytin proteins go through a conformational alternation resulting in the release of transmembrane domain from the surface domain. This process discloses a hydrophobic fusion peptide able to evade the repulsive effect of the adjacent plasma membrane. Subsequently, syncytins seed the target plasma membrane and form a junction linking both membranes resulting in <2 nm proximity between the two cells. Such a process leads to a change in the composition of lipids with the outer plasma membranes that results in phosphatidylserine externalization. A fusion pore is ultimately produced that facilitates inner membrane and cytoplasm union between the merged cells (Renaud and Jeyarajah 2022).

In vitro studies in BeWo cells, a well-known human choriocarcinoma cell line extensively used as a model of trophoblast fusion, illustrated the role of syncytin-1 and syncytin-2 in stimulating cell fusion (Malassine et al. 2008, Fischer et al. 2010). For instance, Fischer et al. reported a role for Galectin-1, a member of the mammalian b-galactoside-binding proteins, in recognition of glycan ligands, including those involved in cell adhesion and growth regulation, on BeWo cells fusion. Forskolin was used as a reference reagent to induce syncytialization. The authors concluded that the cell fusion rates were increased under the influence of Galectin-1 and forskolin. This increase was concurrent with the increased expression of syncytins confirmed at both mRNA and protein levels (Fischer et al. 2010). Moreover, treatment with HERV-W-specific antisense oligonucleotides resulted in the inhibition of cell fusion and differentiation of trophoblastic cells (Mi et al. 2000). The same was observed by Vargas et al. in BeWo as well as primary trophoblast cells. These investigators used RNA interference to suppress *syncytin-1* or *syncytin-2* which resulted in disrupted cell fusion (Vargas et al. 2009).

1.2.2. *Invasive EVT*s

In addition to floating villi formation, anchoring villi establishment is crucial to attach the placenta to the uterine wall and maintain placental perfusion and fetal growth (Vicovac et al. 1995). The formation of the anchoring sites occurs in the second week of pregnancy and includes different types of CTBs. A promptly dividing CTB subpopulation, which plays a role in producing of the cell column bridge between the placental villous tip and maternal decidualized stroma, is located at the proximal ends of the anchoring sites. This cell type provides mechanical support and originates EVT_s. EVT_s are considered the connection between the anchoring villous and uterine decidua basalis. Most EVT_s attached to basement membrane of the anchoring villous proliferate continuously and express epithelial markers such as the villous CTBs (James et al. 2022). Other parts of the EVT_s halt the cell cycle and start to deplete their cell–cell contacts at the distal ends of the columns. As part of their differentiation program, these cells separate from the columns and influenced by decidual factors, they differentiate into interstitial EVT_s (iEVT_s) or endovascular EVT_s (enEVT_s) (Kemp et al. 2002, Yu et al. 2022).

- Interstitial extravillous trophoblast cells – invasion into the uterine stroma

iEVT_s are known to have two different phenotypes: large polygonal iEVT_s (or X cells) and small spindle-shaped iEVT_s. X cells remain close to the placenta-decidua transition. They connect the placenta to the uterus by generating “trophoblast glue”, which consists of a matrix-type fibrinoid (Huppertz 2007, Fu et al. 2013). In contrast, the small iEVT_s invade deeply into the decidua up to the inner third of the myometrium. To ensure their invasiveness, iEVT_s upregulate the expression of several proteases that facilitate the breakdown of the decidual extracellular matrix. These include urokinase-type plasminogen activator (uPA) (Cortina et al. 2017) and several matrix metalloproteinases (MMP), most notably gelatinases MMP-2 and MMP-9 (Cortina et al. 2017, Basu et al. 2018). At their final stage, iEVT_s differentiate into placental bed giant cells, which can produce hormones (hPL and β hCG) like STBs. Additionally, these giant cells contribute to limit the EVT_s invasion in the myometrium by the production of protease inhibitors (Staun-Ram et al. 2004, Yu et al. 2022).

-Endovascular extravillous trophoblast cells – remodelling of the uterine spiral arteries

After 8-12 weeks of pregnancy, placental blood circulation is established and by 20-22 weeks spiral arteries are completely remodeled. enEVTs play a major role in this process leading to the transformation of the spiral arteries from high resistance low-flow muscular vessels to low-resistance high-flow vessels. enEVTs position themselves along the arteries and start disarranging the vascular smooth muscle cell layer. Following, enEVTs invade the lumen of the arteries where they differentiate into the endovascular phenotype. The replacement of endothelial cells by enEVTs occurs through a process termed pseudovasculogenesis or vascular mimicry (Khankin et al. 2010, Knofler et al. 2019).

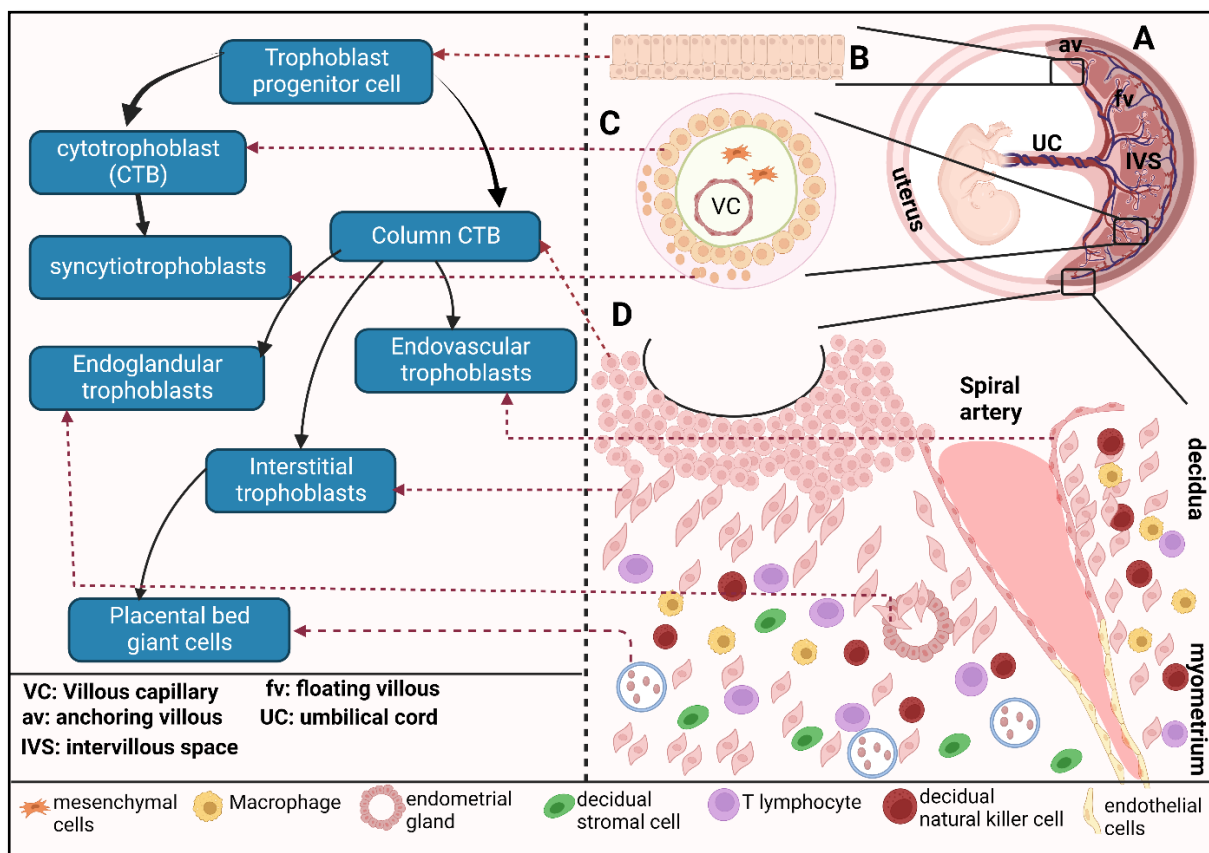


Figure 2. Human placental trophoblast cells differentiation. (A) The growing fetus is bound to the uterus. The umbilical cord includes fetal arteries and veins that give rise to the placental villi. The villi are immersed in maternal blood that is perfused into intervillous spaces. (B) Magnification of chorionic membrane where trophoblast progenitor cells are placed. (C) Magnification of a floating villus. The mononucleated cytotrophoblast cells are coated by a layer of syncytiotrophoblasts. The villous capillaries core and mesenchymal cells are present within the villous core. (D) Anchoring villus magnification. At the distal portion of the column, cytotrophoblast cells detach from the villous and migrate into the decidua. Interstitial trophoblasts invade until the inner third of the myometrium then differentiate into placental bed giant cells. Endovascular trophoblasts (enEVTs) penetrate the uterine spiral artery and substitute the endothelial cells. Endoglandular trophoblasts invade into the endometrial gland. Different immune cells present in the decidua such as macrophage, decidual natural killer cells, and T lymphocytes. The left part of the figure summarizes trophoblast differentiation. Modified from Ji et.al 2013 (Created with Biorender.com).

-Endoglandular trophoblast cells

A new route of trophoblast invasion has been recently described. Endoglandular EVT_s (egEVT_s) replace the glandular cells, and this results in glandular remodeling similar to spiral artery remodeling caused by enEVT_s (Huppertz et al. 2014, Moser et al. 2015). In doing so, egEVT_s locate within the glandular epithelium up to glandular lumen and connect it with the intervillous space of the placenta facilitating the flow of glandular section. Therefore, egEVT_s have a role in histotrophic nutrition of the embryo prior to the establishment of proper placental circulation (Gauster et al. 2022).

The balance between trophoblast proliferation and apoptosis

Early in gestation, the rapidly proliferating CTBs existing beneath the syncytium (which can fuse to form the overlying STBs) are not in direct contact with maternal tissue. Instead, they create projections that push through the primary syncytium to form primary villi which is a CTBs core with a STBs outer layer (Hayder et al. 2018). A new villus may fuse at any segment from the existing tree during a process called random segmental branching. Such a process of CTBs proliferation assists the villous growth and results in comprehensive linear expansion of terminal villi from the second trimester. Later in gestation, the generation of terminal villus develops mainly as a result of fetal vessel expansion, simultaneously with CTBs proliferation decline and increased apoptosis toward term (Turco and Moffett 2019, Gauster et al. 2022).

Partial induction of apoptosis in STBs is essential for CTBs fusion with the STBs layer combined with its normal turnover (Aplin and Jones 2021). Chromatin compaction and margination, cytoplasmic vacuolization, and partially condensed nuclei are considered typical apoptotic characteristics commonly existing in both normal and abnormal placenta (Sun et al. 2020). The occurrence of apoptosis ensures that the nonfunctional cells are cleared without triggering a local inflammatory reaction. Elevation of apoptotic features and reduced expression of the anti-apoptotic protein Bcl-2 in STBs was reported in fetal growth restriction (FGR) and preeclampsia placentas (Farah et al. 2020). Due to their importance in placenta development, trophoblast proliferation and apoptosis processes are investigated in the current study.

1.3. Trophoblasts markers

A set of four criteria have been identified for trophoblastic cell characterization based on i) the expression of protein markers, ii) HLA class I profile, iii) methylation of ELF5, and iv) expression of microRNAs (miRNAs) from the chromosome 19 miRNA cluster (C19MC) (Lee et al. 2016). Out of those markers, E-cadherin and cytokeratine-7 will be further discussed

below as they were used in the present study to evaluate trophoblast cell fusion and identify trophoblast cells, respectively.

As discussed in section 1.1, the first differentiation step of a mammalian zygote is TE formation, which leads to placenta formation. TE cells are polarized and gain the epithelium characteristics of having increased E-cadherin expression and activity (Abou-Kheir et al. 2015). E-cadherin is mainly expressed in anchoring villi and downregulated after the *in vitro* and *in vivo* extravillous differentiation. It was described to be downregulated in distal trophoblast of anchoring villi, iEVTs and enEVTs; however, those cells show increased expression of E-cadherin in preeclamptic placentas (Floridon et al. 2000). The E-Cadherin gene encodes for a calcium-dependent membrane glycoprotein that is necessary for cellular adhesion and polarity maintenance (Burandt et al. 2021). This molecule is located at CTB cells contacts and can be used to visualize cell membrane limits, which are changed with CTBs fusion and formation of STBs. Therefore, E-cadherin was used to assess trophoblasts syncytialization in several studies (Lin et al. 1999, Butler et al. 2009, Gauster et al. 2010, Fischer et al. 2011).

Keratins, formerly known as cytokeratins, are intermediate filaments forming parts that offer mechanical as well as structural support to epithelial cells. Keratins additionally protect from apoptosis as well as regulate cell size and protein synthesis during wound healing and secure the placenta barrier (Abou-Kheir et al. 2015). A total of 54 keratin genes have been identified and classified in type I (acidic) and type II (basic to neutral). Each type is further subdivided into epithelial and hair keratins (Schweizer et al. 2006). As discussed in section 1.2, placental development encompasses trophoblasts differentiation into different subtypes. This process is associated with remodeling of cytoskeletal components including keratin composition to fit with the required structure and function (Gauster et al. 2013). For instance, several keratins are expressed in human placenta, including keratins 7, 8, 13, 18 and 19 in villous trophoblasts and EVT. A summary of the different keratins expressed by human trophoblast is shown in **Table 1**. Keratin 7 is expressed by almost all types of trophoblasts. Therefore, it is used as marker of trophoblast cells (Maldonado-Estrada et al. 2004, Lee et al. 2016, Gauster et al. 2022).

Overall, placental development depends on the appropriate differentiation of all its trophoblast subpopulations. Defective trophoblast differentiation and altered composition of the aforementioned cell populations are associated with placental dysfunction and hence with pregnancy complications including placenta accreta spectrum. This is associated with the increased risk of long-term development of chronic disease in the offspring.

Table 1. Overview of keratins expressed in different trophoblast types

Trophoblast type	Keratin	Reference
Villous trophoblast		
Syncytiotrophoblast	7 [†] , 8, 13, 18, 19	Muhlhauser et al., 1995
Cytotrophoblast	1 [§] , 5, 7, 8, 13, 17*, 18, 19	Muhlhauser et al., 1995; Ahenkorah et al., 2009
Extravillous trophoblast		
Cell column		
Proximal extravillous trophoblast	7, 8, 13, 18, 19	Muhlhauser et al., 1995
Distal extravillous trophoblast	7, 8, 18, 19	Muhlhauser et al., 1995
Interstitial trophoblast	5, 7 [‡] , 8, 18, 19	Proll et al., 1997; Muhlhauser et al., 1995; Ahenkorah et al., 2009
Endovascular trophoblast		
Intramural trophoblast	8, 17, 18, 19	Proll et al., 1997
Intraarterial trophoblast	8, 18, 19	Proll et al., 1997
Endoglandular trophoblast	7 [£]	Moser et al., 2010

[†]: in FFPE placenta detected with antigen-retrieval; *^{*}: only in cells associated with extracellular matrix; [§]: detected with Western blot technique in isolated cytotrophoblasts (Sawicki et al., 2003); [‡]: decreasing expression with increasing invasion distance (Muhlhauser et al., 1995); [£]: others not tested.

Extracted from (Gauster et al. 2013).

1.4. Placenta accreta spectrum

1.4.1. Definition and epidemiology

Placenta accreta spectrum (PAS) was first documented in 1937, describing the pathological condition in which the trophoblast excessively invades into the myometrium and beyond (Jauniaux and Burton 2018). The prevalence of PAS has increased dramatically over the last decades reaching 0.17% of all pregnancies (Conturie and Lyell 2022). The PAS rates per 100,000 births obtained from studies published between 1954 until 2021 are summarized in **Appendix Table 19** and illustrated in **Fig. 3**.

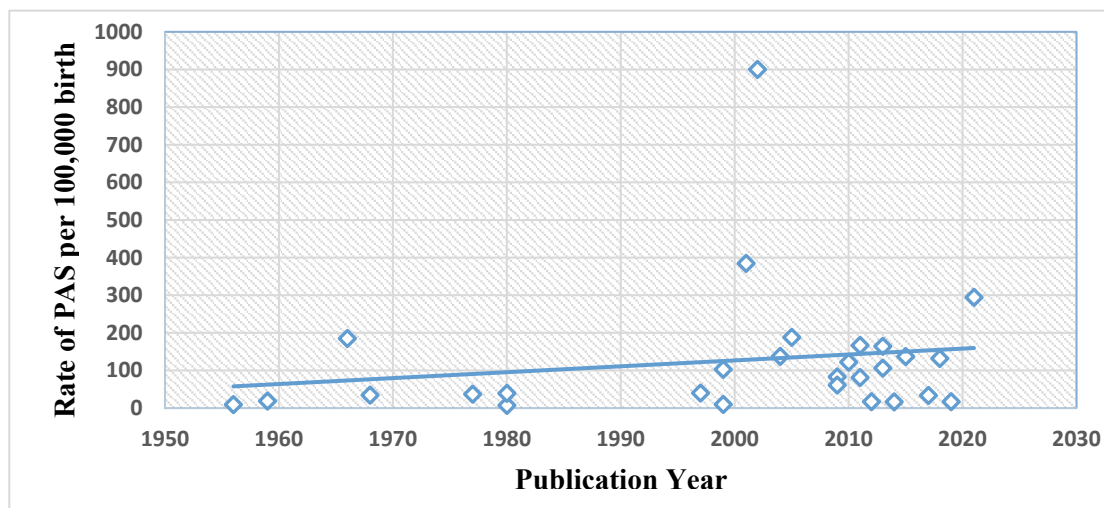


Figure 3. The incidence of placenta accreta spectrum. (A total of 29 studies published between 1954 -2021 were used for incidence calculation). Updated from (Adamczyk 2017).

1.4.2. Pathophysiology

Although the exact PAS pathogenesis is not fully understood, multiple cellular and molecular factors are reported to be involved (Rekowska et al. 2023, Liu et al. 2023). Several hypotheses have been suggested. For instance, an early dysfunction in trophoblast regulatory

mechanisms may result in increased attachment or invasion of the decidua and myometrium. Another hypothesis is based on a secondary defect in the endometrial-myometrial interface due to uterine scar dehiscence, resulting in an abnormal decidualization and abnormal deep placentation (Jauniaux and Burton 2018, Einerson et al. 2020). Alteration in major cellular processes (migration, proliferation, and apoptosis) of trophoblast cells are associated with PAS. These will be further discussed in Chapter 5 in relation with the findings in thesis.

1.4.3. Risk factors

The risk factors for PAS development can be categorized according to the strength and consistency of evidence into three groups, as illustrated in **Table 2**. In an international observational study, 442 PAS cases were registered in the database from 2008 to 2019. A total of 375 cases (84.8%) had placenta previa, when the placenta directly overlies the cervix (Jain et al. 2020), and there was a history of a previous cesarean section (CS) in 329 (74.4%) women (van Beekhuizen et al. 2021). One or multiple CS has been connected to PAS risk, with a linear elevation in both previa and accreta risk depending on the number of prior CS. The risk increased when the placenta was implanted over the previous cesarean scar (Miller et al. 1997, Usta et al. 2005, Grobman et al. 2007, Daltveit et al. 2008). A summary of previous studies reporting the association between PAS and CS, PAS and placenta previa is shown in (**Appendix: Tables 20 and 21**) respectively.

Table 2. Risk factors for PAS

Consistent Evidence from Controlled Studies
<ul style="list-style-type: none"> • Placenta previa • Prior CS(s) (particularly with a placenta previa) • In vitro fertilization (IVF)
Inconsistent evidence from controlled studies
<ul style="list-style-type: none"> • Maternal age ≥ 35 • Prior dilation and curettage of the uterus • Prior myomectomy or other uterine surgery (besides CS) • Maternal smoking
Anecdotal evidence from case series and reports
<ul style="list-style-type: none"> • Prior history of accreta • Uterine synechiae or Asherman's syndrome • Prior endometrial ablation • Prior uterine fibroid embolization • Congenital uterine anomalies (such as a rudimentary horn) • Prior uterine irradiation

Abbreviations: CS, cesarean section; IVF, in vitro fertilization.

Extracted from (Carusi 2017)

1.4.4. *Diagnosis and clinical complications*

Currently, ultrasound is the preferred imaging model for PAS diagnosis during pregnancy (Horgan and Abuhamad 2022). Patients with risk factors are prioritized for sonographic examination (Iacovelli et al. 2020). Magnetic resonance imaging (MRI) can be additionally used with high rates of diagnostic accuracy (Hasegawa et al. 2023, Arakaza et al. 2023). Still, the postpartum histological examination is the definitive diagnosis, which additionally allows performing molecular and immunohistochemical studies to investigate PAS pathogeny (Jauniaux and Burton 2018). Machine learning models have been recently employed to foresee the clinical outcomes of PAS (Shazly et al. 2022).

PAS increases both maternal and perinatal morbidity and mortality. PAS is associated with increased risk of still birth, neonatal death (Baldwin et al. 2017), infection and thrombosis as well as to severe intrapartum and postpartum hemorrhage (O'Rinn et al. 2023). In addition, PAS is one of the leading indications for hysterectomy to avoid massive blood loss (Arakaza et al. 2023).

At present, it is not possible to unambiguously confirm or exclude the diagnosis of PAS through prenatal diagnostics (Garmi and Salim 2012, Conturie and Lyell 2022). Many difficulties remain concerning the prediction and diagnosis of PAS. Thus, the identification of biological markers present in the blood is considered nowadays a potential avenue for diagnostic. There are growing examples of diseases where miRNAs contribute to their pathogenesis and these can be detected in different body fluids, presenting a window of opportunity to evaluate their expression as diagnostic markers.

1.5. miRNAs and control of gene expression

1.5.1. *miRNA*

Each step of gene expression is fine-tuned, from DNA accessibility to RNA transcription, processing, stability, and translation (Chen and Rajewsky 2007). A relatively recent component of the regulatory arsenal of gene expression are miRNAs. They are small (~22 nucleotide) non-coding RNAs with functions as repressors of mRNA expression in all known animal and plant genomes (Pineles et al. 2007). It is estimated that over one third of all human genes are targeted by miRNAs. Therefore, the unique combination of miRNAs that is present in each cell type influences mRNA levels in a specific fashion (Lewis et al. 2005). miRNA genes can be classified based on their genomic locations: intronic miRNAs in protein coding transcription unit (TU), intronic miRNAs in noncoding TU, and exonic miRNAs in noncoding TU. 'Mixed' miRNA genes can be assigned to one of the above groups depending on the given splicing pattern (Kim and Nam 2006, Kabekkodu et al. 2018).

1.5.2. miRNA clusters and families

miRNAs arranged in closed proximity in the genome generate miRNA clusters to allow their expression in a concerted manner (Kabekkodu et al. 2018, Kabekkodu et al. 2020). It has been estimated that 20- 40% of more than 1800 human miRNA sequences are arranged in polycistrons (clusters) that are transcribed together (Pidikova et al. 2020). miRNA cluster consist of 2-8 miRNAs; however, more than 60% of clusters have only two miRNAs (Guo et al. 2014). The clusters can be categorized in two groups: homologous clusters and heterologous clusters. The former consists of miRNAs belong to the identical family whereas the later composed of miRNA genes from different families (Wang et al. 2016). Gene families are groups of homologous genes with similar functions and the same seed sequence (O'Brien et al. 2018). miRNA families and clusters have complex distributions in the genome. One miRNA family can be found in one or more clusters and one cluster can be implicated in one or more families. Above 60% of miRNA clusters in the human genome encompass miRNAs from the same family (Pidikova et al. 2020).

1.5.3. Biogenesis pathways

miRNA genes can be transcribed from their own promoters, and clustered miRNAs are generated as polycistronic primary transcripts (pri-miRNAs). The transcription is mediated by RNA polymerase II (pol II) which yields pri-miRNAs containing both cap structures and poly (a) tails (Cai et al. 2004, Hayder et al. 2018). The miRNA maturation model is shown in **Fig. 4**. pri-miRNAs transcripts are subsequently shortened into hairpin intermediates (pre-miRNAs) (Kim 2005, Yao 2016) by nuclear RNase III Drosha followed by their cleavage by Dicer (another RNase III enzyme) into mature miRNAs. The catalytic activities are compartmentalized into the nucleus and the cytoplasm. Consequently, the nuclear export of pre-miRNA is necessary for the cytoplasmic processing to occur (Lee et al. 2002, O'Brien et al. 2018). Mature miRNAs are integrated into effector complexes called miRNA-containing RNA-induced silencing complex (miRISC) (Knight and Bass 2001, Yi et al. 2003, Matsuyama and Suzuki 2019).

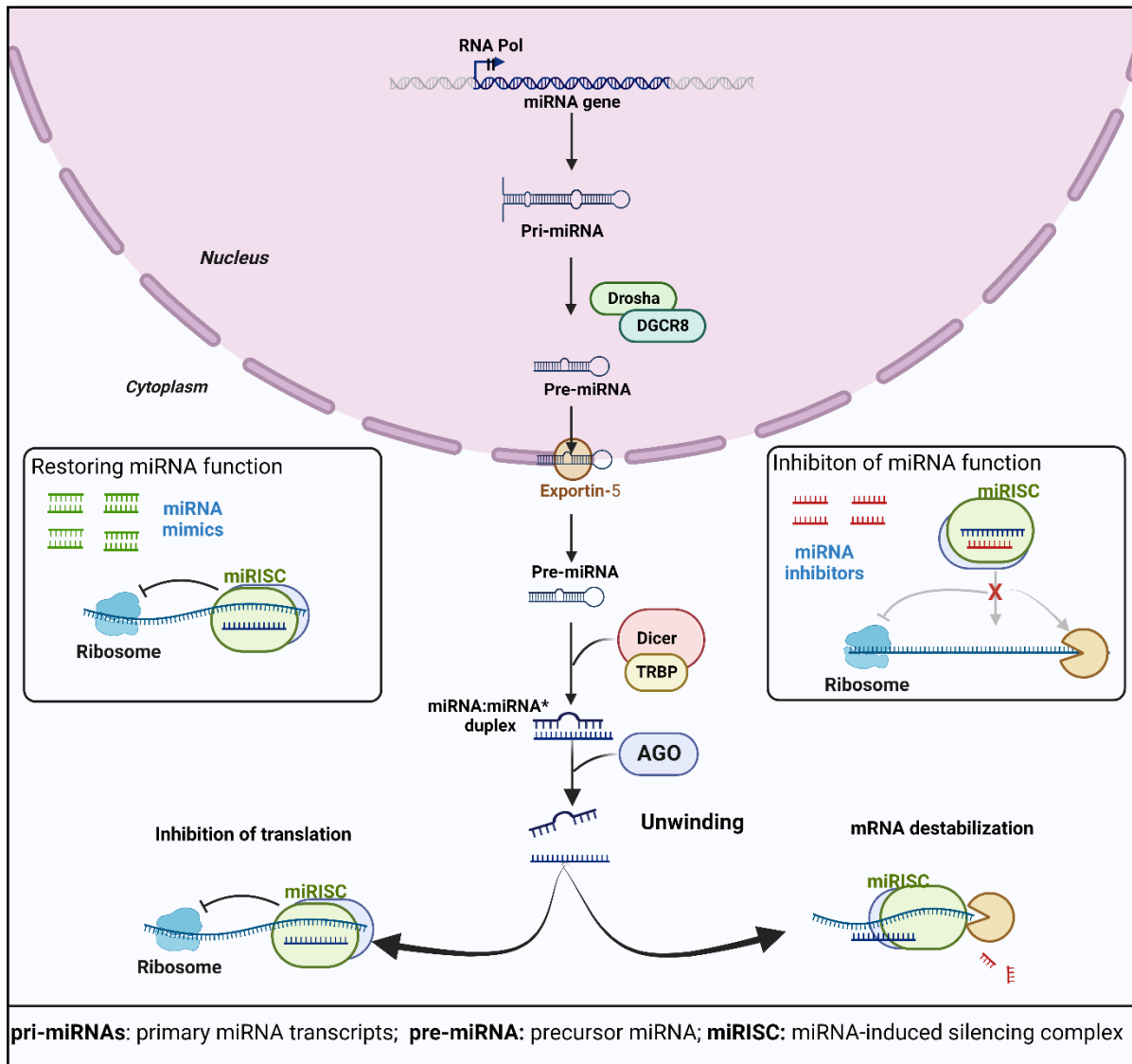


Figure 4. miRNA biogenesis and modification of its activity by miRNA mimics and miRNA inhibitors oligonucleotides. RNA polymerase II transcribed miRNA genes into long pri-miRNA which is digested in the nucleus by the Drosha–DGCR8 complex to pre-miRNA hairpin structures (~ 70 nucleotides). Pre-miRNAs are transported into the cytoplasm and processed by Dicer–TRBP complex to imperfect miRNA: miRNA* duplexes (~ 22 nucleotides). In the cytoplasm, miRNA duplexes are introduced into Argonaute-containing miRISC, followed by unwinding of the duplex and retention of the mature miRNA strand in miRISC. The mature miRNA works as a guide molecule for miRISC by leading it to partially complementary sites in the target mRNAs, resulting in translational repression and/or mRNA degradation. To date, two strategies have been applied to manipulate miRNA activity: restoring miRNA function using double-stranded miRNA mimics and inhibiting of miRNA function using single-stranded anti-miR oligonucleotides (Created with Biorender.com).

1.5.4. Experimental strategies to modulate miRNA levels

-miRNAs downregulation

The principle of Watson and Crick base-pairing guides the binding between miRNAs and their target mRNAs. In order to manipulate this binding, anti-miRNA oligonucleotides (AMOs) have been used to directly compete with endogenous miRNAs (Lima et al. 2018)

(Fig.4). Anti-sense studies have shown that targeting of miR-21, a miRNA that is over-expressed in many cancer types, effectively reduced tumor size in a xenograft mouse model based on MCF-7 cells. AMOs antagonists conjugated to cholesterol were generated and efficiently inhibited miRNA activity in-vivo (Esau et al. 2006).

The generation of miRNA sponges is another method for interfering with the interaction between miRNAs and their targets. miRNA sponges are synthetic mRNAs that have multiple binding sites for endogenous miRNAs. Sponges which were synthesized with multimeric seed sequences have been confirmed to successfully repress miRNA families sharing the same seed sequence (Thomson and Dinger 2016). Although these oligonucleotide-based methods have been shown to work successfully, they can elicit off-target side effects and unwanted toxicity. This is due to the capability of miRNAs to regulate hundreds of genes coordinating pivotal cellular processes (Budhu et al. 2010).

miR-masking is an alternative strategy that utilizes a sequence with perfect complementarity to the target mRNA 3' untranslated regions (UTR) such that duplexing will occur with higher affinity than that between the target mRNA and its endogenous miRNA, which commonly includes mismatches (Addo et al. 2020). In doing so, the miR-mask prevents the availability of the seed sequence of the mRNA to its miRNA (Wang 2011). This gene-specific miRNA interfering strategy has been shown to reduce the activities of miR-1, miR-133, and miR-430 in several model systems (Xiao et al. 2007, Choi et al. 2007).

-miRNAs overexpression

Promoting the expression of miRNAs that have a tumor suppression activity is a method to stimulate cellular tumor inhibitory functions. This can be done by using viral or liposomal delivery mechanisms (Zhang et al. 2012). Several miRNAs have been introduced into cells via these methods, including miR-34, miR-15, miR-16 and let-7 (Xie et al. 2015). For instance, the use of adenovirus-associated virus (AAV) to systematically deliver miR-26, a tumor suppressive miRNA in Hepatocellular carcinoma (HCC), in animal model led to cell proliferation inhibition and tumor-specific apoptosis (Janaiah Kota 2009).

miRNA precursors have been used to obtain long-term stable expression of miRNAs by inserting the miRNA precursor sequence downstream of RNA polymerase III (Pol III)-driven or Pol II-driven promoters in a vector system. For example, miR-124 precursor plasmid was introduced into mouse subventricular zone stem cells (Zhang et al. 2012). The use of viral based method has high gene transfer efficiency, but the residual viral elements can elicit immunogenic

effect. This can lead to a preference for non-viral methods for gene transfer such as cationic liposome mediated system. The liposomes are promising transfer method but they lack tissue specificity and have a lower transfection efficiency compared with viral vector-based methods (Budhu et al. 2010).

miRNA mimics have also been used to increase miRNA expression within cells (**Fig.4**). They are small, chemically modified double-stranded RNA molecules that mimic endogenous mature miRNAs (Lu and Rothenberg 2018). These mimics are now commercially available and reasonable results have been reported with systemic delivery methods using lipid and polymer-based nanoparticles. Oligofectamine and Lipofectamine are commonly used cationic lipids that form complexes with the negatively charged nucleic acid molecules to avoid electrostatic repulsion of the cell membrane (Fus-Kujawa et al. 2021). Since miRNA mimics do not have vector-based toxicity, they are favorable tools for therapeutic treatment of tumors (Martinez et al. 2002). They are introduced by endocytosis to cells as a complex of cationic lipids and nucleic acids in liposomes, which are released into the cytoplasm. It is an advantageous method due to its high transfection efficiency for various types of cells including primary cells, adherent cell lines and cell lines cultured in suspension (Ewert et al. 2010). It permits the delivery of DNA, RNA and proteins of different molecular weights to the cell and it can be applied for either stable or transient transfection (Zhi et al. 2018).

1.6. miRNA in pregnancy

The discovery in 1997 of the fetal release of cell-free DNA into the maternal circulation opened new avenues for noninvasive prenatal diagnosis (Rafi and Chitty 2009). Current medical use of circulating fetal DNA analysis include determination of fetal sex for prenatal management of sex-linked diseases and RhD blood group genotyping for the detection and management of RhD incompatibility (Chiu and Lo 2013). In addition to DNA, placenta-derived RNAs, including miRNAs, have been detected in maternal plasma. Placental miRNAs offers the possibility for noninvasive investigation of placental function and the detection of diseases associated with placental dysfunction (Chiu and Lo 2010).

Placental miRNAs are main regulators of various physiological processes such as proliferation, apoptosis, stem cell differentiation, angiogenesis and immune responses (Hayder et al. 2018). Vital molecules for miRNA biogenesis including Argonaute 2 (Ago2), Drosha, Exportin 5, and Dicer were detected in trophoblast cells (Rezaei et al. 2019). There are more than 1900 miRNAs expressed in the human placenta (Morales-Prieto et al. 2020). The pattern of placental miRNA expression changes during pregnancy with a total of 208 miRNA

transcripts differentially expressed between the first and third trimester (Gu et al. 2013). Remarkably, definite cluster expression profiling demonstrated that the highly expressed miRNAs in the first trimester, control proliferative and angiogenic genes, whereas miRNAs that are highly expressed in third trimester induce cell differentiation and inhibit proliferation (Gu et al. 2013). Three pregnancy-associated miRNA clusters have been identified, namely C14MC, C19MC and miR-371-3.

The chromosome 14-encoded miRNA cluster (C14MC) contains 52 miRNA genes and is located within two nearby segments spanning about 40 kb (Dini et al. 2018, Dini et al. 2019). It is exclusively expressed from the maternally inherited chromosome. Differential methylation of distal intergenic germline-derived regions plays a role in C14MC regulation. C14MC was amplified by tandem duplication, which was then preserved without structural changes and exclusively expressed in placental mammals (Morales-Prieto et al. 2013). C14MC expression decreases across the gestation (Gu et al. 2013).

C19MC has 46 highly homologous miRNA genes within a ~100 kb genomic region (Donker et al. 2012). These miRNAs are mainly expressed in primate placenta, some fetal tissues and certain tumor cells. Throughout the gestation, they are highly expressed in trophoblasts, released into maternal circulation via EVs, and cleared after delivery (Rippe et al. 2010, Morales-Prieto et al. 2013). miR-517a, miR-517b, miR-516b, miR-525-5p, miR-512-3p, and miR-515-3p are considered the most highly expressed C19MC miRNAs. They are potential biomarkers for pregnancy-associated complications including preeclampsia, obesity, ectopic pregnancies, gestational diabetes, FGR, preterm birth, and recurrent pregnancy loss (Addo et al. 2020). miR-519, miR-517a, and miR-517c are some members of C19MC that display tumor suppressive activity by stimulating cell senescence or cell proliferation inhibition (Xu et al. 2021).

miR-371-3 encodes only six mature miRNAs. The miR-371-3 cluster is located on chromosome 19 within a 1050 bp region neighboring the C19MC cluster (Morales-Prieto et al. 2013). The expression of this clusters is limited to only a few tissues mainly during embryonic and fetal development, restricted to extraembryonic tissues and in particular the placenta (Gottlieb et al. 2021).

1.6.1. *miRNAs and PAS*

The association between PAS and miRNAs dysregulation has been reported several times in the literature. A summary of these studies is shown in **Table 3** and a more detailed explanation is illustrated below.

Umemura et al. described a significant decrease of miR-34a expression in PAS placenta. Such decrease of miR-34a was concurrent with the increased expression of plasminogen activator inhibitor-1 (PAI-1) suggesting it as a target of miR-34a. Using JAR human choriocarcinoma cell line, they detected increased expression of miR-34a with addition of IL-6 and IL-8. JAR cells invasion was enhanced with the decreased expression of miR-34a (Umemura et al. 2013). The expression of miR-29a/b/c in PAS tissue was also significantly downregulated. miR-29a/b/c induce apoptosis when its mimic was transfected to HTR-8/SVneo trophoblastic cells. Myloid cell leukemia 1 (MCL1) was confirmed to be its target mRNA using a luciferase activity assay (Gu et al. 2016). Later, the same group demonstrated the downregulation of miR-125a in PAS placenta and its function in apoptosis. MCL1, which was upregulated in PAS tissue, was reported to be a potential target of miR-125a (Gu et al. 2019a).

Yang and collaborators used RNA sequencing to compare mRNA, lncRNA, and miRNA expression profiles between PAS and normal pregnancy (NP) placentas as well as plasma samples. A total of 8,806 lncRNAs, 128 miRNAs, and 1,788 mRNAs were revealed to be differentially expressed between PAS and NP placentas. Out of the 128 miRNA that were assessed, seven miRNAs were significantly upregulated (miR-490-3p, miR-488-3p, miR-770-5p, miR-193a-3p, miR-133a-3p, miR-103a-3p, and miR-501-3p) and two miRNAs were significantly downregulated (miR-137-3p, miR-34b-5p) in the placentas of PAS. Additionally, miR-490-3p and miR-133a-3p were positively correlated to operation-related blood volume loss. Thus, those two miRNAs may serve as potential biomarkers for PAS prognosis (Yang et al. 2020).

miR-518b is elevated in PAS and positively correlated with the expression of osteopontin (OPN) and vascular endothelial growth factor (VEGF) (Long et al. 2019). OPN is a secretory, phosphorylated glycoprotein that contributes to cell migration, adhesion and extracellular matrix (ECM) formation (Kariya et al. 2021). VEGF is involved in placental angiogenesis as it has an effect on endometrial vascular endothelial cells. VEGF promotes their proliferation, migration and increases the vascular permeability. VEGF has other roles in increasing trophoblast invasion that is relevant to PAS etiology (Long et al. 2019).

miR-17-5p, miR-21-5p, miR-25-3p, miR-92a-3p, and miR-320a-3p were upregulated in peripheral blood of pregnant women with PAS and correlated with the severity of the disease. These miRNAs are potential regulators of clusterin, which is expressed by almost all tissues and present in body fluids. This molecule is involved in several signaling pathways, including those related to IGF1 (Bass-Stringer et al. 2020), TGF- β (Jin and Howe 1999), VEGF, AKT/MAPK, and Wnt, and also regulates EMT (Pereira et al. 2018, Rodriguez-Rivera et al. 2021, Timofeeva et al. 2021). Clusterin has 3 isoforms and the secreted form was significantly downregulated in plasma of PAS patients. This suggested that the quantification of the secretory form of clusterin and those miRNAs in the first trimester of pregnancy may have a predictive value to assess PAS development (Timofeeva et al. 2021).

Another study reported that miR-139-3p, miR-196a-5p, miR-518a-3p, and miR-671-3p are downregulated in PAS and could be used for non-invasive prenatal PAS screening. These miRNAs were selected out of 42 miRNAs that were screened by miRNA array in plasma samples from third trimester NP and PAS pregnancies. Using bioinformatic tools, their target mRNAs and functions were predicted. They include angiogenesis, embryonic development, cell migration and adhesion, and tumor-related pathways, which are associated with PAS pathogenesis (Chen et al. 2020).

miR-193a-3p was investigated in PAS by Li et al. revealing that this miRNA was upregulated in PAS placenta and its mRNA target, Ephrin-B2, was downregulated. Trophoblastic HTR-8/SVneo cells were used to examine the role of miR-193a-3p in migration and invasion. Both processes were enhanced by miR-193a-3p. Epithelial-mesenchymal transition (EMT) was activated as determined by the elevated expression of N-cadherin, vimentin, MMP2, and MMP9 as well as reduced E-cadherin in HTR-8/SVneo cells transfected with miR-193a-3p-mimics or si-EFNB2 and validated in the PAS samples (Li et al. 2020).

A recent study revealed an elevated expression of miR-1296 in PAS that is inversely correlated with the expression of angiogenic factor with G-patch and FHA domains 1 (AGGF1), a novel P53-dependent oncogenic suppressor that inhibit tumor progression through the P53 signaling axis. AGGF1 was confirmed by dual-luciferase assay as a primary target of miR-1296. The reduced expression of AGGF1 promoted by miR-1296 upregulation in HTR-8/SVneo trophoblast cells enhanced proliferation, invasion and migration as well as reduced apoptosis (Wang et al. 2023).

miR-24-3p, miR-193b-3p, miR-331-3p, miR-376c-3p, miR-382-3p, miR-495-3p, miR-519d-3p and miR-3074-5p were upregulated, and miR-106b-3p, miR-222-3p, miR-370-3p,

miR-454-5p, miR-3615-3p, and miR-137-3p were downregulated in PAS placenta tissue in comparison to placenta tissue collected from NP which were assessed by RNA-sequencing and qPCR (Murrieta-Coxca et al. 2023). The properties of miR-193b-3p will be further described in the next section.

Table 3. Summary of miRNAs dysregulated in PAS

miRNAs	Expression	Targets	Functions *	Sample type	References
miR-34a	Downregulated	PAI-1	↓ Invasion	Placenta	(Umemura et al. 2013)
miR-29a/b/c	Downregulated	MCL1	↑Apoptosis	Placenta	(Gu et al. 2016)
miR-125a	Downregulated	MCL1	↑Apoptosis	Placenta	(Gu et al. 2019a)
miR-518b	Upregulated	ND	ND	Placenta	(Long et al. 2019).
miR-490-3p, miR-488-3p, miR-770-5p, miR-193a-3p, miR-133a-3p, miR-103a-3p, and miR-501-3p	Upregulated	ND	ND	Placenta and plasma	(Yang et al. 2020)
miR-34b-5p and miR-137-3p	Downregulated				
miR-139-3p, miR-196a-5p, miR-518a-3p, and miR-671-3p	Downregulated	ND	ND	Plasma	(Chen et al. 2020)
miR-193a-3p	Upregulated	Ephrin-B2	↑Migration, invasion, epithelial-mesenchymal transition	Placenta	(Li et al. 2020)
miR-17-5p, miR-21-5p, miR-25-3p, miR-92a-3p, and miR-320a-3p	Upregulated	Clusterin	ND	Plasma	(Timofeeva et al. 2021).
miR-1296	Upregulated	AGGF1	↑Migration, invasion and proliferation. ↓ Apoptosis	Placenta	(Wang et al. 2023)
miR-24-3p, miR-193b-3p, miR-331-3p, miR-	Upregulated	ND	ND	Placenta	(Murrieta-Coxca et al. 2023)

376c-3p, miR-382-3p, miR-495-3p, miR-519d-3p and miR-3074-5p					
miR-106b-3p, miR-222-3p, miR-370-3p, miR-454-5p, miR-3615-3p, and miR-137-3p	Downregulated				

* Experimentally assessed function; PAI-1: plasminogen activator inhibitor-1; AGGF1: angiogenic factor with G-patch and FHA domains 1; MCL1: myeloid cell leukemia 1; ↑: increase; ↓: decrease; ND: not detected.

1.6.2. *miR-193b-3p*

The miR-193 family contains 56 sequences, including miR-193a and miR-193b that are located on chromosome 17 (chr17: 31559996– 31560083) and 16 (chr16: 14303967–14304049), respectively (Khordadmehr et al. 2019). miR-193b is located within the same cluster with miR-365a (chr16: 14309285-14309371) (miRBase. 2019). miR-193b-3p has effects on proliferation in a tissue-specific manner. For example, chondrocyte proliferation and auricular chondrocyte ECM were enhanced after miR-193b-3p-mimic transfection. The increase in ECM synthesis in chondrocytes was accompanied by the decreased expression of MMP16, which was confirmed as a primary target of miR-193b-3p (Chen et al. 2019b). However, this miRNA has also an anti-proliferative effect as a part of miR-193b/miR-365a cluster, suggesting its role in cell differentiation. For instance, it inhibits myogenesis leading to brown adipose tissue differentiation (Sun et al. 2011). Similarly, upregulation of miR-193b leads to aging-related senescence of chondrocyte (Ukai et al. 2012). miR-193b overexpression was examined in normal human keratinocytes after calcium-induced differentiation and regulated the terminal differentiation program of keratinocytes (Hildebrand et al. 2011). miR-193b was reported to play a vital role in drug susceptibility, DNA methylation, and tumor metastasis (Gao et al. 2011). It has an inhibitory function in various tumors and tumor cell lines including prostate cancer, breast cancer, glioma, pancreatic cancer, melanoma, hepatocellular carcinoma, and ovarian cancer. Nevertheless, it was reported to function as an oncogene in colorectal cancer and cervical cancer (Khordadmehr et al. 2019). An overview of miR-193b-3p reported functions is summarized in **Table 4**.

It was reported in two different studies that miR-193b-3p is involved in pregnancy-associated diseases such as preeclampsia and intrauterine growth restriction (IUGR). For instance, miRNA sequencing of preeclamptic and NP placentas identified 25 miRNAs which

were significantly dysregulated between the two groups. Ten of them were further validated by qPCR, which showed that miR-193b-3p was the most significantly upregulated miRNA. *In vitro* analysis of miR-193b-3p functions using HTR-8/SVneo trophoblast cells concluded that miR-193b-3p decreases their migration and invasion. Transforming growth factor- β 2 (TGF- β 2) was confirmed to be a miR-193b-3p target, which is downregulated in preeclamptic placentas (Zhou et al. 2016).

In a case control study, the placentas from FGR and control women were subjected to miRNA sequencing analysis. Out of 1870 detected miRNAs, miR-193b-3p and miR-3679-5p were significantly upregulated in FGR placentas. Six miRNAs were significantly downregulated (miR-379-3p, miR-335-3p, miR-4532, miR-519e-3p, miR-3065-5p, and miR-105-5p). Bioinformatics analysis indicated that four of these miRNAs, including miR-193b-3p, were involved in insulin-IGF pathway, suggesting their influence on fetal growth via a growth-promoting system (Ostling et al. 2019). Another study showed that 6 miRNAs and 22 genes were differentially expressed between placentas from healthy, IUGR, preeclampsia, and preeclampsia with IUGR patients. miR-193b-3p was significantly upregulated in all of the three disease groups (Awamleh et al. 2019).

miR-193b-3p was shown to be upregulated in placenta accereta spectrum (PAS) detected by sequencing and qPCR and mainly localized in STBs (Murrieta-Coxca et al. 2023).

Table 4. Studies involving miR-193b-3p

Pathology/ Model	miR-193b-3p expression	Target	Function	Reference
Lung cancer, (A549 cells)	Downregulated	Cyclin D1, uPA	↓ Migration ↓ Proliferation ↓ Invasion	(Hu et al. 2012)
HNSCC, (FaDu: the human hypopharyngeal HNSCC)	Upregulated	NF1	↑ Migration ↑ Invasion ↑ Proliferation	(Lenarduzzi et al. 2013)
Epidermal squamous cell carcinoma, (HaCaT, CAL27, CAL60, A431 cell lines and NHK)	Downregulated	K-Ras	↓ Proliferation ↓ Migration	(Gastaldi et al. 2014)
Preeclampsia, (HTR-8/SVneo trophoblastic cell line)	Upregulated	TGF- β 2	↓ Migration ↓ Invasion	(Zhou et al. 2016)
Ovarian carcinoma, (A2780, SKOV3, OVCAR3, and HeyC2 cells)	Downregulated	PAK3	↓ Proliferation	(Zhang et al. 2017b)

Osteoarthritis	Downregulated	MMP-19	↑ Cartilage extracellular matrix COL2A1 and aggrecan expression in PHCs	(Chang et al. 2018)
Breast cancer, (MCF-7 cells)	Downregulated	Era, uPA	↓ Migration ↓ Invasion	(Hashemi et al. 2018)
T2DM	Upregulated in T2DM ectosomes	ND	Regulate angiogenesis	(Stepien et al. 2018)
Microti, (chondrocyte isolated from microtia patients were used)	ND	MMP16	↑ Proliferation ↑ ECM formation	(Chen et al. 2019b)
AML, (human normal bone marrow CD34+ cells and AML cell lines MV-4-11, AML-193, HL-60, and KG-1 cells)	Downregulated	MCL1	↓ Proliferation ↑ Apoptosis	(Wang et al. 2021)
Placenta accreta spectrum	Upregulated	ND	ND	(Murrieta-Coxca et al. 2023)

AML: Acute Myeloid Leukemia; COL2A1: type II collagen gene; ECM: Extracellular matrix; Era: estrogen receptor α ; HNSCC: head and neck squamous cell carcinomas; MCL1: Myloid cell leukemia 1; MMP: matrix metalloproteinases; ND: not detected; NF1: Neurofibromin 1; NHK: normal human keratinocyte; OC: ovarian cell line; PAKs: P21-activated kinases; PHCs: primary human chondrocytes; T2DM: type 2 diabetes mellitus; uPA: urokinase-type plasminogen activator; TGF- β 2: transforming growth factor- β 2.

1.7. Extracellular Vesicles

Extracellular vesicles (EVs) are membrane-enclosed nanoscale particles containing proteins, lipids, RNA, and DNA produced by all prokaryotic and eukaryotic cells and are potential carriers of miRNAs. They can convey instructions between cells via the extracellular space and influence the recipient cells phenotype by the exchange of biomolecules (O'Brien et al. 2020). Pan and Jonsotne (1983) were among the first researchers who described the existence of EVs. It was previously thought that EVs release was a disposal mechanism to get rid of the waste material from the cells. Further research revealed that EVs are essential mediators of intercellular communication that is vital in physiological and pathological processes (Abels and Breakefield 2016, Doyle and Wang 2019). Aside from the blood, EVs can also be isolated from different body fluids such as urine, cerebrospinal fluid, breast milk,

semen, saliva and amniotic fluid (Yanez-Mo et al. 2015). EVs are composed of different types of proteins (CD63, CD9, CD81, and other tetraspanins, heparin sulfate proteoglycans, integrins, immunoglobulins, and lectins), lipids (phosphatidylserine, sphingoglycolipids and cholesterol) and nucleic acids (mRNA, miRNA and other ncRNA) (Doyle and Wang 2019, Veziroglu and Mias 2020). This content is protected from proteases and nucleases in the extracellular space and may vary depending on the biogenesis, cell type, and cellular conditions (Abels and Breakefield 2016).

1.7.1. Extracellular vesicles classification

Based on their size, content, and origin, EVs can be classified into exosomes, microvesicles and apoptotic bodies (**Fig. 5**). Due to limitations in their isolation, it has also been proposed to classify them into fractions containing exosome-enriched small vesicles (sEVs) and microvesicles-enriched large vesicles (lEVs) (Favaro et al. 2021).

Exosomes (50 – 150 nm) are produced by the endocytic pathway, through inward budding of endosomal compartments, called multivesicular bodies (MVBs) that are formed by invagination of the cell membrane. Exosomes release into the extracellular environment requires fusion of the MVB to the plasma membrane (Favaro et al. 2021, Gurung et al. 2021). Exosomes express endosomal membrane markers (Tetraspanins: CD63, CD9, CD81, TSG101, and Alix); RNA species (miRNA, other non-coding RNAs, and mRNAs); and are highly enriched in glycosphingolipids, cholesterol, and phosphatidylserine (Jankovicova et al. 2020, Larios et al. 2020, O'Brien et al. 2020).

Microvesicles (150 – 1,000 nm) are released from the plasma membrane to the extracellular space by its outward blebbing. Therefore, they have a similar lipid composition as the plasma membrane. They are also enriched with CD40, MMP2 and CK18 proteins and have a similar composition in terms of RNA species with exosomes (Escudero et al. 2016, Willms et al. 2018).

Apoptotic bodies (1,000 – 5,000 nm) are generated from cells undergoing programmed cell death. They are enriched in histones, fragmented DNA, and contain cellular organelles and cytosolic components (Escudero et al. 2016, Tannetta et al. 2017, Favaro et al. 2021).

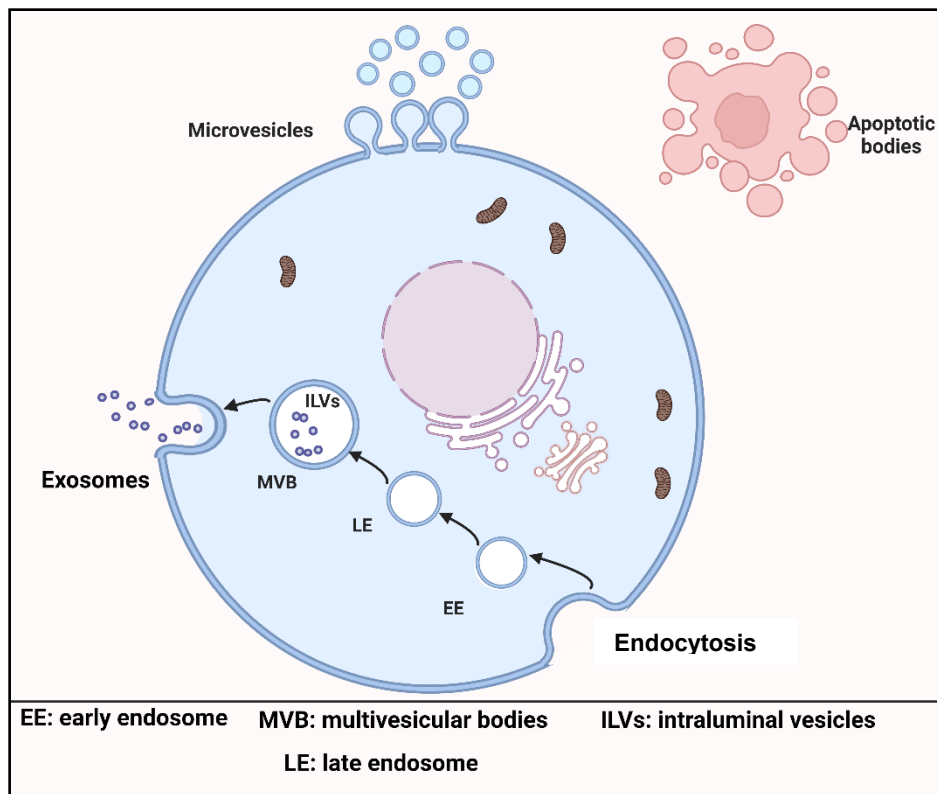


Figure 5. Various types and biogenesis pathways of extracellular vesicles (EVs). The EVs generated by outward invagination of the plasma membrane are microvesicles (form by healthy cell) and apoptotic bodies (formed during programmed cell death). Exosomes are produced by inward budding of LE resulting in the generation of MVB containing multiple intraluminal vesicles. MVBs are then released into extracellular spaces (Created with Biorender.com).

1.7.2. Mechanisms of extracellular vesicles uptake

The mechanisms of EVs uptake as illustrated in **Fig. 6** include:

- **Macropinocytosis:** A mechanism that involves the invagination of the plasma membrane followed by pinching off into intracellular compartment. This process permits EVs internalization within the plasma membrane (Bloomfield and Kay 2016).
- **Membrane Fusion:** This involves membrane fusion of two lipid bilayer which ended by pore formation where the hydrophobic cores are mixed (Fuhrmans et al. 2015).
- **Clathrin-mediated endocytosis:** This process encounters the internalization of the EVs, which are coated by clathrin. Then clathrin coated- EVs deform the membrane which collapses into vesicular bud and pinches off after maturation. Then clathrin un-coating of the EVs occurs allowing the release of EVs contents after endosome fusion (Kaksonen and Roux 2018).
- **Caveolin-dependent endocytosis:** Caveolae are small cave-like structures in the plasma membrane which are able to be internalized into the cell. They are replete of sphingolipids and

cholesterol. One of the required proteins for caveolae formation is Caveolin-1 which is clustered within membrane invaginations (Verdera et al. 2017).

- **Lipid raft mediated endocytosis:** Lipid rafts are microdomains of the plasma membrane with high cholesterol and glycosphingolipids abundance (Pike 2003). Raft mediated endocytosis is a mechanism of EVs internalization which is facilitated by those domains (Wei et al. 2020). Because of their physical properties explained by the heterogeneous composition, they can recruit the assembly of signaling complexes. Their prospective role in influencing EVs uptake was confirmed by studies employing inhibitors of cholesterol and glycosphingolipid synthesis (Mulcahy et al. 2014).

- **Phagocytosis:** Encompasses a receptor-mediated event in which invagination formation of the surrounding material has occurred. It has been shown that small particles with a size of 85 nm in diameter can be internalized, raising the possibility that EVs can be also internalized in this way (Rudt and Muller 1993).

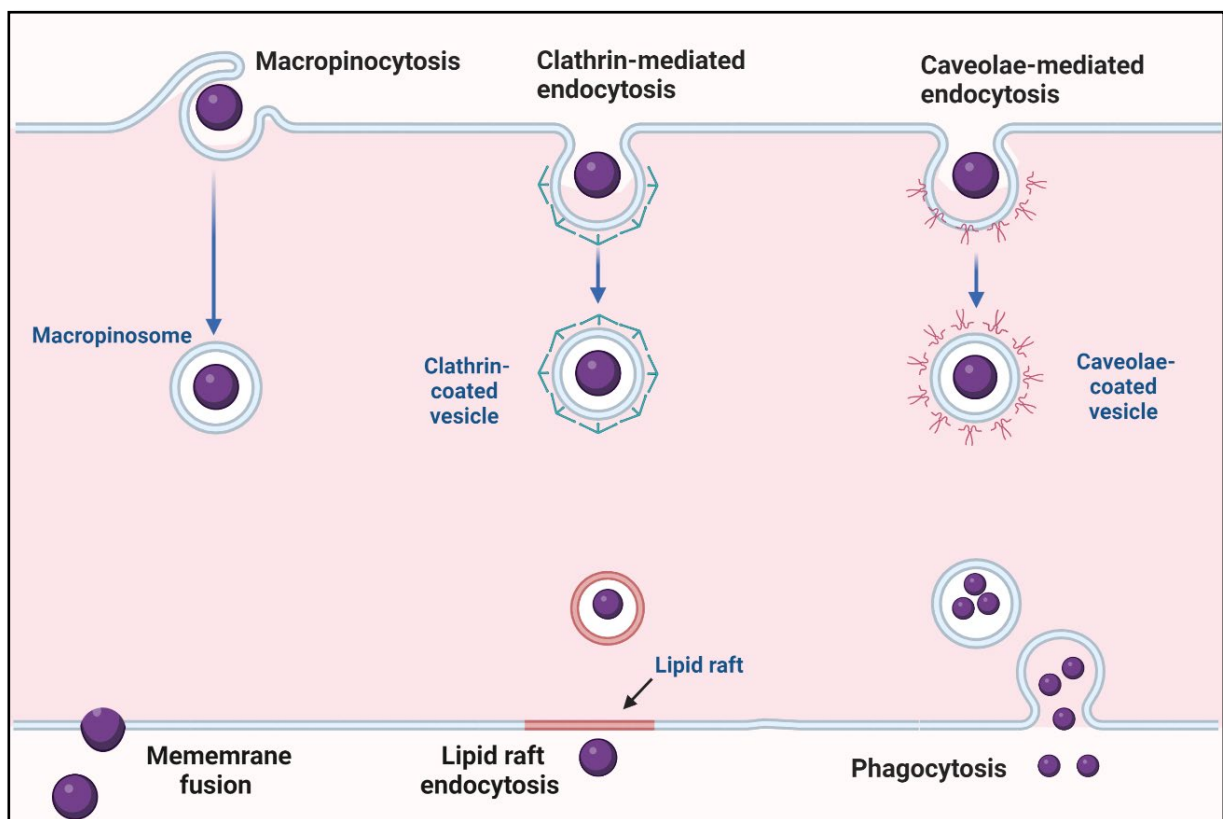


Figure 6. The pathways involved in extracellular vesicles (EVs) uptake by target cells. EVs can be taken up by micropinocytosis, clathrin- and caveolin-mediated endocytosis, and phagocytosis. EVs cargo can be additionally internalized after their fusion with the plasma membrane of recipient cells (Created with Biorender.com).

In summary, the role of miRNAs in regulating placental development and trophoblast function has been extensively demonstrated in the literature. Furthermore, miRNAs are packaged into EVs and released by trophoblast cells to facilitate fetal-maternal communication

and support maternal adaptations during pregnancy. Alterations in their expression have been demonstrated in various pregnancy complications, highlighting their importance for early diagnosis, prognosis, and potential treatment of the diseases. PAS, a pregnancy complication that threatens maternal life, is associated with alterations in miRNAs expression. Although miR-193b-3p expression is changed in placental diseases, the functions of this miRNA in trophoblast cells have not been comprehensively studied. miR-193b-3p was reported to be involved in cell migration, invasion, and proliferation processes that are altered in PAS. Therefore, miR-193b-3p was selected for this study to investigate its role in trophoblast cell function and its possible association with PAS.

2.HYPOTHESIS AND OBJECTIVES

2.1. Hypothesis

miR-193b-3p was reported to be dysregulated in placental diseases. Furthermore, this miRNA regulates different cellular processes in human cells including proliferation, migration, and apoptosis, which are altered in PAS. Therefore, it was hypothesized that miR-193b-3p regulates trophoblast functions that may be associated to PAS pathogenesis.

2.2. Objectives

2.2.1. *General*

This study aimed to investigate the expression and localization of miR-193b-3p human placentas as well as the functions and potential targets of this miRNA in trophoblast cells. In addition, the uptake and influence of trophoblast-derived miR-193b-3p-enriched EVs in immune cell proliferation was examined.

2.2.2. *Specific objectives*

- To examine miR-193b-3p expression and localization in human placentas by miRNA in situ hybridization;
- To evaluate the expression of miR-193b-3p by qPCR in primary trophoblast cells and trophoblastic cell lines JEG-3, HTR-8/SVneo, and BeWo as well as HUVECs and Jurkat T cells;
- To upregulate or downregulate miR-193b-3p expression in trophoblastic cells by transfecting them with miRNA-mimic or -inhibitor, respectively, to investigate their effects on trophoblast cell migration, proliferation, apoptosis, and syncytialization;
- To isolate and characterize miR-193b-3p-enriched EVs derived from trophoblastic JEG-3 cells transfected with miR-193b-3p-mimic;
- To examine the uptake of miR-193b-3p-enriched EVs by flow cytometry and confocal microscopy and their influence on miR-193b-3p levels over a period of 10 days in Jurkat T cells;
- To investigate the effect of miR-193b-3p-enriched EVs on Jurkat T cells proliferation;
- To analyze the effects of miR-193b-3p downregulation on trophoblastic JEG-3 cells proteome;
- To validate changes in gene and protein expression from proteomic data via qPCR and Western blot, respectively, in JEG-3 cells.

3. MATERIAL AND METHODS

3.1. Materials

Table 5. List of equipment

Equipment	Manufacturer
Automated Rotary Microtome	Leica Biosystems, Germany
Axiomager A2 microscope	Carl Zeiss Microscopy, USA
AxiObserver Z.1 + Incubator Zeiss microscope	Carl Zeiss Microscopy, USA
Beckman Coulter CytoFLEX flow cytometer	Brea, USA
BOX Chemi XX6	Syngene, USA
Confocal scanning fluorescence microscope, LSM 880	Carl Zeiss Microscopy, USA
Cryo-TEM	CM 120, Netherlands
CytoBrite hybridizer	SciGene, USA
Eppendorf mastercycler	Eppendorf, Germany
JuLI™ Stage automated cell imaging system	NanoEnTek, Korea
MCF-2360 mini-centrifuge	LMS, Korea
NanoDrop ND-1000 spectrophotometer	Thermo Fisher Scientific, USA
NanoSight version 2.3	NanoSight Ltd., UK
Optima XPN-100 Ultracentrifuge	Beckman coulter, USA
QIAXpert Spectrophotometer	Qiagen, Germany
Realtime-PCR qTower 3G	Analytik Jena, Germany
Slide scanner	NanoZoomer-SQ, Japan
SPECTROstar Omega ELIZA reader	BMG LABTECH, Germany
SpeedVac centrifugation	Thermo Fisher Scientific, USA
Stratagene Mx300P Thermal cycler	Agilent Technologies, Germany
xCELLigence® Real-Time Cell Analyzer	ACEA Biosciences Inc., USA
XL-100 Ultracentrifuge	Beckman coulter, USA

Table 6. List of materials

Name	Cat. #	Manufacturer
0.2 ml Semi-skirted 96-well PCR plate white 25 plates	AB-0900/W	Thermo Fisher Scientific, USA
0.8/0.2 µm pore-size filters Acrodisc® Syringe Filters with Supor® Membrane	4658	Cornwall, UK
6-well cell culture plate	657160	Greiner bio-one, Germany
8-chamber culture slides	354118	Corning, USA
96-well PCR plate	AB0900	Thermo Fisher Scientific, USA
Cell culture flasks red filter screw cap 250 ml	658175	Greiner bio-one, Germany
Cell scraper with 2- position Blade	83.3950	Sarstedt, Germany
Coverslips	10767371	Thermo Fisher Scientific, USA
Cryo-holder	626-DH	Gatan, USA
Dako Pen	H-4000	Vector Laboratories, Germany
E-Plate® 16	2801185	Omni Lifescience, Germany
Falcons 15 ml	188 271	Greiner bio-one, Germany
Filter tips 100-1000 µl	A1000S-MR	Kiesker, Germany
ibidi™ culture inserts	80206	Ibidi GmbH, Germany
Microcentrifuge tube 0.65 ml RNase/DNase free	3206	Costar, USA
Microcon filter-30	MRCF0R030	Millipore, USA
Optically clear flat 8 cap Strips, Natural 120 of 8 Caps	AB-0866	Thermo Fisher Scientific, USA
Pipette filter tips	713117	ClearLine, Germany
Pipettes 5 ml, 10 ml	606 180, 607 180	Greiner bio-one, Germany

PVDF Transfer membrane	88518	Thermo Fisher Scientific, USA
QIAxpert slide-40 (25)	990700	Qiagen, Germany
Superfrost Plus slides	J1800AMN2	Thermo Fisher Scientific, USA
Ultra-Clear centrifuge tubes	344057	Beckman Coulter, USA
Ultra-Clear centrifuge tubes	344059	Beckman Coulter, USA
Ultra-Clear Centrifuge tubes	344060	Beckman Coulter, USA
UltrAuFoil R 2/2, pore size 2 µm, 300 mesh	-	Quantifoil Micro Tools, Germany

Table 7. List of Chemicals

Name	Cat. #	Manufacturer
10x RIPA Buffer	ab156034	Abcam, UK
1x DPBS, sterile	14190-094	Gibco, Germany
20x SSC buffer, ultrapure	15557-044	Gibco, Germany
5% Formaldehyde	02653137	Otto Fischer Chemicals, Germany
7-AAD	51-68981E	BD Pharmingen, USA
Acetonitrile	75-05-8	Sigma-Aldrich, USA
Acid-phenol: Chloroform	AM9720	Ambion, Germany
Albumin fraction V	8076.5	Carl Roth GmbH, Germany
Ammonium bicarbonate	1066-33-7	Sigma-Aldrich, USA
Antibody diluent with background-reducing components, ready-to-use diluent	S302283-2	Dako, Denmark
Benzonase	E1014-25KU	Sigma-Aldrich, USA
Collagenase type IV	C5138-500 mg	Sigma-Aldrich, USA
Cytobond	2020-00-1	SciGene, USA
Dithiothreitol	A39255	Thermo Fisher Scientific, USA
DNase type IV	DN25-100 mg	Sigma-Aldrich, USA
Dynabead (Goat anti-mouse IgG)	110.33	Invitrogen, Germany

Ethanol	9065.2	Carl Roth GmbH, Germany
Fibronectin	F1056-1MG	Sigma-Aldrich, USA
Forskolin	F3917-10MG	Sigma-Aldrich, USA
Formic acid	64-18-6	Sigma-Aldrich, USA
GlycoBlue™ blue coprecipitant	AM9516	Ambion, Germany
Hematoxylin Mayer solution	T865.1	Roth, Germany
Hoechst 33342	875756-97-1	Sigma-Aldrich, USA
Iodoacetamide	144-48-9	Sigma-Aldrich, USA
Isopropanol (2-Propanol)	C2432	Sigma-Aldrich, USA
Laemmli 2× Concentrate	S3401	Sigma-Aldrich, USA
Levamisole hydrochloride	31742	Sigma-Aldrich, USA
Luminata Forte, Western HRP Substrate	WBLUF0100	Sigma-Aldrich, USA
miRNA ISH buffer 2x	90-012	Exiqon, USA
Mounting medium	03989	Sigma-Aldrich, USA
NBT/BCIP ready-to-use tablets	11697471001	Roche Diagnostics, Germany
Nuclear Fast Red	H-3403	Vector Laboratories, Germany
Nuclease-free water	AM9930	Ambion, Germany
Oligofectamine™ Transfection reagent	12252011	Thermo Fisher Scientific, USA
Percoll	17-0891-02	GE Healthcare, USA
Phosphatase-Inhibitor-Mix I	39050.02	Serva, Germany
Protease type IV	P5147-1 g	Sigma-Aldrich, USA
Protease-Inhibitor Mix HP	39106.01	Serva, Germany
RBC lysis buffer	420301	Biozol, Germany
RNA later	AM7021	Ambion, Germany
RNase Zap	AM 9780	Ambion, Germany
SERVA Gel™ TG PRIME™	43263.01	Serva, Germany
SERVA Triple Color Protein Standard II	39257.01	Serva, Germany

Sheep serum	013-000-121	Jackson, UK
Sodium dodecyl sulfate (SDS)	L4509	Sigma-Aldrich, USA
Spectra™ Multicolor High Range Protein Ladder	26625	Thermo Fisher Scientific, USA
TaqMan Universal Master Mix II	4440040	Thermo Fisher Scientific, USA
Tris/HCl	1185-53-1	Sigma-Aldrich, USA
TRIzol	15596018	Invitrogen, Germany
Tween-20	93773	Sigma-Aldrich, USA
Urea	57-13-6	Sigma-Aldrich, USA
Xylene	28973.328	VMR chemicals, Germany

Table 8. List of kits

Name	Cat. #	Manufacturer
ARCHITECT Total β hCG Chemiluminescent Microparticle assay	B7K780	Abbott, Germany
Cell proliferation ELISA, BrdU (colorimetric)	11647229001	Roche Diagnostics, Germany
High-Capacity cDNA Reverse Transcription Kit	4368814	Thermo Fisher Scientific, USA
Micro BCA™ Protein Assay Kit	23235	Thermo Fisher Scientific, USA
PKH26 Red Fluorescent Cell Linker Kit for General Cell Membrane Labeling	PKH26GL-1KT	Sigma-Aldrich, USA
PKH67 Green Fluorescent Cell Linker Kit for General Cell Membrane Labeling	PKH67GL-1KT	Sigma-Aldrich, USA
TaqMan miRNA Reverse Transcription Kit	4366597	Thermo Fisher Scientific, USA
TaqMan® Advanced miRNA cDNA Synthesis Kit	A25576	Thermo Fisher Scientific, USA
VECTASTAIN® Elite ABC kit	PK6102	Vector Laboratories, Germany

Table 9. List of buffers and solutions

Name	Composition
Antibody blocking solution	PBS, 0.1% Tween, 2% Sheep serum, 1% BSA
Antibody diluent solution	PBS, 0.05% Tween, 1% sheep serum, 1% BSA
Proteinase-K buffer	5 ml of 1 M Tris-HCl (pH7.4), 2 ml of 0.5 M EDTA, 0.2 ml of 5 M NaCl
PBS-T (0,1%), pH7.4	1 ml of Tween-20 to 1 L of PBS
KTBT buffer	50 mM Tris-HCl, 150 mM NaCl, 10 mM KCl
AP substrate	NBT-BCIP tablet in Milli-Q water, 0.2 mM Levamisol
Antibody blocking solution and Antibody diluent solution	Mix 6 ml PBS-T and 120 μ l sheep serum to make solution 1. Take 4 ml of solution 1 and add 132 μ l 30% BSA to make blocking solution. Take 2 ml of solution 1 and add 2 ml PBS and 132 μ l 30% BSA to make diluent solution

Table 10. List of probes

Name	miRNA Sequence	RNA Tm	Cat. #
miR-193b-3p	5'AACUGGCCCUCAAAGUCCCGCU	84.3°C	YD00611218
U6 snRNA	CACGAATTTGCGTGTCATCCTT	84°C	YD00699003
Scramble	GTGTAACACGTCTATACGCCCA	87°C	YD00699004

Table 11. List of antibodies

Name	Cat. #	Manufacturer
Rabbit anti-human ALIX	92880S	Cell-signaling, Germany
Annexin V-PE	31490014	Immunotools, Germany
Anti-DIG-AP	11093274910	Roche Diagnostics, GmbH
Mouse Anti-human E-cadherin	610181	BD Transduction Laboratories TM , Switzerland
Anti-human CD45	21270451X2	ImmunoTool, Germany
Anti-human CD82	21270086	ImmunoTool, Germany

Rabbit anti-human TMPPE	PA5-55484	Thermo Fisher Scientific, USA
Anti-mouse cyanine 3	A10521	Thermo Fisher Scientific, USA
Mouse Anti-human cytokeratin-7	M7018	Dako, Denmark
Horse anti-mouse-HRP	7076P2	Cell-signaling, Germany
Mouse anti-human CD63	10628D	Thermo Fisher Scientific, USA
Rabbit anti-human AKT1	9272	Cell-signaling, Germany
Rabbit anti-human CD47	63000	Cell-signaling, Germany
Rabbit anti-human GAPDH	2118S	Cell-signaling, Germany
Secondary antibodies goat anti-rabbit-HRP	4074S	Cell-signaling, Germany
Secondary antibodies horse anti-mouse-HRP	7076	Cell-signaling, Germany

Table 12. List of TaqMan™ miRNA Primers

Gene	Assay ID	Source
ath-miR-159a	478411_mir	Thermo Fisher Scientific, USA
hsa-miR-193b-3p	002367	
hsa-miR-193b-3p	A25576	
hsa-miR-3648	464401_mat	
RNU48	001006	

Table 13. List of miRNA sequence

Type	Assay ID	Source
hsa-miR-193b-inhibitor	MH12383	mirVana® miRNA inhibitor, Ambion
hsa-miR-193b-mimic	MC12383	mirVana® miRNA mimic, Ambion

SCR-inhibitor	4464076	mirVana™ miRNA inhibitor negative control #1; Ambion
SCR-mimic	4464058	mirVana™ miRNA mimic negative control #1; Ambion
Spike in control, ath-miR159a	478411_mir	Thermo Fisher Scientific, USA

Table 14. List of TaqMan™ Gene expression assays

Gene symbol	Gene name	Assay ID	Source
<i>ABI2</i>	abl-interactor 2	Hs01048244_m1	Thermo Fisher Scientific, USA
<i>AKT1</i>	AKT serine/threonine kinase 1	Hs00178289_m1	
<i>ARPC5</i>	Actin related protein 2/3 complex subunit 5	Hs00271722_m1	
<i>CALM1</i>	Calmodulin 1	Hs00300085_s1	
<i>ERVFRD-1</i>	Endogenous retrovirus group FRD member 1	Hs01652148_m1	
<i>ERVW-1</i>	Endogenous retrovirus group W member 1	Hs01926764_u1	
<i>GAPDH</i>	Glyceraldehyde-3-phosphate dehydrogenase	Hs03929097_g1	
<i>K-Ras</i>	K-Ras proto-oncogene, GTPase	Hs00364284_g1	
<i>MCL1</i>	BCL2 family apoptosis regulator	Hs06626047_g1	
<i>NF1</i>	Neurofibromin 1	Hs01035108_m1	
<i>PTK2</i>	Protein tyrosine kinase 2	Hs01056457_m1	
<i>SHMT2</i>	Serine hydroxymethyltransferase 2	Hs01059263_g1	
<i>TMPPE</i>	Transmembrane protein with metallophosphoesterase domain	Hs02760287_s1	
<i>YWHAZ</i>	Tyrosine 3-monooxygenase/tryptophan 5-monooxygenase activation protein zeta	Hs01122445_g1	

Table 15. List of medium and buffers used for cell culture

Medium	Cat. #	Sources
DMEM	41965039	Gibco, Germany
DMSO	D8418-50ML	Sigma-Aldrich, USA
Endothelial Cell Growth Medium	C-22010	PromoCell, Germany
Exosome-depleted FBS	A2720801	Gibco, Germany
Ham's F-12 Nutrient Mix	21765037	Thermo Fisher Scientific, USA
Opti-MEM™ I Reduced Serum Medium	31985047	Thermo Fisher Scientific, USA
PBS DULBECCO'S	14190169	Thermo Fisher Scientific, USA
RPMI 1640 Medium	21875091	Thermo Fisher Scientific, USA
Trypan blue stain 0.4%	T10282	Thermo Fisher Scientific, USA
Trypsin-EDTA (0.05%), phenol red	25300054	Thermo Fisher Scientific, USA

Table 16. List of cell lines

Medium	Description	Growth Properties	Cell type	Medium
JEG-3	This is one of six clonally derived lines with epithelial morphology isolated from the Woods strain of the Erwin-Turner tumor by Kohler and associates (Olivier et al. 2021).	Adherent	Trophoblast	F-12 Nutrient Mix+10% FBS+ 1%P/S
HTR-8/SVneo	It was derived by transfecting the cells that grew out of chorionic villi explants of human first-trimester placenta with the gene encoding for simian virus 40 large T antigen (Msheik et al. 2020).	Adherent	Trophoblast	RPMI 1640 + 10% FBS+ 1% P/S
HUVEC	Primary Human Umbilical Vein Endothelial Cells isolated from the vein of the umbilical cord of single,	Adherent	Endothelial cell	Endothelial Cell Growth Medium + 10% FBS

	pooled or pre-screened donors (Kocherova et al. 2019).			
Jurkat T cells	It was established from the peripheral blood of a 14-year-old boy by Schneider et al., and was originally designated JM (Gioia et al. 2018).	Suspension	T lymphoblast	RPMI 1640 +10% FBS+ 1%P/S
BeWo	These cells were initiated from a malignant gestational choriocarcinoma of the fetal placenta (Heaton et al. 2008).	Adherent	Trophoblast	F-12 Nutrient Mix+10% FBS+1% P/S

FBS: Fetal bovine serum; P/S: penicillin and streptomycin.

Table 17. List of software

Software	Provider
GraphPad Software, Version 6	GraphPad, USA
qPCRsoft, Software for REAL-TIME PCR Thermal Cycle	Analytik Jena, Germany
MxPro Mx3005p®	Agilent Technologies, Germany
ImageJ software 1.49b	Wayne Rasband, USA
ZEN Blue 3.0	Carl Zeiss Microscopy, USA
GeneSys Softwar version 1.5.6	Syngene, USA
CytExpert Acquisition and Analysis Software Version 2.4	Bechman coulter, USA

3.2. Methods

3.2.1. *Human placenta samples collection*

The Placenta Lab obtained approval for studies on human placenta at all stages of pregnancy by the Ethics Committee of the Jena University Hospital (1509-03/05). Eight healthy participants signed an informed consent form before collection and processing of their samples and medical data. Placentas were collected following vaginal delivery (17%) or caesarian section (83%). The samples were collected by the nurses of the Department of Obstetrics and placenta lab members of the Jena University Hospital. Placenta samples were collected from participants of an average of 29 years, 39 weeks of gestation, 3351 grams of birth weight, and 51.2 cm of birth height. Samples with other medical, obstetrical, or surgical complications were not included in the study. The samples were used to perform histological analysis in which placental villi and decidua were not separated. They were harvested immediately after delivery and washed twice with sterile phosphate buffer saline (PBS) to remove blood. They were fixed in formalin for 48 h before embedding in paraffin blocks.

3.2.2. *RNA Extraction*

RNA was isolated from trophoblastic cells and EVs using TRIzol reagent according to the manufacturer's instructions. In summary, 500 μ l of TRIzol was added to each well of the culture plate for cells lysis and the resulting homogenate was collected in 1.5 ml tubes. Next, 100 μ l of chloroform was added, mixed, and incubated for 10 min on ice. The samples were centrifuged for 15 min at 12,000 rpm (4°C). The resulting homogenate was separated into an upper aqueous layer (containing RNA), an interphase, and a red lower organic layer (containing the DNA and proteins). The aqueous phase was transferred into a new tube and 1.5 μ l of Glycoblue was added for RNA staining. After addition of 250 μ l of isopropanol and incubation for 10 min at room temperature (RT), the samples were placed in a centrifuge for 10 min at 4 °C / 12,000 rpm. The supernatant was discarded, and the pellet was washed twice with 500 μ l of 75% ethanol. The supernatant was discarded, the pellet was air dried for 5–10 min, and 25 μ l RNase free water was added. Total RNA concentration was measured using a NanoDrop ND-1000 spectrophotometer. Samples with A260/A280 ratio >1.8 were stored at –80°C.

3.2.3. *cDNA Synthesis, and Quantitative real time PCR (qPCR)*

Expression of miR-193b-3p and miR-3648 was analyzed using individual TaqMan miRNA assays following the manufacturer's protocol. Reverse transcription was performed with miRNA specific stem-loop RT primers and TaqMan miRNA Reverse Transcription Kit. Real-time PCR was performed using specific TaqMan Assays and TaqMan Universal PCR

Master Mix. Fold changes were calculated by the formula $2^{-\Delta\Delta Ct}$ using RNU48 as a reference control.

The expression of *syncytin-1*, *syncytin-2*, *K-Ras*, *MCL1*, *TMPPE*, *ARPC5*, *ABI2*, *AKT1*, *CALM1*, *YWHAZ*, *SHMT2*, *PTK2* and *NFI* was determined by reverse transcription using High-Capacity RNA-to-cDNA™ Kit followed by qPCR. qPCR was performed using the corresponding TaqMan assays and TaqMan Universal PCR Master Mix reagents. Expression of individual mRNA was normalized using the $2^{-\Delta Ct}$ method relative to *GAPDH*.

For analysis of miR-193b-3p in EVs, *Arabidopsis thaliana* miRNA ath-miR159a was added as spike-in control to the samples at a final concentration of 10 pM. TaqMan miRNA assays were used to evaluate miR-193b-3p and ath-miR159a levels. The expression of miR-193b-3p was normalized using the $2^{-\Delta\Delta Ct}$ method relative to ath-miR-159a. All reactions were run in duplicates including no-template controls in 96-well plates on a Realtime-PCR qTower 3G or Stratagene Mx300P.

3.2.4. *miRNA in situ hybridization (miRNA-ISH)*

Determining the localization of miR-193b-3p expression was achieved using the miRCURY LNA™ miRNA ISH Optimization Kit (FFPE) according to the manufacturer's protocol. In brief, placenta samples embedded in paraffin were cut in 6 µm slices. Sections were deposited on SuperFrost®Plus slides and stored at 4 °C for no more than 7 days before the ISH experiments. The sections were melted in 60 °C oven for 30 min followed by deparaffinization for 5 min in xylene and subsequent hydration in ethanol with decreasing concentrations (99.9%, 96%, 70%), followed by washing with PBS.

A hydrophobic barrier was applied around tissue sections using a Dako Pen followed by proteinase-K digestion, which was done by deluting the stock immediately before using it in its buffer to have 200 µl for each slide, which was then incubated for 10 min at 37 °C in a hybridizer. The slides were then placed in a glass jar with PBS to be washed twice for 2 min in PBS. After that, 50 µl of hybridization mixture containing a specific double-labelled digoxigenin (DIG) probe for miR-193b-3p was applied to each tissue section. A sterile coverslip was placed over it, avoiding air bubbles. To prevent the evaporation of the solution, cytoBond was used to seal the coverslips. The slides were placed in the hybridizer for 1 h at 55 °C. Next, cytoBond was removed with tweezers and the coverslips were carefully detached. Stringent washing steps using different concentrations of SSC buffers (once in 5x SSC, twice in 1x SSC and twice in 0.2x SSC) at 55 °C were performed which was ended by final washing in 0.2x SSC and PBS both at RT.

Next, the slides were placed in a humidifying chamber and 200 µl of blocking solution (block non-specific binding of the anti-DIG antibody) was added to each tissue section and incubated for 15 min at RT. Later, the blocking solution was removed and 200 µl of sheep anti-DIG antibody diluted in antibody diluent (1:1000) was added per section and incubated for 1 hour (h) at RT. The slides were then washed 3x3 min with PBS containing 0.1 % Tween-20. Afterwards, a freshly prepared alkaline phosphatase (AP) substrate (ready to use tablet of 4-nitro-blue tetrazolium and 5-bromo-4-chloro-3'-indolylphosphate) was dissolved in water containing 0.2 mM levamisole and applied to the sections for 2 h at 30 °C in the humidifying chamber, protected from light during the reaction. Thereafter, KTBT buffer (2x5 min) was added to each slide to stop the AP reaction. For nuclear counterstaining, Nuclear Fast Red™ was passed through a filter to remove undissolved precipitates and then diluted 1:10 in water of which 250 µl was applied to each section for 1 min. The slides were rinsed with running tap water for 10 min and dehydrated through an increasing gradient of ethanol solutions. To terminate the preparation, the slides were mounted using a mounting medium. The slides were analysed using a light microscope - AxioImager A.2.

3.2.5. *Immune staining of Cytokeratin-7*

For the identification of trophoblast cells, the following procedure was used. Paraffin-embedded tissue was serially sectioned. One cut was served for miRNA-ISH and one for immune staining of cytokeratin-7 performed by using a VECTASTAIN® Elite ABC kit following the manufacturer's protocol. In summary, sections were deparaffinized, rehydrated in graded xylene (2x20 min) and ethanol (2x5 min of 100% ethanol, 2x5 min of 96% ethanol, 2x5 min of 70% ethanol).

The endogenous peroxidase was blocked with 0.9% hydrogen peroxidase for 20 min. Boiling citrate buffer was applied for antigen retrieval followed by washing of slides in 2x2 min PBS. Thereafter, sections were incubated with blocking buffer (200 µl blocking serum for 20 min) and cytokeratin-7 (1:300) primary antibody was applied (200 µl overnight incubation at 4 °C). After washing with PBS, the samples were incubated with a biotinylated secondary antibody (200 µl for 30 min at RT) for subsequent exposure to the avidin-peroxidase complex and ABC substrate (200 µl for 30 min at RT). Mayer's hematoxylin was used for counterstaining followed by washing with increasing alcohol concentration (2x1 min of 70% ethanol, 2x1 min of 96% ethanol, 2x1 min of 100% ethanol) followed by mounting the slides and analysis using a light microscope type AxioImager A.2. The serial cuts from miRNA-ISH and cytokeratin-7 immune staining were digitally processed using the slide scanner.

3.2.6. *Isolation of primary trophoblast cells (PTC)*

PTC were isolated from term placentas as documented before (Murrieta-Coxca et al. 2020). In summary, placental villi were cut into small pieces followed by washing in sterile PBS with 1% penicillin/streptomycin. In three cycles of 12 min at 37 °C, they were subjected to a digestive enzymes solution containing 0.1 mg/ml DNase type IV, 0.5 mg/ml collagenase type IV, and 1 mg/ml protease type IV in Dulbecco's Modified Eagle's Medium (DMEM) serum-free medium. An equal amount of DMEM supplemented with 10% FBS and 1% penicillin/streptomycin was added to stop the enzymatic activity. The cell suspension was filtered through 100 µm cell strainers, centrifuged for 20 min at 700 x g and resuspended in DMEM supplemented with 10% FBS and 1% penicillin/streptomycin. A density gradient was applied to isolated cells using Percoll™. After centrifugation step at 750 x g for 30 min without brake, the cell layer between 25% and 60% Percoll™ was collected followed by washing it twice with supplemented DMEM medium and spinning at 700 x g for 5 min. RBC lysis buffer was used to get rid of contaminating erythrocytes. For depletion of leukocytes and fibroblasts, Dynabeads® coated with anti-CD45 and anti-CD82 antibodies were used. The suspension containing unbound trophoblast cells was spun at 350 x g for 5 min. The trophoblast pellet was resuspended and cultured in supplemented DMEM using a 6-well plate at 37 °C in 5% CO₂ for further experiments.

3.2.7. *Cell culture*

BeWo and JEG-3 cells were cultured in Ham's F-12 Nutrient medium. Jurkat T cells were cultured in RPMI 1640 medium. All culture media were supplemented with 10% FBS and 1% penicillin/streptomycin antibiotic solution. Cell cultures were performed at 1×10^6 cells in a 75 cm² flask and maintained under standard culture conditions (37 °C, 5% CO₂ and humid atmosphere).

3.2.8. *Western Blot*

JEG-3 cell pellets were lysed using RIPA lysis buffer containing protease and phosphatase inhibitors. To analyze EVs markers, EVs fractions (20 µg) were mixed with non-reducing Laemmli loading buffer (375 mM Tris-HCl, 9% SDS, 50% glycerol, and 0.03% bromophenol blue). Protein concentration was measured using Pierce BCA™ Protein-Assay. Protein extracts were loaded on a 12% precast gel SERVA Gel™ and transferred to a nitrocellulose membrane. Non-specific binding was blocked by incubation with TBST containing 5% (w/v) non-fat dried milk for 1 h at RT. Membranes were immunoblotted with specific primary antibodies overnight at 4 °C. The following primary antibodies were used at a 1:500 dilution: rabbit anti-human

TMPPE, mouse anti-human CD63, rabbit anti-human GAPDH, rabbit anti-human ALIX and rabbit anti-human CD47. Rabbit anti-human AKT1 was used at a 1:1000 dilution. The following secondary antibodies were used at 1:5000 dilution: anti-rabbit-HRP or anti-mouse-HRP. Blots were developed using enhanced chemiluminescence detection kit. The analysis of densitometric measurements of single protein was done using Image J and the protein expression was normalized to GAPDH.

EVs from ex vivo human placenta perfusate were used as a positive control and collected by colleagues, Dr Jinlu Ji and Dr Rodolfo Favaro, as described in their previous publication (Zabel et al. 2021).

3.2.9. *Cell transfection*

JEG-3 and BeWo cells were cultured in 6-well plates and allowed to attach overnight to reach 40 – 60% confluence. To overexpress miR-193b-3p, cells were transfected with miR-193b-3p-mimic. To reduce miR-193b-3p expression, cells were transfected with miR-193b-3p-inhibitor. To estimate the transfection specificity with miR-193b-3p-mimic or –inhibitor, cells were transfected with non-genomic scrambled sequences, labelled as SCR-mimic and SCR–inhibitor, respectively. All mimics were used at a final concentration of 20 nM, the inhibitors at 50 nM. Transfection was performed by using Oligofectamine™ transfection reagent according to the manufacturer's recommendations. In brief, a total of 200 µl of the RNA solution was mixed with Oligofectamine™ and OPTI-MEM™ and left for a 20 min incubation at RT. The cells were washed once with 1 ml OPTI-MEM™ and 800 µl of OPTI-MEM™ was added to each well followed by the addition of 200 µl sequence mix. Non-transfected cells (NTC) were also used as a mock control in which they receive a mixture of OPTI-MEM™ and Oligofectamine™. After a 4 h incubation with mimics and 24 h after incubation with the inhibitors, medium containing 30% exosome-depleted FBS (ED-FBS) was added to stop the transfection. The cells were left for overnight incubation under standard culture condition. To minimize the toxicity, the medium was replaced the next day with 4 ml of medium containing 10% FBS exosome-depleted.

3.2.10. *BeWo syncytialization*

BeWo cells were used for 3 different types of experiments: to investigate if the expression of miR-193b-3p is changed after forskolin-induced syncytialization, whether it influences the expression of the syncytialization markers, and to assess if it affects the ability of BeWo cells to form syncytium.

To monitor miR-193b-3p expression, 400,000 BeWo cells were cultured in 6-well plates until they reached 50-60% confluency, followed by treatment with forskolin (final concentration 100 μ M) or DMSO as solvent control for 48 h and 72 h. At the end of each time point, the supernatants were collected for hormone analysis which was performed at the Department of Clinical Chemistry at the Jena University Hospital. Total β hCG was quantified by an ARCHITECT Total β hCG Chemiluminescent Microparticle assay. β hCG concentration was normalized to that in DMSO treated NTC supernatants. The remaining BeWo cells have been treated with TRIzol for RNA isolation to assess the expression of miR-193b-3p along with the expression of the syncytialization markers (*syncytin-1*, *syncytin-2* and miR-3648).

For assessing the expression of syncytialization markers, BeWo cells were transfected as described before. Then the cells were treated with forskolin, cells and supernatants were collected as described before. The cells were collected for RNA isolation followed by qPCR to check the transfection efficiency, *syncytin-1* and *syncytin-2* expression after the transfection with miR-193b-3p-mimic and miR-193b-3p-inhibitor. The supernatants were collected to measure β hCG production after the transfection.

To examine the cell fusion rate, a protocol for immunofluorescence staining after transfection needed to be established. The following parameters were first tested: cell number to be seeded (10,000 or 20,000 or 30,000), the dilution factor of the E-cadherin antibody (1:25 or 1:50 or 1:100) and the appropriate fixative (formalin or acetone). After optimization, the following conditions were adhered to. A total of 10,000 BeWo cells were seeded in 8-chamber culture slides. Thereafter, they were transfected, followed by forskolin treatment as described above. Acetone was used to fix the cells followed by treatment of 1% PBS/BSA for 30 min to block unspecific binding. Mouse anti-human E-cadherin antibody (1:200) was applied for 60 min followed by using anti-mouse cyanine 3 at a 1:1000 dilution for 60 min at 37 °C in a humid chamber. Cell nuclei were counterstained with Hoechst 33342. The images were taken using an AxioObserver Z.1 + Incubator Zeiss microscope. Around fifteen images were taken per each condition. The nuclei in the syncytium were counted and divided by the total number of nuclei in the image field to yield the fusion index.

3.2.11. Wound Healing assay (cell migration)

For the migration assay, ibidi™ culture inserts were used. These inserts consist of two chambers separated by a 0.5 mm divider, each chamber has a growth area of 0.22 cm². After setting inserts into the wells of a 24-well plate by using sterile tweezers, 70,000 cells from the different transfection conditions were transferred to each chamber and were cultured overnight

to allow them to adhere. After insert removal, the cells migrate and progressively close the gap. This process was monitored by live-cell microscopy for 24 h using a JuLI™ Stage automated cell imaging system.

3.2.12. Cell proliferation

Proliferation of JEG-3 and Jurkat T cells was assessed using a xCELLigence® Real-Time Cell Analyzer (RTCA). E-Plate®16 were used for seeding of 10,000 JEG-3 cells for each transfection condition. For the culturing and capturing of Jurkat T cells, 40 µl of 170 µg/ml fibronectin was used to coat the wells in order to induce cell attachment. This concentration was chosen based on the manufacturer's recommendation and previously published research (Martinez-Serra et al. 2014). To assess the effect of fibronectin on cell attachment, two tests were conducted. Both tests started after the addition of fibronectin to each well of an E-Plate and then leaving the plate for 2 h at RT. For the first test, Jurkat T cells were added and left in cell culture incubator. After 24 h, cells in the presence (F+) or absence (F-) of fibronectin were investigated under the microscope. The cell culture medium was removed by the cell culture pump and the cells were observed again under the microscope. For the second test: the cells with (F+) and (F-) coating were seeded in E-Plate and their corresponding proliferation cell index (CI) was measured. CI represent the changes in electrical impedance which results from the increase of Jurkat T cell numbers.

To determine the appropriate cells number of Jurkat T cells to be seeded, different amounts of Jurkat T cells were initially seeded (20,000, 40,000, 60,000, 80,000, 100,000 and 120,000 cells/well) in (F+) or (F-). A cell count of 60,000 cells was subsequently used in our experiments. Fibronectin was added to each well of E-Plate and left for 2 h at RT under the cell culture hood. Each well was then washed 3 times with the RPMI medium. Background was measured before cell seeding by putting 100 µl medium. Then, 60,000 cells/well (of each transfection condition) were seeded and the measurements were started.

For investigating the effect of JEG-3 EVs (collected after miR-193b-3p transfection) on Jurkat T cell proliferation, wildtype cells were seeded as mentioned above. After 24 h, EVs from transfected JEG-3 cells (IEV_{miR-193b-3p}, sEV_{miR-193b-3p}) were added. As a control, EVs collected from SCR-mimic transfected JEG-3 cells (IEV_{SCR-mimic}, sEV_{SCR-mimic}) and EVs from NTC JEG-3 cells (IEV_{NTC}, sEV_{NTC}) were used.

To independently assess the results obtained in Jurkat T cells proliferation using xCELLigence system, an established reference method in the placenta lab was employed. This method is the colourimetric BrdU-incorporation ELISA and was used according to the

manufacturer's instructions. In brief, Jurkat T cells (5000 cells/well) were seeded in 96-well plates (transfected and wildtype) in 200 μ L medium. The medium contained 10% FBS (transfected cells) or 10% ED-FBS (wildtype). Wild-type Jurkat T cells were treated with IEVs (125 ng) or sEVs (125 ng) fractions of each transfection condition as described before. BrdU (10 μ l/well) was added and left for 2 h. The labeling solution was removed and the cells were dried for 15 minutes. The fixation step was then applied by the addition of 200 μ l/well FixDenat to each well and incubated for 30 min at +15 to +25 $^{\circ}$ C. The fixation solution was removed followed by incubation with 100 μ l/well anti-BrdU-POD working solution for 90 min at +15 to +25 $^{\circ}$ C. The antibody solution was removed followed by three times washing steps. A total of 100 μ l/well substrate solution was added and incubated at +15 to +25 $^{\circ}$ C until a sufficient color development for photometric detection is reached. The absorbance at 370 nm was measured using an ELISA reader.

3.2.13. *Apoptosis assay*

Transfected JEG-3 cells were harvested (after 72 h of tranfection) and washed twice with cold PBS. The supernatant was discarded and 200,000 cells were washed with 1x Binding Buffer. Then, 100 μ l of 1x binding buffer was added, followed by 15 min incubation with 5 μ l of Annexin V and 5 μ l of 7-AAD. A total of 400 μ l of 1x binding buffer was added to each tube which were subsequently mixed before the measurements at a Beckman Coulter CytoFLEX flow cytometer. Unstained cells and single stained (Annexin V or 7-AAD) cells were used as controls. The percentage of early and late apoptotic cells was evaluated after collection of 10,000 cell counting events. Annexin V-positive/7-AAD-negative cells were considered as early apoptotic cells and Annexin V-positive/7-AAD-positive cells were considered as late apoptotic cells.

3.2.14. *EVs isolation*

The isolation of enriched-EVs fractions (IEVs and sEVs) was accomplished using sequential centrifugation steps as described by (Zabel et al. 2021) and illustrated in **Fig. 7**. A total of 5 ml of the conditioned medium was collected 24 h after transfection and centrifuged for 10 min at 380 x g to get rid of cellular debris. The supernatant was transferred to a new tube (Ultra Clear Centrifuge Tubes) and centrifuged for 10 min at 10,000 x g to exclude the apoptotic bodies. The supernatant was transferred to a new tube, and centrifuged at 18,890 x g for 30 min. These pellets were washed in PBS, centrifuged again at 18,890 x g for 30 min, and resuspended in 100 μ l of PBS to obtain a IEVs-enriched pellet. Meanwhile, the supernatant was passed through 0.8/0.2 μ m pore-size filter and centrifuged at 100,000 x g for 70 min. The supernatant

was discarded, the pellet was washed with PBS and centrifuged again at 100,000 x g for 70 min to obtain sEVs. Pellets were resuspended in 100 µl of PBS. Both pellets (IEVs and sEVs) were stored at -80 °C until further analysis.

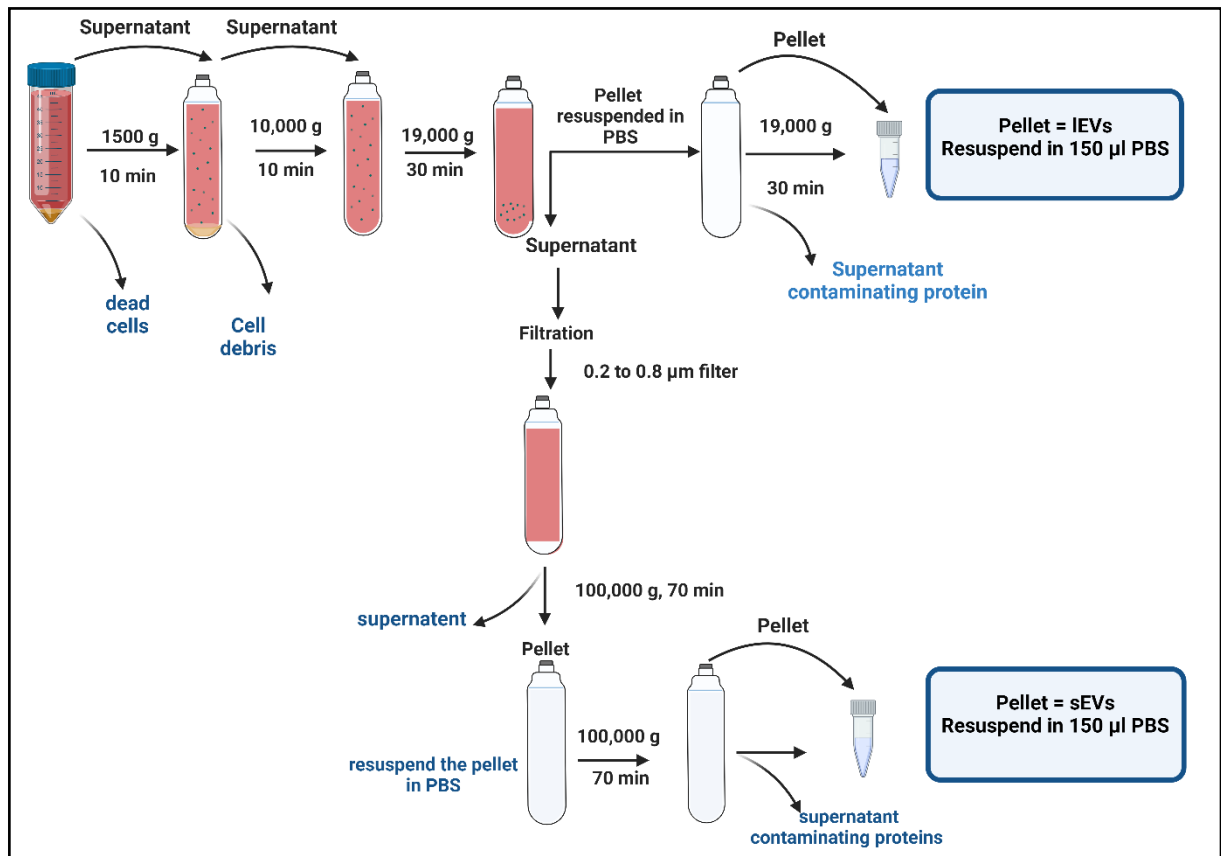


Figure 7. Diagram depicting the enrichment of small extracellular vesicles (sEVs) and large extracellular vesicles (IEVs) by serial ultracentrifugation (Created with Biorender.com).

3.2.15. Nanoparticle Tracking Analysis

To determine the size of EVs and their concentration in suspensions, NTA on a NanoSight version 2.3 was used as described before (Ospina-Prieto et al. 2016). The NTA instrument composed of a laser beam that illuminates the particles in suspension, a microscope connected to a camera, a hydraulic pump and a measuring chamber (Szatanek et al. 2017). The light scattered by each particle is gathered by the microscope into the camera, which differentiates them individually, being tracked and recorded over a certain period. Based on their Brownian motion, the software calculates the size and number of particles (Gardiner et al. 2013). The isolated EVs were diluted in PBS over a range of concentrations to obtain 10 to 100 particles per image before analysis with the NTA system. Then, the samples were offered to the sample chamber at RT and the chamber was washed with PBS between samples measurements. Twenty

seconds of videos were processed and analyzed using optimized instrument settings. Values were expressed as means of 4 isolated populations.

3.2.16. Transmission Electron Microscopy

The imaging of EVs was done at the TEM facility of the Jena University Hospital by Mr. Frank Steiniger who followed the protocol below.

A small droplet (5 μ l) of EVs was put on a holey gold film (UltrAuFoil R 2/2, pore size 2 μ m, 300 mesh). Excess liquid was blotted between two strips of filter paper. Subsequently, the sample was rapidly plunged into liquid ethane (cooled to about -180 °C with liquid nitrogen) in a Cryobox. The frozen specimen was transferred with a cryo-holder into a precooled Cryo-TEM operated at 120 kV and viewed under low dose conditions. Cryo-TEM images were recorded with a 2 K CMOS Camera.

3.2.17. JEG-3 cell-derived EVs uptake

IEVs and sEVs were resuspended in 500 μ l PBS and labelled with 2 μ M PKH67 and PKH26 dye, respectively, for 5 min. For the PKH67-PBS and PKH26-PBS control, an equivalent volume of pure PBS was used as starting material. The reaction was stopped by adding an equal volume of 1% ED-FBS in PBS. Pellets containing labelled EVs were washed twice in PBS by centrifugation at 100,000 x g for 70 min. A total of 200,000 Jurkat T cells were seeded into 24-well plates and incubated with 5 μ g/ml PKH67-labelled IEVs and PKH26-labelled sEVs for 24 h in 1 ml RPMI medium containing ED-FBS. After washing, fluorescence in recipient cells was detected at a CytoFLEX flow cytometer and analyzed using the manufacturer's software.

For confocal microscopy, 200,000 Jurkat T cells were seeded in 48-well plates in 500 μ l ED-FBS medium and treated with 5 μ g PKH67 stained IEVs and PKH26 stained sEVs or an equivalent volume of PKH67-PBS and PKH26-PBS. After 24 h, the cells were washed 3 times with cooled PBS and fixed with 2.5% formaldehyde for 10 min at RT; 1:2000 Hoechst 33342 staining was used to visualize the nuclei. Images were acquired and recorded with a confocal scanning fluorescence microscope with Airyscan using a Plan-Apochromat 63 \times /1.4 oil DIC M27 objective and analyzed with the ZenBlue software. The microscope was located at the Institute of Human Genetics in the Jena University Hospital, and operated by Dr. Federico Ribaldo.

In order to determine the kinetics of miR-193b-3p levels in Jurkat T cells upon the uptake of miR-193b-3p-enriched EVs, the following procedure was followed. A total of 60,000 cells

were seeded in 24-well plate, 500 μ l of RPMI medium supplemented with 10% of ED-FBS were added to the cells. A total of 125 ng modified JEG-3 EVs (IEV_{miR-193b-3p} and sEV_{miR-193b-3p}), EVs collected after SCR-mimic transfection (IEV_{SCR-mimic} and sEV_{SCR-mimic}) and EVs collected from NTC cells (IEV_{NTC} and sEV_{NTC}) were added to the cells. Ten of 24-well plates were seeded in the same way for each experiment so that the cells were collected in 1.5 ml tubes at the end of each day until the tenth day. The tubes were then centrifuged (1500 rpm for 5 min) to remove the medium followed by TRIzol based RNA isolation. Reverse transcription and qPCR were performed as described before to examine the miR-193b-3p expression under each condition.

3.2.18. LC-MS/MS Proteomic analysis

Cells preparation

The cells were transfected as described before in section 3.2.9. The transient transfection was repeated independantly 5 times. After 48 h of tranfection, cells were washed with PBS and each sample was collected using 100 μ l of 1% SDS and heated for 5 min at 95 °C. The samples were treated with 5 μ l of Benzonase for 1 h at 37 °C followed by addition of 5.25 μ l of 1M Dithiothreitol (DTT) and boiling for 10 min at 95 °C. The samples are then stored at – 20 °C until the next step which was done with the assistance of Dr Andre Schmidt, Placenta Lab, Jena University Hospital, Jena, Germany.

FASP sample preparation

The samples collected after 5 times tranfection were processed all together for protien digestion and mass spectormetry measurements. A total of 110.25 μ l of each sample were thawed followed by mixing with 400 μ l urea buffer (UA: 8 M urea in 0.1 M Tris/HCl pH 8.5) then transferred to a 30 kDa Microcon filter unit. The samples were centrifuged and washed once with 200 μ l urea solution at 14 000 x g for 40 min and the flow-through was discarded. A total of 100 μ l alkylation solution (0.1 M iodoacetamide in urea buffer) was added to the samples and left for 10 min in dark followed by centrifugation at 14 000 x g for 20 min. The alkylation solution and SDS was removed by centrifugation followed by 3 washing steps (14 000 x g for 40 min) with 200 μ l of 8 M urea buffer. Subsequently, the samples were washed twice with 200 μ l of 50 mM ammonium bicarbonate buffer. The samples were then digested by addition of 30-40 μ l trypsin in ammonium bicarbonate buffer (trypsin:protein ratio roughly 1:50). The digestion was done for 16 h at 37 °C and the peptides were eluted by centrifugation. The peptides were dried by vacuum centrifugation, and reconstituted by adding 20 μ l of 0.3% formic acid/H₂O. Peptide concentrations (A280) were measured with a Nanodrop at A280 and

adjusted to 0.38 - 1.0 mg/ml by adding 0.3% formic acid/H₂O. The samples were frozen at – 20 °C until further use. Subsequently, the samples were analyzed by mass spectrometry by Dr. Mario Müller of ZIK Septomics, University Hospital Jena. A total of 2 µg of peptides generated by tryptic digestion were analyzed in each run with a Dionex Ultimate3000 UHPLC coupled to an Orbitrap Fusion in data dependent acquisition (DDA) mode. Peptides were loaded onto a trap column and separated using a 50 cm analytical C18 column (Easy-Spray PepMap 2 µm C18). Full mass spectrometric scans were acquired at a resolution of 120,000 (full width at half maximum) in the Orbitrap (m/z range 350-1570, quadrupole isolation) for 150 min using a nonlinear gradient of 2% to 95% acetonitrile/0.1% formic acid. MS1 ions were fragmented using higher energy collisional dissociation (HCD) and 20 fragment spectra were recorded in the ion trap in rapid mode per cycle.

The following conditions and parameters were used: spray voltage 2.0 kV; heated capillary at 275 °C; S-lenses: 60%; maximum automatic gain control (AGC) value 4×10^5 for MS1, or a maximum ion accumulation time of 50 ms; maximum AGC value 1×10^4 for MS2 or maximum ion accumulation time of 35 ms; dynamic exclusion time window of 30 seconds with maximum mass window 10 ppm.

All raw data were searched against the human reference proteome (UniProt database, version May 2016) using MaxQuant software (version 1.6.17.0) run with default or standard parameters. False discovery rates were set to 0.01 on PSM and protein level. Statistical analysis was done using Perseus software. Label-free quantitative values of identified proteins were uploaded and “revers”, “only-by-site” and “possible contamination” identifications removed. Missing values were imputed using default parameters (width 0.3 and down shift 1.8). To compare the results of different groups, Student's T test was performed and p-values were adjusted according to Benjamini Hochberg procedure. The test was performed between the measurements of NTC and miR-193b-3p-inhibitor transfected cells. Significant expression changes were defined as fold change ≥ 2 and $p\text{-value}_{B.H.adj.} \leq 0.05$. The analysis of LC-MS/MS Proteomic data, and the processing of (**Fig. 20**) was done by Dr. Müller. The information in (**Table 18**) were provided by him as well.

3.2.19. Bioinformatic Prediction of miR-193b-3p Target Gene

Putative miR-193b-3p targets were selected from the bioinformatics platforms miRNA (<https://www.microrna.org>), miRtarBase (<https://mirtarbase.cuhk.edu.cn>) and miRPathDB v.2.0 (<https://mpd.bioinf.uni-sb.de/mirna.html>). Targets were confirmed by qPCR and Western blotting as described above.

3.2.20. Statistical Analysis and figures

Experiments were repeated independently at least 3 times. After assessing normal distribution using the normality and lognormality tests, the appropriate test was used. The data are presented as mean \pm SEM (standard error of the mean). Where appropriate and stated in the figure legends statistical comparisons were performed using a One or two tailed student t-test, One-way or Two-way ANOVA with Bonferroni Multiple Comparisons. GraphPad Prism software version 6 was used and a p-value <0.05 was considered significant. Figures 2, 4, 5, 6, 7, and 22 were created with Biorender.Com.

4. RESULTS

4.1. miR-193b-3p localization and expression in human placenta

To localize the expression of miR-193b-3p and cytokeratine-7 (trophoblast marker) in human placenta (n= 8), sequential cutting was performed in the paraffin blocks of each sample. A tissue cut served for miRNA-ISH and the subsequent for cytokeratine-7 detection via IHC. In the placental villi, miR-193b-3p was found to be mainly present in STBs and endothelial cells (**Fig. 8A-B**). In the decidual layer, miR-193b-3p was expressed by different cells. Cytokeratine-7 staining showed that these miR-193b-3p positive cells were iEVTs, characterized by single or grouped cytokeratin-7 positive cells in the decidua, and enEVTs, cytokeratin-7 positive trophoblast cells that substitute endothelial cells in the lumen of spiral arteries. Some of cytokeratine-7 negative cells expressing miR-193b-3p were present in the decidual layer (**Fig. 9A-B**). For control of background staining, a probe recognizing a non-genomic SCR sequence was employed and a negligible staining was observed (**Fig. 8C**).

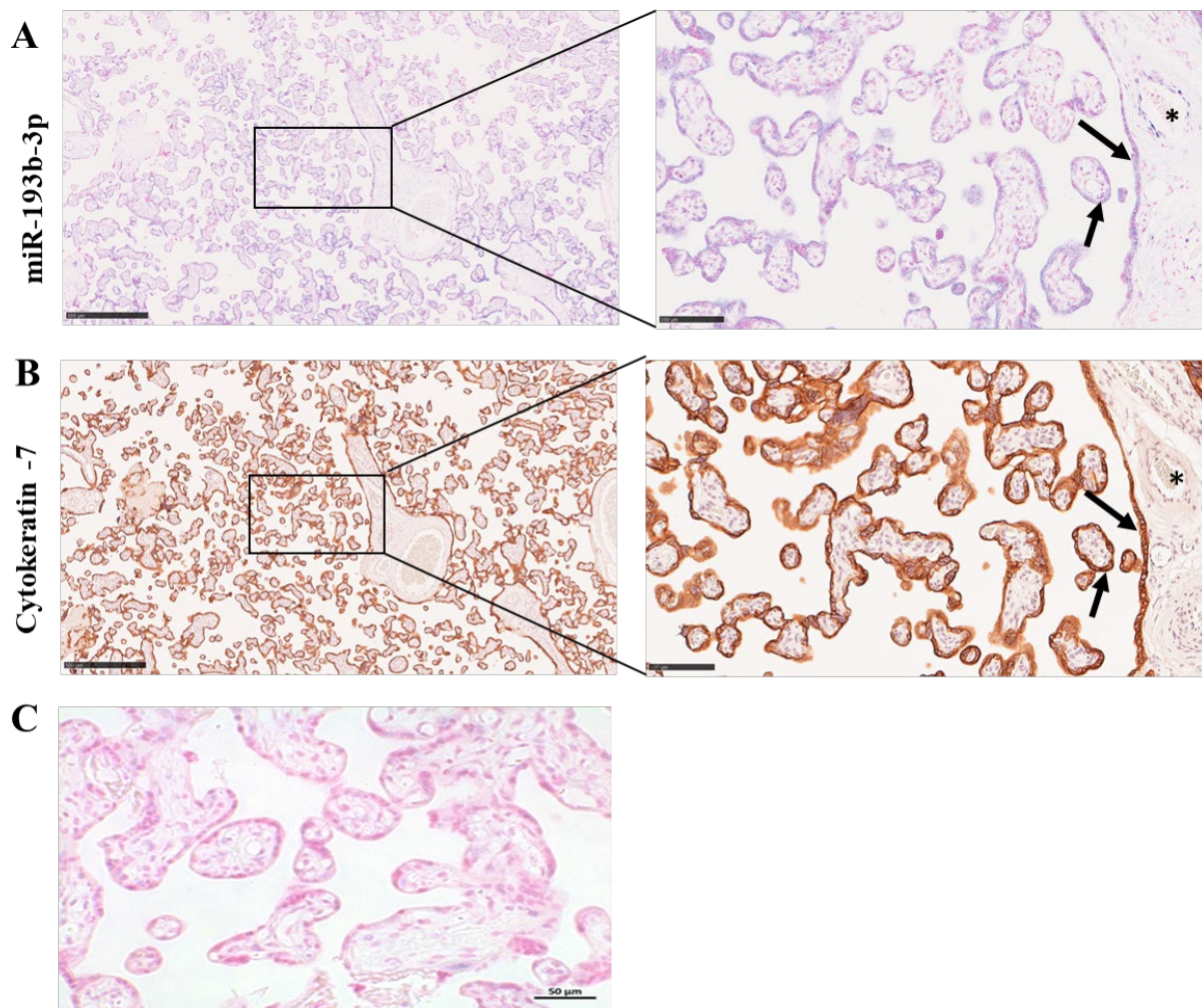


Figure 8. miR-193b-3p expression and localization in the villous tree of human placentas. (A) miR-193b-3p localization using miRNA-ISH in human placenta tissue (n=8) (scale bar: 500 μ m). A representative image of each stain was chosen, and a higher magnification is shown to the right of the corresponding image (scale bar: 100 μ m). (B) Immunohistochemistry against cytokeratine-7 (brown) and a higher magnification is shown to the right of the corresponding images. The miR-193b-3p positive staining (blue) is observed in syncytiotrophoblast cells (arrows), which are positive to cytokeratin-7, and endothelial cells of villous blood vessels (asterisks). (C) Negative control staining with scramble sequence probe (SCR).

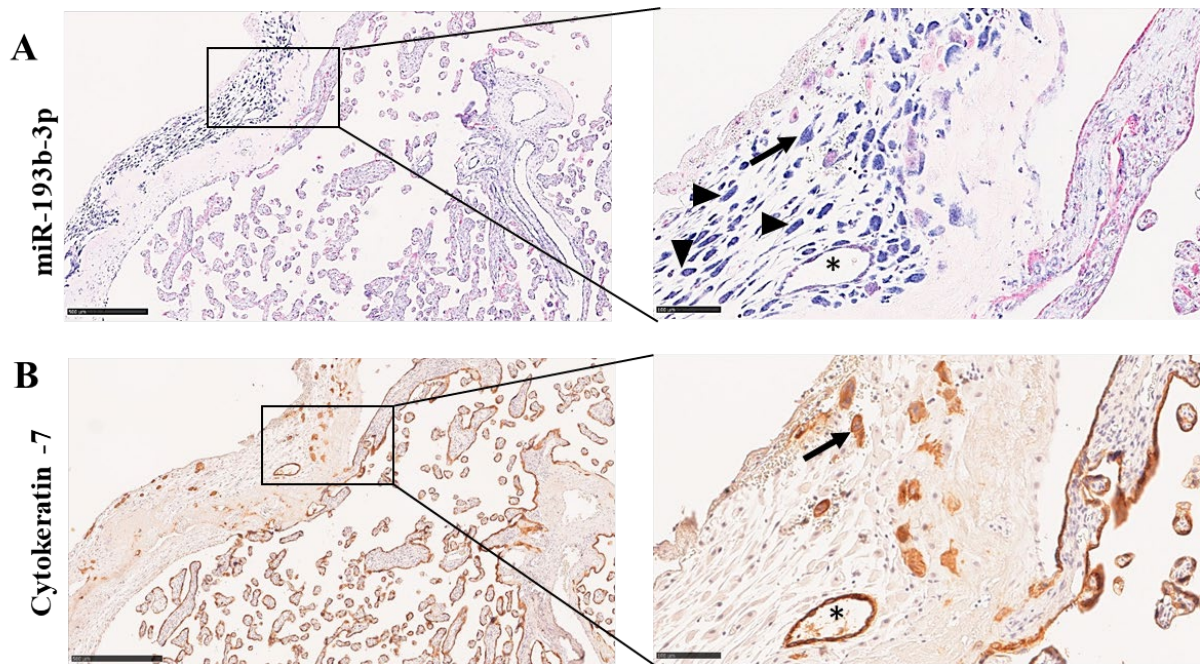


Figure 9. miR-193b-3p localization in the decidual layer human placenta. (A) miR-193b-3p localization using miRNA-ISH (n=8) (scale bar: 500 μ m) and a higher magnification is shown to right of the corresponding image (scale bar: 100 μ m). (B) Immunohistochemistry against cytokeratine-7 (brown) and a higher magnification is shown to right of the corresponding image. The miR-193b-3p staining (blue) is observed in interstitial trophoblast cells (arrows) and endovascular trophoblast cells (asterisks). miRNA-193b-3p is expressed by interstitial trophoblast cells (iEVTs; arrows), characterized by single or grouped cytokeratin-7 positive cells in the decidual, and endovascular trophoblast cells (enEVTs), which are cytokeratin-7 positive cells within the lumen of spiral arteries (asterisks). miR-193b-3p-positive and cytokeratine-7 negative cells (arrowheads) are also present.

4.2. miR-193b-3p expression in cells

The basal expression of miR-193b-3p was evaluated in JEG-3, HTR-8/SVneo, BeWo, and Jurkat T cells. PTC and HUVECs served as references of miR-193b-3p expression in primary human cells. The highest expression of miR-193b-3p was detected in JEG-3 cells followed by PTC and BeWo, whereas similar levels were observed between HUVEC, HTR-8/SVneo, and Jurkat T cells (**Fig. 10A**).

miR-193b-3p-mimic transfected JEG-3 cells had a 205-fold higher miR-193b-3p expression in comparison to NTC and SCR-mimic transfected cells, whereas miR-193b-3p-inhibitor transfected cells had a 12-fold reduction on miR-193b-3p expression (Fig. 10B-C). The transfection of BeWo cells with miR-193b-3p-mimic increased miR-193b-3p expression by 86-fold, whereas the transfection with miR-193b-3p-inhibitor decreased its expression to one-fifth (Fig. 10B-C). Transfected cells were subjected to functional assays to investigate the effects of miR-193b-3p on trophoblast syncytialization (BeWo cells), migration, proliferation, and apoptosis (JEG-3 cells).

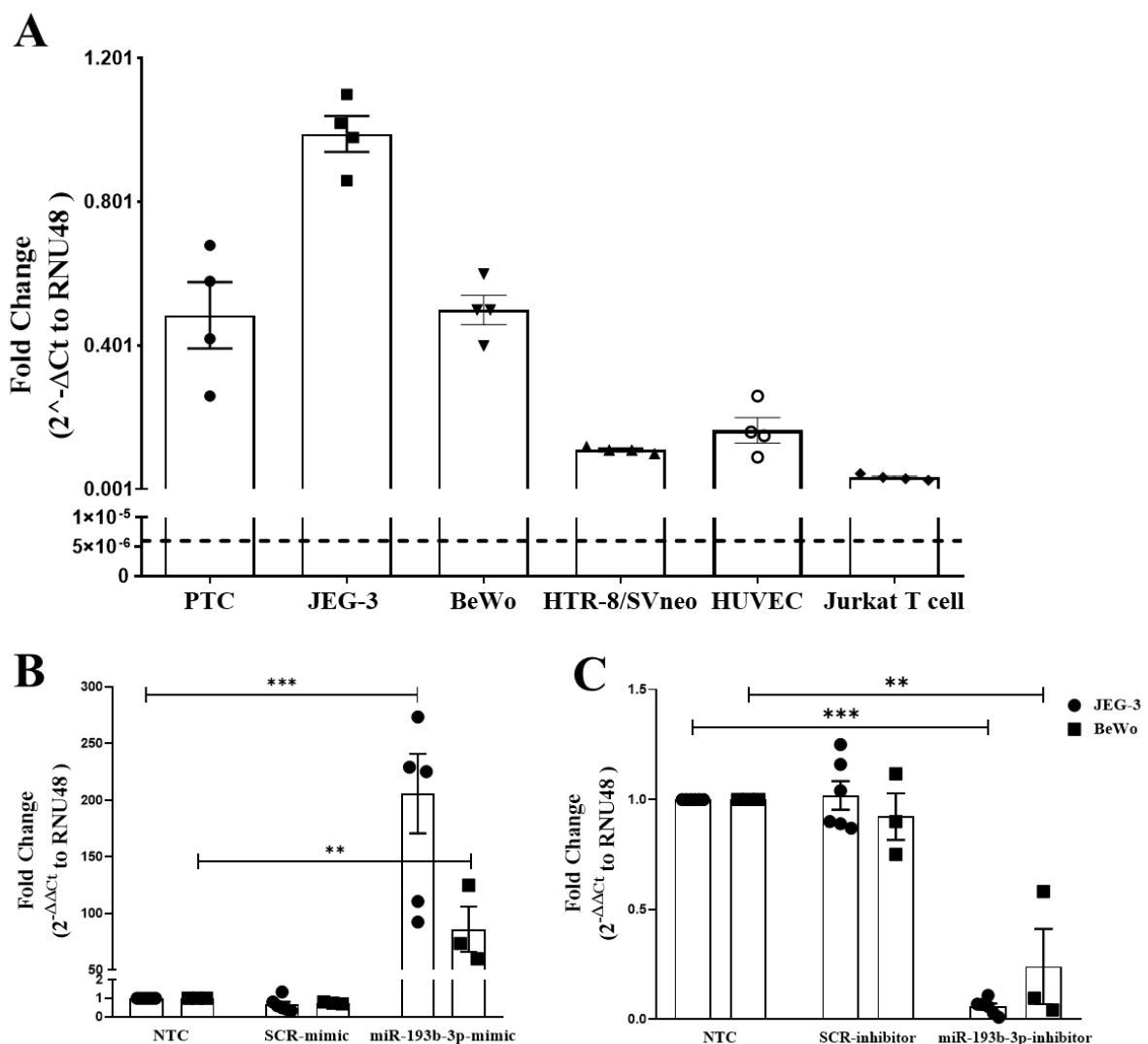


Figure 10. miR-193b-3p expression in cells. (A) The expression of miR-193b-3p in primary trophoblast cells (PTC), JEG-3, HTR-8/SVneo, BeWo, Jurkat T cells, and HUVECs. The dot line corresponds to Ct=40. miR-193b-3p expression was determined by qPCR in JEG-3 and BeWo cells transfected with mimic (B) or inhibitor sequences (C) and normalized to housekeeper RNU48. Bars represent means \pm SEM, $n \geq 3$. One-way ANOVA followed by Bonferroni multiple comparison test. ** $p < 0.01$, *** $p < 0.001$. HUVEC: primary Human Umbilical Vein Endothelial Cells; NTC: non-transfected cells; PTC: primary trophoblast cells.

4.3. The role of miR-193b-3p in BeWo cells syncytialization

The results from miRNA-ISH showed that miR-193b-3p is expressed by STBs. Therefore, the influence of this miRNA in syncytialization (cell fusion), a critical process for the formation of STBs, was investigated. To this end, BeWo trophoblast cells treated with forskolin for 48 h and 72 h were used as a model. Since both time points were equivalent, only results from 48 h experiments are shown. *Syncytin-1* and *syncytin-2* mRNA expression as well as β hCG levels in the supernatant, which are markers of syncytialization, were found to be upregulated by forskolin (**Fig. 11A-B**). Analysis of cell fusion with the aid of E-cadherin immunofluorescence confirmed the induction of the syncytialization process (presented below). Although miR-3648, another marker of syncytialization (Dubey et al. 2018), was upregulated by forskolin, miR-193b-3p expression did not change (**Fig. 11C**).

Next, to examine whether miR-193b-3p can alter trophoblast syncytialization, BeWo cells were transfected with miR-193b-3p-mimic or inhibitor followed by forskolin treatment. *Syncytin-1* and *syncytin-2* expression and β hCG production were decreased by the miR-193b-3p-mimic (**Fig. 12A-C**) and significantly elevated by miR-193b-3p-inhibitor (**Fig. 12D-F**). Quantification of cell fusion showed that control DMSO-treated BeWo cells had a spontaneous fusion of 3%. Forskolin treatment elevated the cell fusion rate to 25%. Transfection of cells with miR-193b-3p-mimic followed by forskolin treatment reduced cell fusion to 12%, whereas miR-193b-3p-inhibitor transfected BeWo cells elevated the fusion rate to 35% (**Fig. 13A-B**).

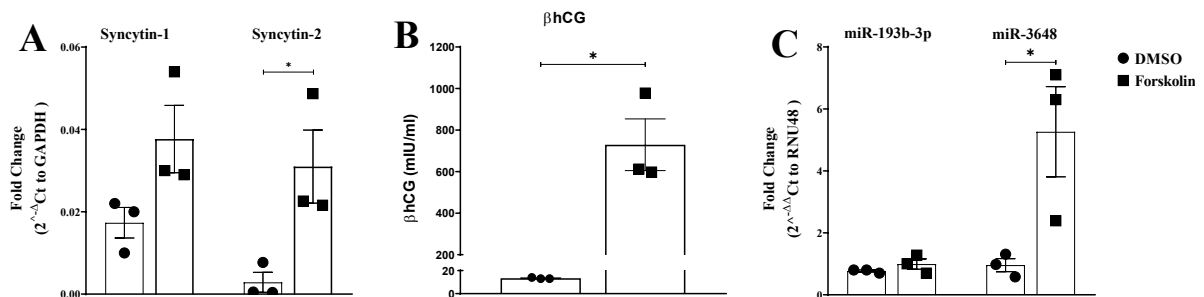


Figure 11. Forskolin treatment of BeWo cells induces syncytialization markers expression without altering miR-193b-3p expression. (A) Expression of *Syncytin-1* and *Syncytin-2*, (B) β hCG production, and (C) miR-193b-3p and miR-3648 expression in BeWo cells treated with forskolin for 48 h. *Syncytin-1* and *Syncytin-2* expression was normalized to housekeeper *GAPDH*. The expression of miR-193b-3p and miR-3648 was normalized to housekeeper *RNU48*. Bars represent means \pm SEM, n = 3. Two tailed Student's t test in B; Two-way ANOVA followed by Bonferroni multiple comparison test in A and C, * $p < 0.05$.

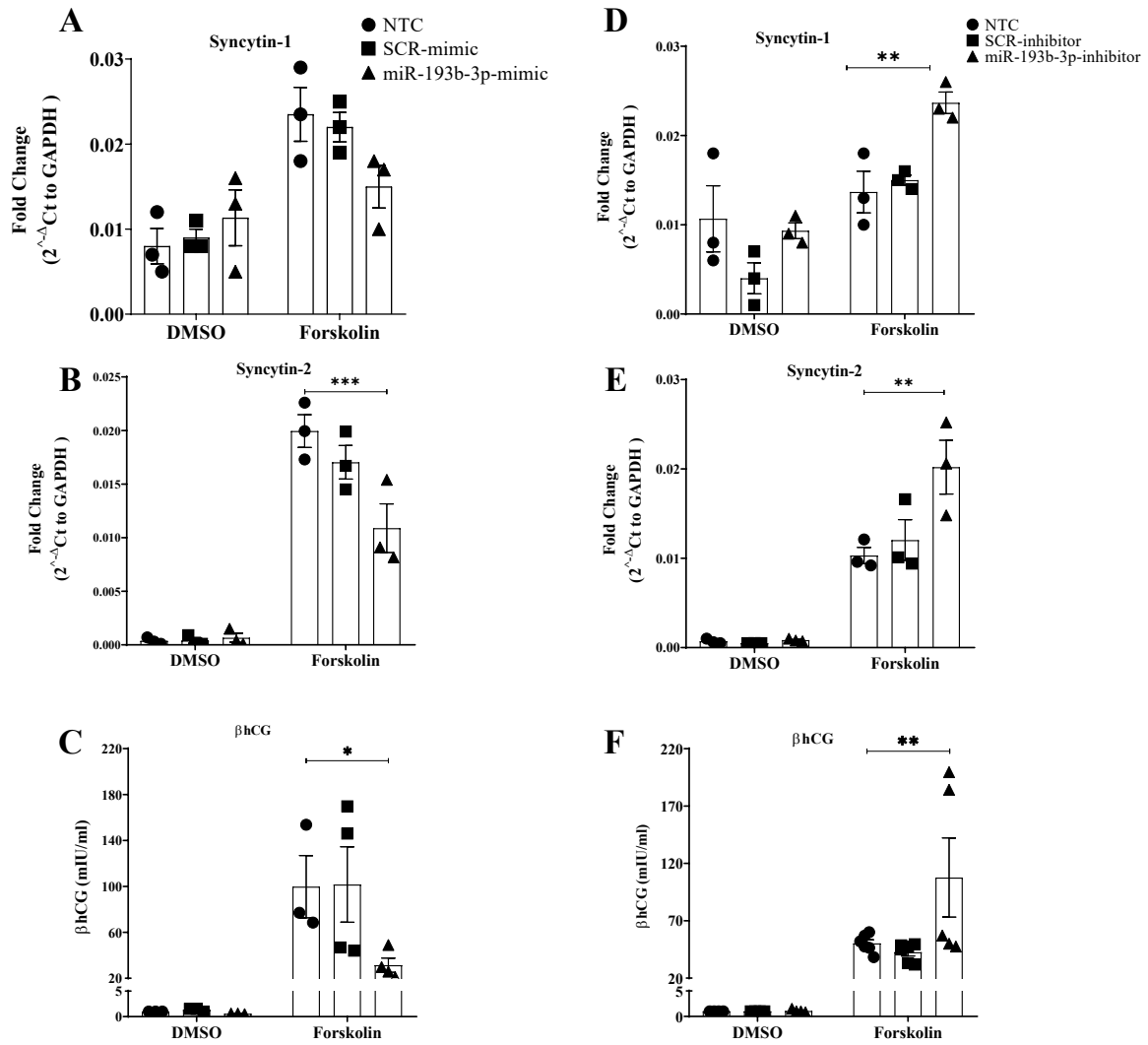


Figure 12. Influence of miR-193b-3p on syncytialization markers in BeWo cells treated with forskolin for 48 h. Expression of *Syncytin-1*, *Syncytin-2*, and β hCG production in miR-193b-3p-mimic (A, B, and C respectively) or miR-193b-3p-inhibitor (D, E, and F respectively) transfected BeWo cells 48 h after forskolin treatment. Bars represent means \pm SEM, $n \geq 3$. Two-way ANOVA followed by Bonferroni multiple comparison test; * $p < 0.05$, ** $p < 0.01$, *** $p < 0.001$. NTC: non-transfected cells.

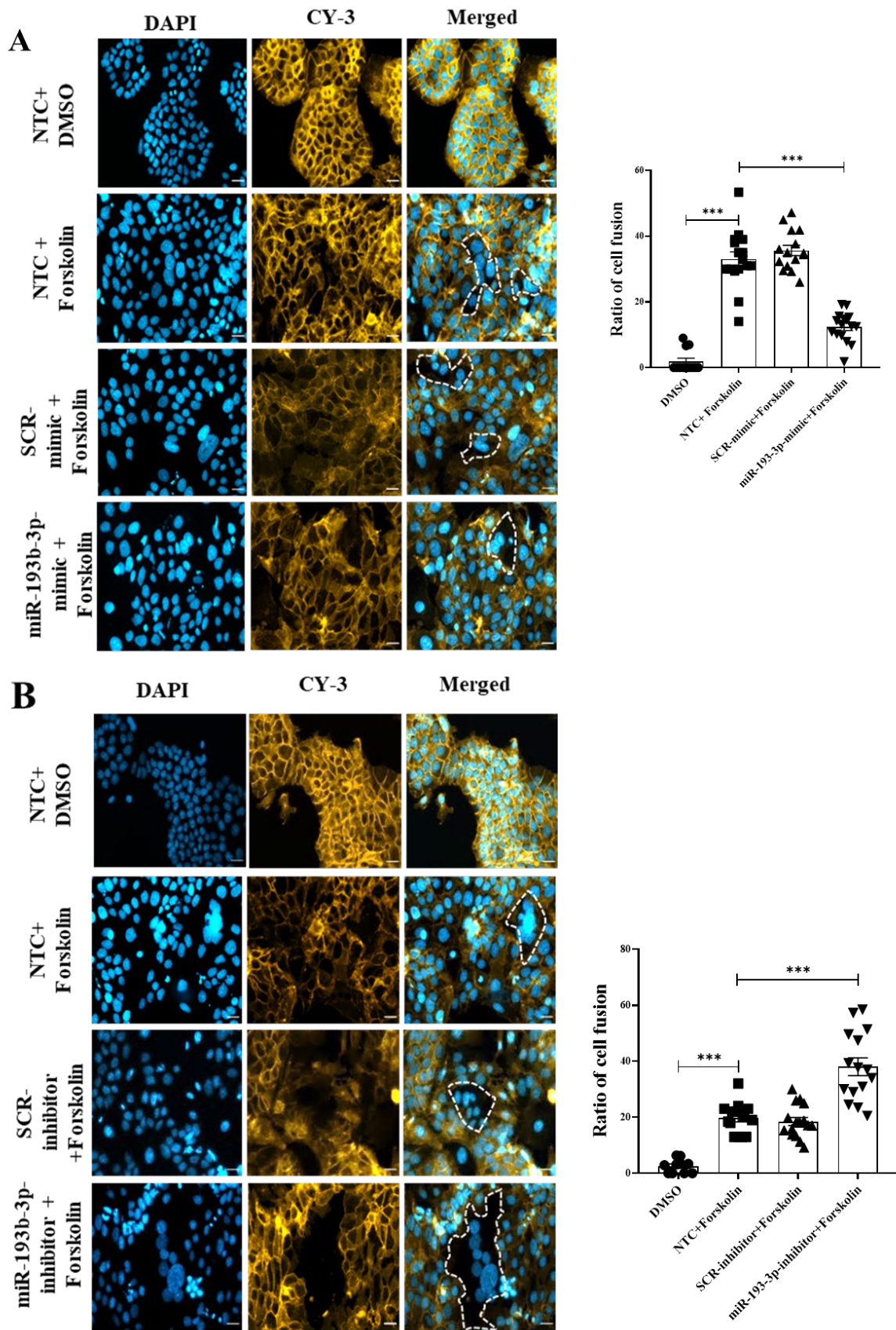


Figure 13. Effects of miR-193b-3p on BeWo cells syncytialization. Syncytium formation in BeWo cells transfected with miR-193b-3p-mimic (A) or inhibitor (B) followed by 48 h of forskolin treatment.

Cells are immunostained against E-cadherin (Cy3, orange) and nuclei are counterstained with DAPI (blue); (scale bar: 50 μ m). The white dotted line indicates syncytialized cells, characterized by nuclei without membrane divisions. Bars represent means \pm SEM, n = 3. One-way ANOVA with Bonferroni multiple comparison test; *** p < 0.001. NTC: non-transfected cells.

4.4. Cell migration

The migratory capacity of JEG-3 cells was assessed in a wound-healing assay monitored by live microscopy. Cell migration was quantified by assuming that the wound area reduces over time in an approach referred as closure rate method (Bobadilla et al. 2019). miR-193b-3p-mimic transfected cells had a significant reduction in their migration compared to NTC and SCR-mimic. In contrast, transfection of JEG-3 cells with miR-193b-3p-inhibitor significantly increased cell migration (Fig. 14).

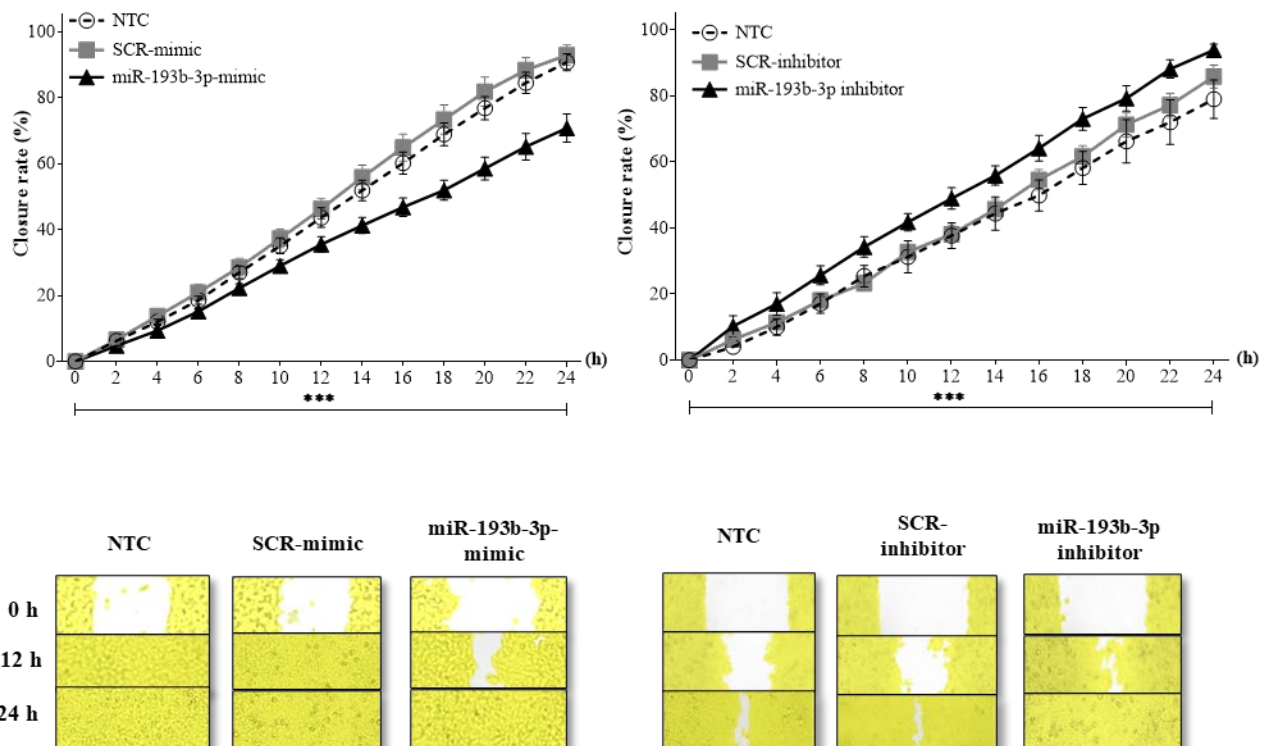


Figure 14. miR-193b-3p reduces JEG-3 cell migration. JEG-3 cells were transfected with miR-193b-3p-mimic, SCR-mimic, miR-193b-3p-inhibitor, or SCR inhibitor. The cells were subjected to wound healing migration assay monitored by JuLI™ Stage imaging system every 2 h for a period of 24 h. The closure rate is shown in images at 0, 12, and 24 h. Data are presented as means \pm SEM, n = 4. Two-way ANOVA followed by Bonferroni multiple comparison test. *** p < 0.001 compared to non-transfected cells (NTC).

4.5. Cell proliferation

The proliferation of JEG-3 cells was evaluated using RTCA. The xCELLigence instrument measures the electrical impedance promoted by cells attachment to E-plates, which is expressed as CI. Changes in cells number result in different CI values which is continuously

recorded by the machine. The data showed that, transfection of JEG-3 cells with miR-193b-3p-mimic significantly stimulated JEG-3 proliferation compared to NTC and SCR-mimic transfected cells, whereas miR-193b-3p-inhibitor transfected cells had a significantly lower proliferation index (**Fig. 15A**).

4.6. Cell apoptosis

The percentage of apoptotic cells was measured by flow cytometry after Annexin V/PE and 7-AAD staining. Early apoptotic cells expose phosphatidyl serine at the cell surface that is identified by Annexin V and late apoptotic cells become permeable to 7-AAD, which stains their DNA (Banfalvi 2017). Late apoptosis of JEG-3 cells was significantly reduced after miR-193b-3p-mimic transfection, while miR-193b-3p-inhibitor transfected cells had a significant increase in both early and late apoptosis (**Fig. 15B**).

4.7. Characterization of isolated EVs

To examine the effect of miR-193b-3p-enriched trophoblast EVs in the communication with Jurkat T cells, EVs were isolated from the conditioned medium of miR-193b-3p-mimic transfected JEG-3 cells. To validate the EVs enrichment protocol, sEVs and IEVs fractions were characterized based on their morphology, size, and marker expression. EVs morphology was visualized by TEM (**Fig. 16B**) and particle size distribution and concentration were determined via NTA. sEVs had a mean size of 120 nm and IEVs of 220 nm. Both EVs fractions had similar concentrations ($\sim 2.5 \times 10^8$ particles/ml) (**Fig. 16C**). A qualitative assessment of EV markers was performed by Western blot. The expression of EVs marker proteins CD63 and ALIX were present in sEVs from JEG-3 cells and placental perfusate. However, CD63 and ALIX were almost absent in IEVs. CD47 and GAPDH levels were found to be present in sEVs and IEVs fractions from JEG-3 and placenta perfusate (**Fig. 16D**).

To confirm that EVs collected from JEG-3 cells transfected with miR-193b-3p-mimic had higher levels of miR-193b-3, their content was investigated by qPCR. miR-193b-3p levels were significantly higher in both IEV- (IEV_{miR-193b-3p}; 1500 folds) and sEV-enriched fractions (sEV_{miR-193b-3p}; 400 folds) when compared to those from non-transfected (IEV_{NTC} and sEV_{NTC}) or scramble transfected cells (IEV_{SCR-mimic} and sEV_{SCR-mimic}) (**Fig. 16A**).

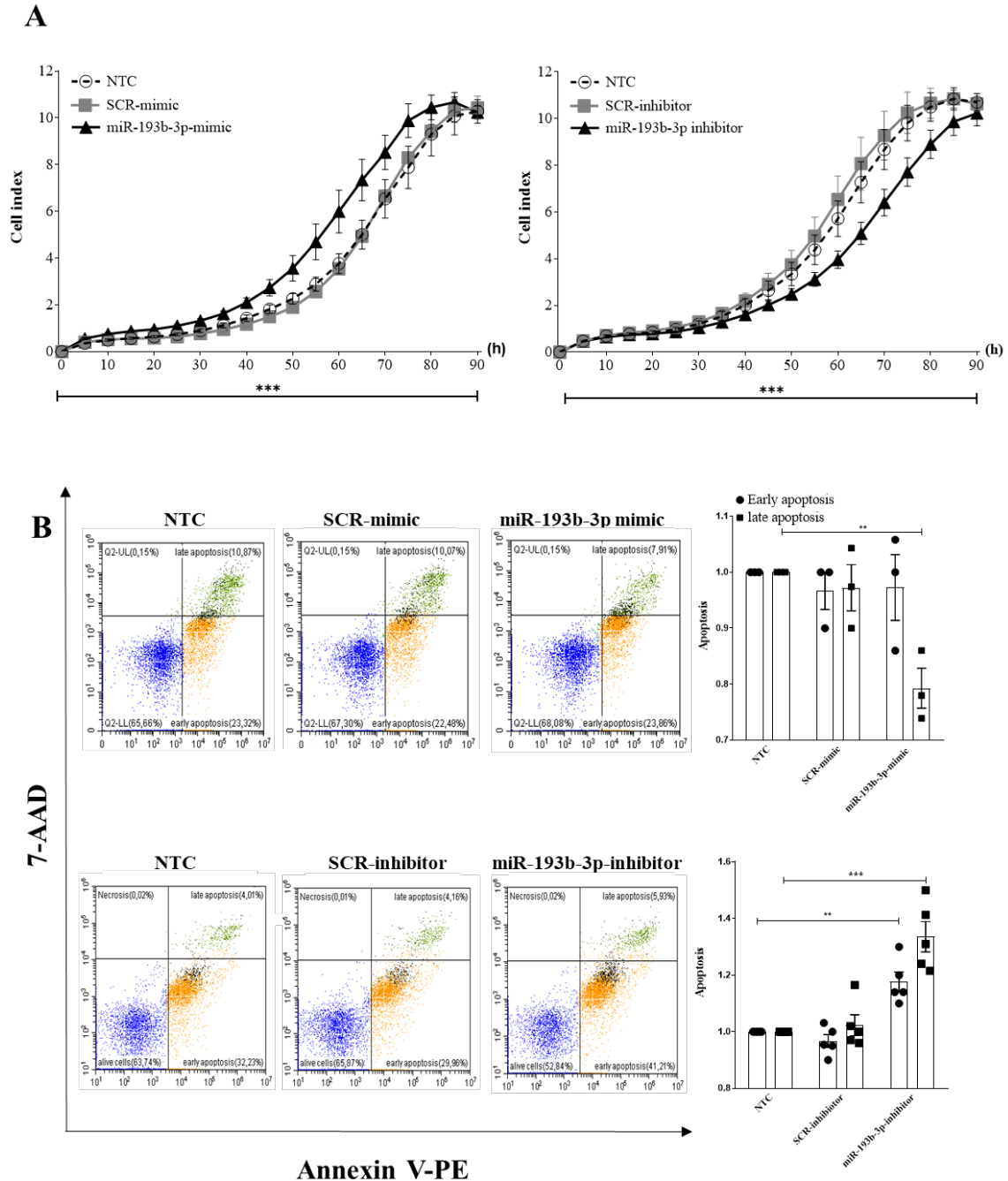


Figure 15. The influence of miR-193b-3p on JEG-3 cell proliferation and apoptosis. **(A)** Proliferation assay using xCELLigence® Real-Time Cell Analyzer. **Left:** JEG-3 cells transfected with miR-193b-3p-mimic and **Right:** JEG-3 cells transfected with miR-193b-3p-inhibitor. The cell proliferative index was assessed every 10 h for a period of 90 h. Data are presented as means \pm SEM, $n = 4$. **(B) Left:** Flow cytometric analysis of apoptosis in JEG-3 cells transfected with miR-193b-3p-mimic, SCR-mimic, miR-193b-3p-inhibitor, or SCR inhibitor. Viable cells (Annexin V-/7-AAD-) can be observed in the lower left quadrant, dead cells (Annexin V+/7-AAD+) in the upper left quadrant, early apoptotic cells (Annexin V+/7-AAD-) in the lower right quadrant, and late apoptotic cells (Annexin V+/7-AAD+) in the upper right quadrant. **Right:** The percentage of late and early apoptotic cells. Data are presented as means \pm SEM, $n \geq 3$. Two-way ANOVA followed by Bonferroni multiple comparison test. ** $p < 0.01$, *** $p < 0.001$. NTC: non-transfected cells.

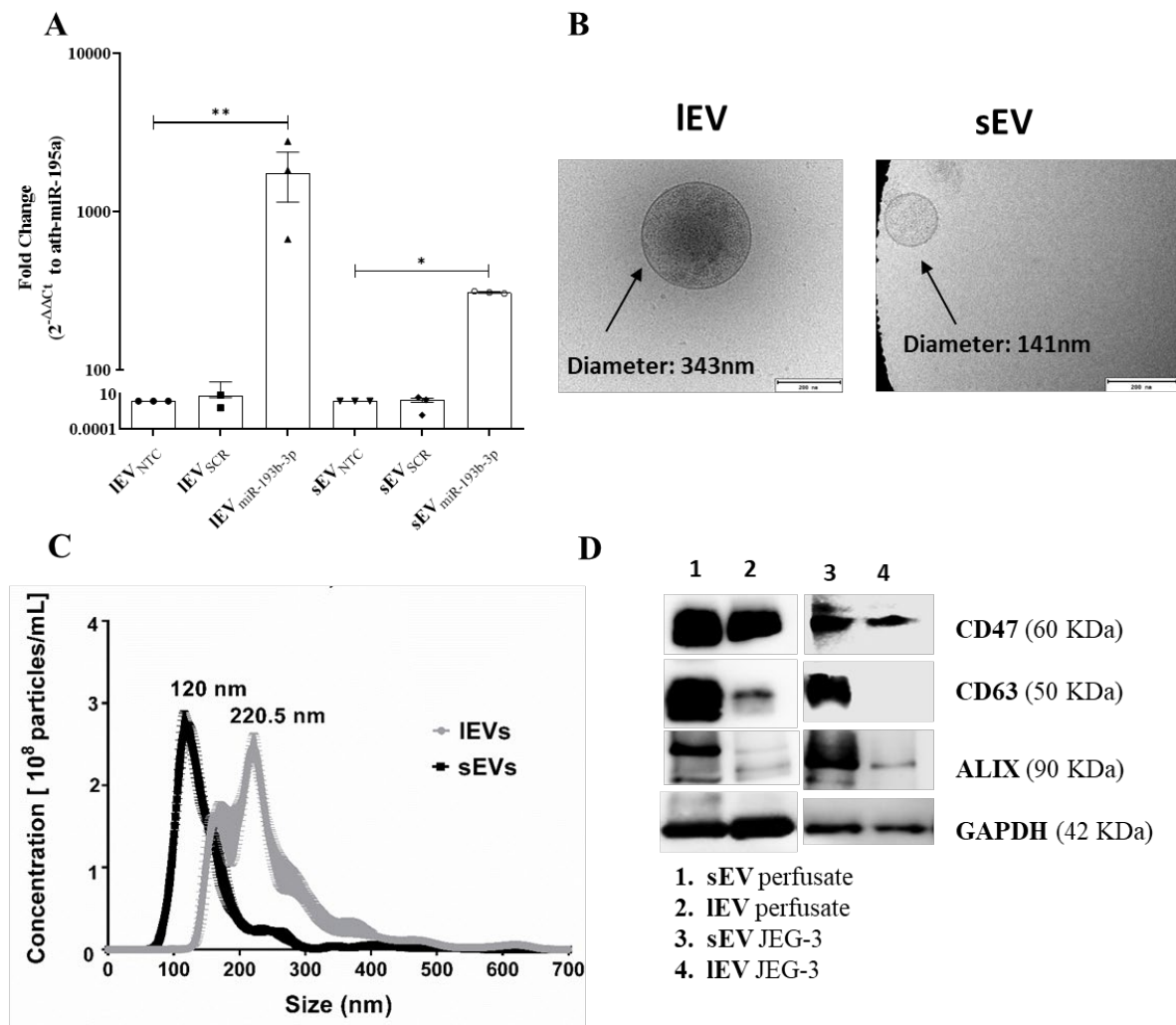


Figure 16. Characterization of JEG-3 EVs fractions. (A) miR-193b-3p expression in JEG-3 EVs collected after miR-193b-3p-mimic transfection determined by qPCR and normalized to ath-miR-159a spike-in control. Bars represent means \pm SEM, $n = 3$. One-way ANOVA with Bonferroni multiple comparison test. * $p < 0.05$, ** $p < 0.01$. (B) Transmission electron microscopy of membranous vesicles with diameters of 343 nm and 141 nm from IEV- and sEV-enriched fractions, respectively. (C) Particle size distribution and concentration in IEV- and sEV-enriched fractions from JEG-3 cells supernatant, $n = 4$. (D) Western blot analysis of EVs markers CD63, CD47, ALIX, and GAPDH. sEVperfusate and IEVperfusate are extracellular vesicles-enriched fractions from placental perfusate.

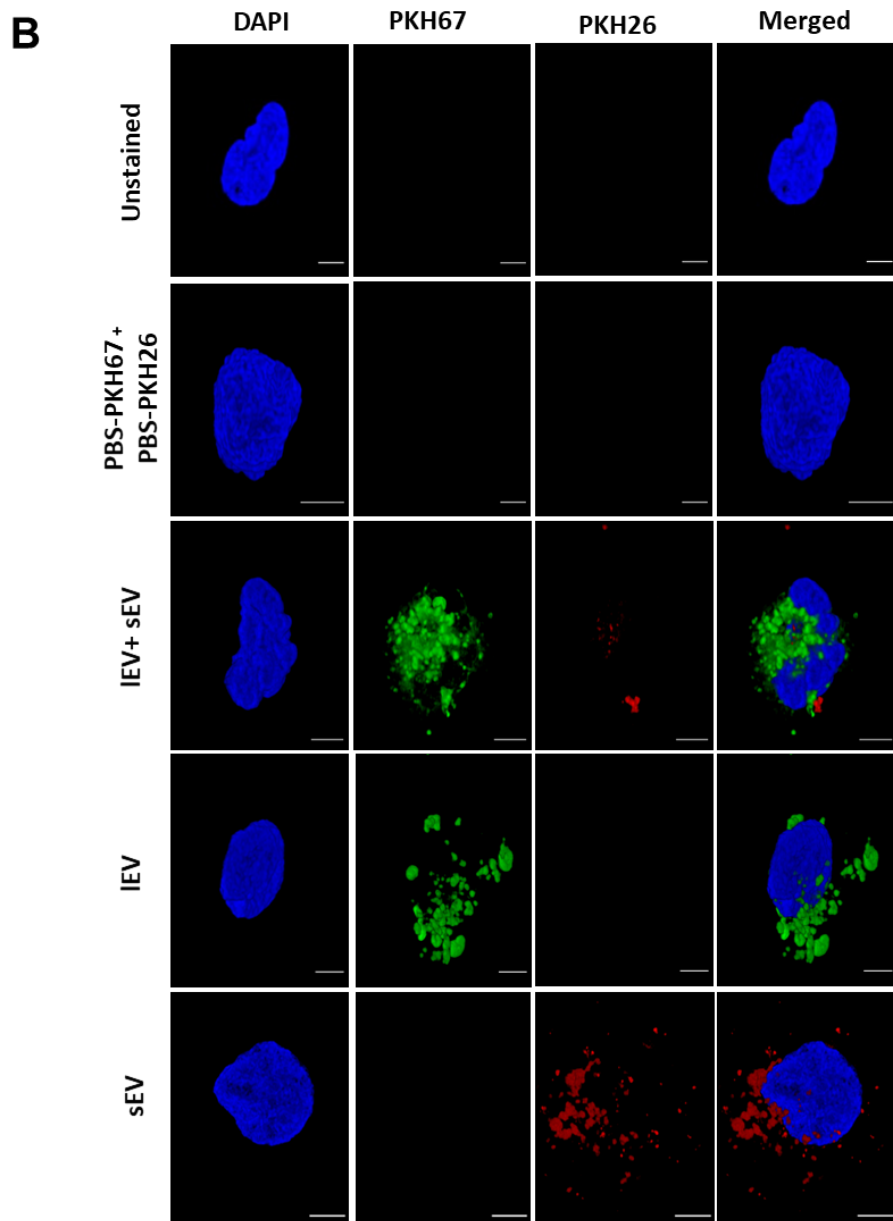
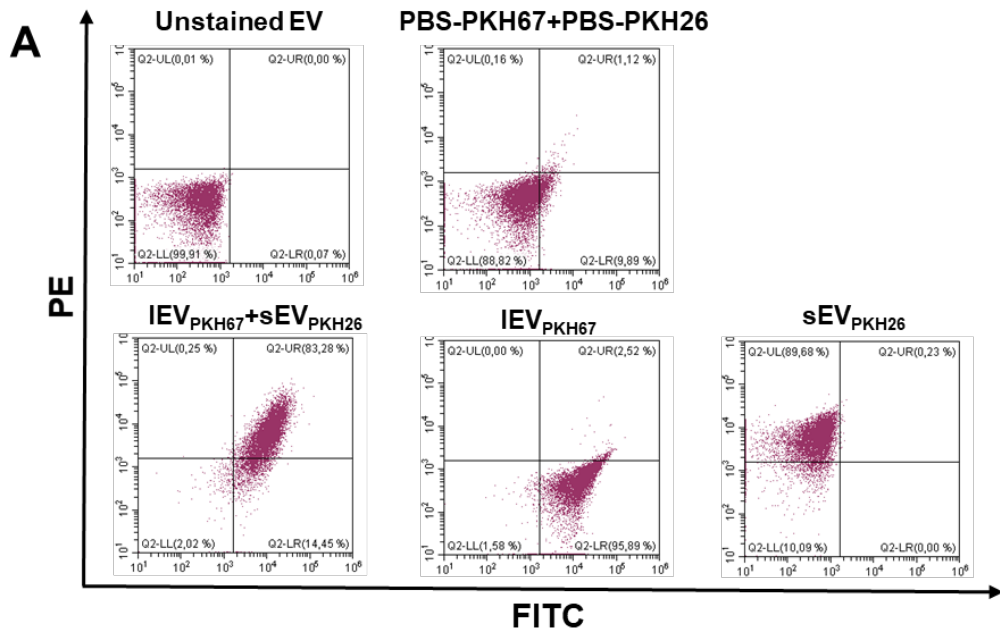
4.8. The effect of miR-193b-3p-enriched trophoblast EVs on Jurkat T cells uptake and proliferation

To examine the uptake of trophoblast EVs by Jurkat T cells, IEVs were stained with PKH67 (IEV_{PKH67}) and sEV with PKH26 (sEV_{PKH26}) and added to cell cultures. After 24 h, EVs uptake was investigated by flow cytometry and confocal microscopy. Flow cytometry data showed that 95.9% of Jurkat T cells incorporated IEVs and 89.7% sEVs when EVs fractions were applied separately. When Jurkat T cells were incubated with both EVs fractions, 83.3% incorporated both IEVs and sEVs, whereas 14.5% only IEVs. To evaluate the non-specific

uptake, the cells were incubated with PBS-PKH67+PBS-PKH26. Around 9.8% showed PKH67 signals (**Fig. 17A**). Additionally, the uptake of sEVs and IEVs by Jurkat T cells was visualized by confocal microscopy. When both EVs fractions were applied together, mean fluorescence intensity in IEV_{PKH67}-treated cells was significantly higher than that of sEV_{PKH26}-treated cells. PBS-PKH67 and PBS-PKH26 controls showed a very small background fluorescence intensity caused by non-specific uptake of the dyes (**Fig. 17B-C**).

The kinetics of miR-193b-3p levels in Jurkat T cells upon uptake of IEV_{miR-193b-3p} and sEV_{miR-193b-3p} was analyzed daily during a period of 10 days. On the first day, cells treated with both IEV_{miR-193b-3p} and sEV_{miR-193b-3p} presented an increased expression of miR-193b-3p. In addition, IEV_{miR-193b-3p}-treated cells had a significantly higher levels of miR-193b-3p compared to those treated with sEV_{miR-193b-3p}. miR-193b-3p upregulation lasted for 5 days in both IEV_{miR-193b-3p} and sEV_{miR-193b-3p}-treated Jurkat T cells (**Fig. 18A**).

miR-193b-3p-mimic transfected Jurkat T cells had a significant increase of miR-193b-3p expression compared to NTC and SCR-mimic transfected cells (**Fig. 18B**). Those cells were tested for their proliferation rate by using RTCA. Fibronectin was used to induce cells' attachment. In order to compare the results with a conventional method used for cell proliferation measurements, a colorimetric BrdU incorporation test was carried out. The proliferation rate, examined as cell index, was significantly reduced after treatment of Jurkat T cells with IEV_{miR-193b-3p}, sEV_{miR-193b-3p}. These results were confirmed by colorimetric BrdU incorporation. To confirm that the previous results were due presence of miR-193b-3p in EVs, the proliferation of transfected Jurkat T cells was assessed by both methods which caused a significant reduction of proliferation in miR-193b-3p-mimic transfected cells compared to NTC and SCR-mimic (**Fig. 19A-B**).



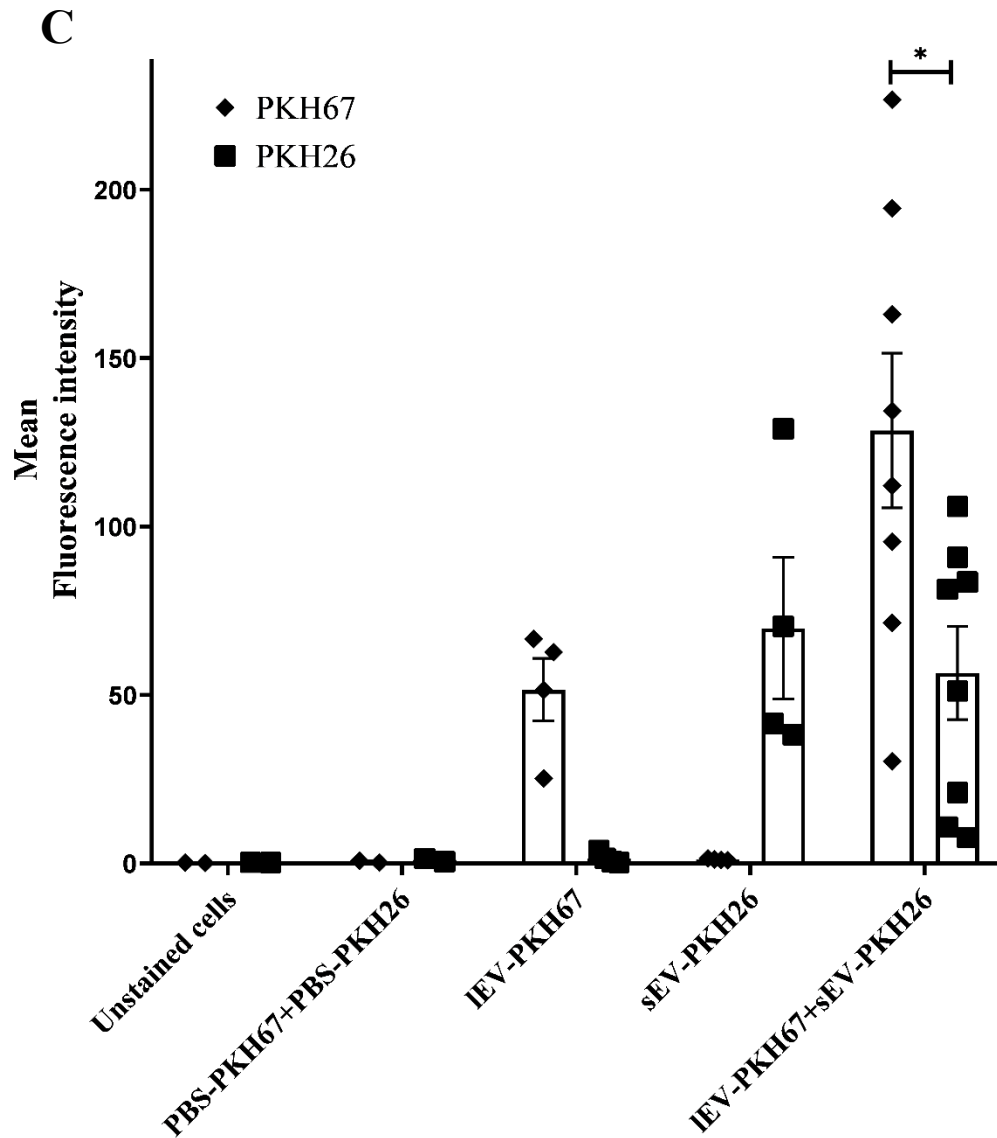


Figure 17. Uptake of JEG-3 EVs by Jurkat T cells. Jurkat T cells were treated for 24 h with either PKH67-stained IEVs, PKH26-stained sEVs, or both. The uptake was assessed by: **(A)** Flow cytometry analysis showing no EVs uptake in the lower left quadrant, sEVs uptake in the upper left quadrant, IEVs uptake in the lower right quadrant, and sEVs+IEVs uptake in the upper right quadrant. **(B)** Laser scanning confocal microscopy shows the uptake of PKH67-stained IEVs (green) and PKH26-stained sEVs (red) individually or combined. Scale bar = 4 μ m. **(C)** The relative mean of PKH67 and PKH26 fluorescence intensity in recipient cells. The results are presented as mean \pm SEM. Two tailed student t-test, * $p < 0.05$.

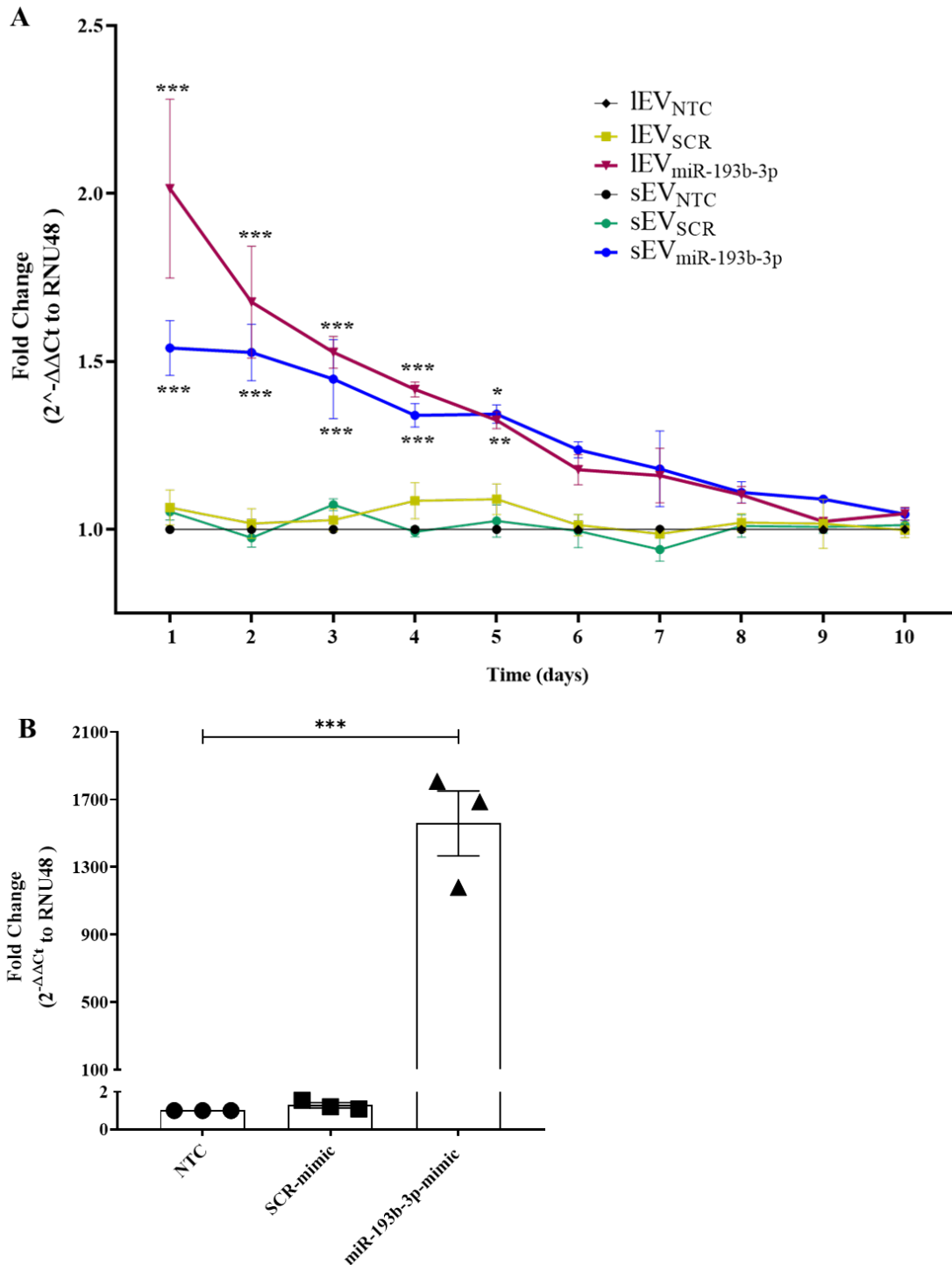


Figure 18. The influence of miR-193b-3p enriched JEG-3 EVs on miR-193b-3p expression in Jurkat T cells. (A) Expression of miR-193b-3p evaluated by qPCR in Jurkat T cells over a period of 10 days after treatment with IEV_{miR-193b-3p}, sEV_{miR-193b-3p}, IEV_{SCR-mimic}, sEV_{SCR-mimic}, IEV_{NTC} and sEV_{NTC} and normalized to RNU48. **(B)** Expression of miR-193b-3p in Jurkat T cells after miR-193b-3p-mimic transfection. Bars represent means ± SEM, n = 3. Two-way ANOVA with Bonferroni multiple comparison test. * p < 0.05, ** p < 0.01, *** p < 0.001

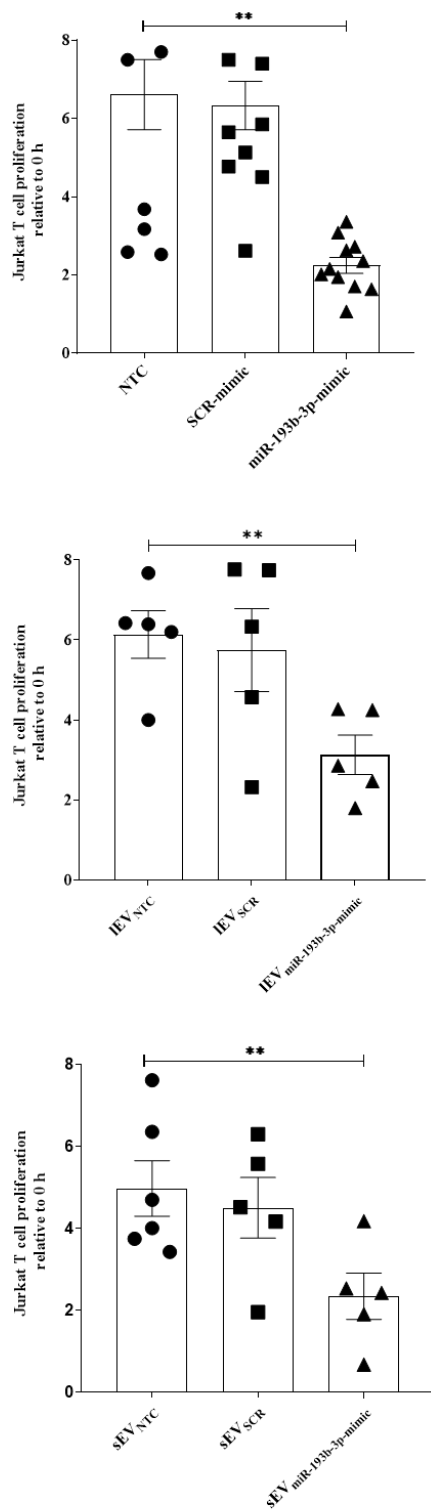
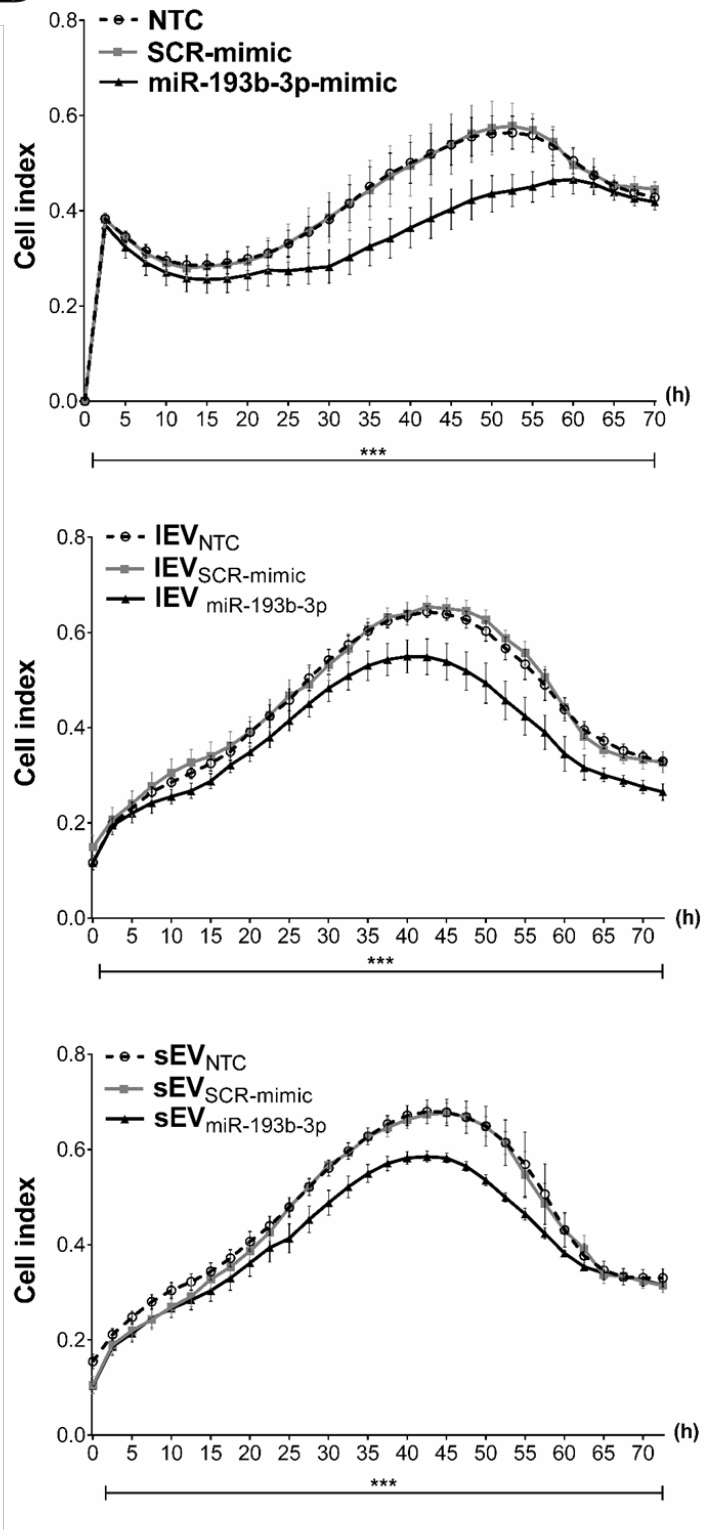
A**B**

Figure 19. miR-193b-3p enriched JEG-3 EVs reduce Jurkat T cells proliferation. The proliferation of Jurkat T cells transfected with miR-193b-3p-mimic or treated with EVs measured by (A) xCELLigence® Real-Time Cell Analyzer and (B) colourimetric BrdU incorporation. Bars represent means \pm SEM, $n \geq 3$. Two-way ANOVA with Bonferroni multiple comparison test. ** $p < 0.01$, *** $p < 0.001$.

4.9. Effects of miR-193b-3p on JEG-3 cells proteome

Global protein expressions analysis of transfected cells was employed to investigate the effects of miR-193b-3p inhibition on the JEG-3 cellular proteome. After transfection of JEG-3 cells with miR-193b-3p-inhibitor, the protein levels were evaluated using a LC-MS/MS approach. A total of 4112 proteins were detected in the data set and 35 proteins (33 with a $FC > 2$) (Fig. 20) were significantly differentially expressed between miR-193b-3p-inhibitor transfected cells and controls. Seventeen proteins were upregulated, and 18 proteins were downregulated (Table 18).

Table 18. Significantly changed proteins in miR-193b-3p-inhibitor transfected JEG-3 cells in comparison to non-transfected cells

No.	Protein symbol	Protein name	Differential expression	Log P value	Fold change
1	POLG2	DNA polymerase subunit gamma-1	Upregulated	5.66	3.17
2	DIABLO	Diablo homolog, mitochondrial	Upregulated	3.77	4.26
3	HSD17B1	Estradiol 17-beta-dehydrogenase 1	Upregulated	4.27	4.308
4	TMPPE	transmembrane protein with metallophosphoesterase domain	Upregulated	5.41	3.801
5	CCT3	T-complex protein 1 subunit gamma	Upregulated	3.38	0.63
6	C10orf54	Platelet receptor Gi24	Upregulated	4.09	2.52
7	IDH3B	Isocitrate Dehydrogenase (NAD (+)) 3 Non-Catalytic Subunit Beta	Upregulated	5.13	2.94
8	POLR1B	DNA-directed RNA polymerase I subunit B	Upregulated	5.18	3.09
9	APAF1	Apoptotic protease-activating factor 1	Upregulated	5.00	3.42
10	ZC3H7A	Zinc finger CCCH domain-containing protein 7A	Upregulated	5.35	3.53
11	NDC1	Nucleoporin NDC1	Upregulated	5.23	3.93
12	MRPL9	39S ribosomal protein L9, mitochondrial	Upregulated	6.92	4.88
13	UTP6	U3 small nucleolar RNA-associated protein 6 homologs	Upregulated	5.22	4.56
14	FNDC3A	Fibronectin type-III domain-containing protein 3A	Upregulated	4.55	4.75

15	RER1	Protein RER1	Upregulated	3.94	3.27
16	QRSL1	Glutamyl-tRNA(Gln) amidotransferase subunit A, mitochondrial	Upregulated	3.90	3.75
17	FKBP4	Peptidyl-prolyl cis-trans isomerase FKBP4; N-terminally processed	Upregulated	4.06	0.46
18	BRD2	Bromodomain-containing protein 2	Downregulated	5.72	-3.41
19	SMARCA1	Probable global transcription activator SNF2L1	Downregulated	5.47	-3.71
20	ZWILCH	Protein zwilch homolog	Downregulated	5.225	-2.31
21	TWF1	Twinfilin-1	Downregulated	5.00	-2.36
22	PDE6D	Retinal rod rhodopsin-sensitive cGMP 3,5-cyclic phosphodiesterase subunit delta	Downregulated	4.38	-3.38
23	FIGNL2	Putative fidgetin-like protein 2	Downregulated	4.50	-2.32
24	ATG5	Autophagy protein 5	Downregulated	4.53	-1.94
25	POMP	Proteasome maturation protein	Downregulated	4.11	-3.11
26	ADPGK	ADP-dependent glucokinase	Downregulated	4.10	-2.85
27	CCM2L	Cerebral cavernous malformations 2 protein-like	Downregulated	3.90	-4.37
28	PMPCA	Mitochondrial-processing peptidase subunit alpha	Downregulated	3.61	-3.99
29	MRPL24	39S ribosomal protein L24, mitochondrial	Downregulated	3.76	-3.74
30	ANKRD11	Ankyrin repeat domain-containing protein 11	Downregulated	3.81	-3.07
31	CYB5R2	NADH-cytochrome b5 reductase 2	Downregulated	3.78	-2.61
32	POLB	DNA polymerase beta	Downregulated	3.81	-2.02
33	TFB1M	Dimethyladenosine transferase 1, mitochondrial	Downregulated	3.40	-3.08
34	TNIK	TRAF2 and NCK-interacting protein kinase	Downregulated	4.50	-1.06
35	RELL1	RELT-like protein 1	Downregulated	5.70	-4.09

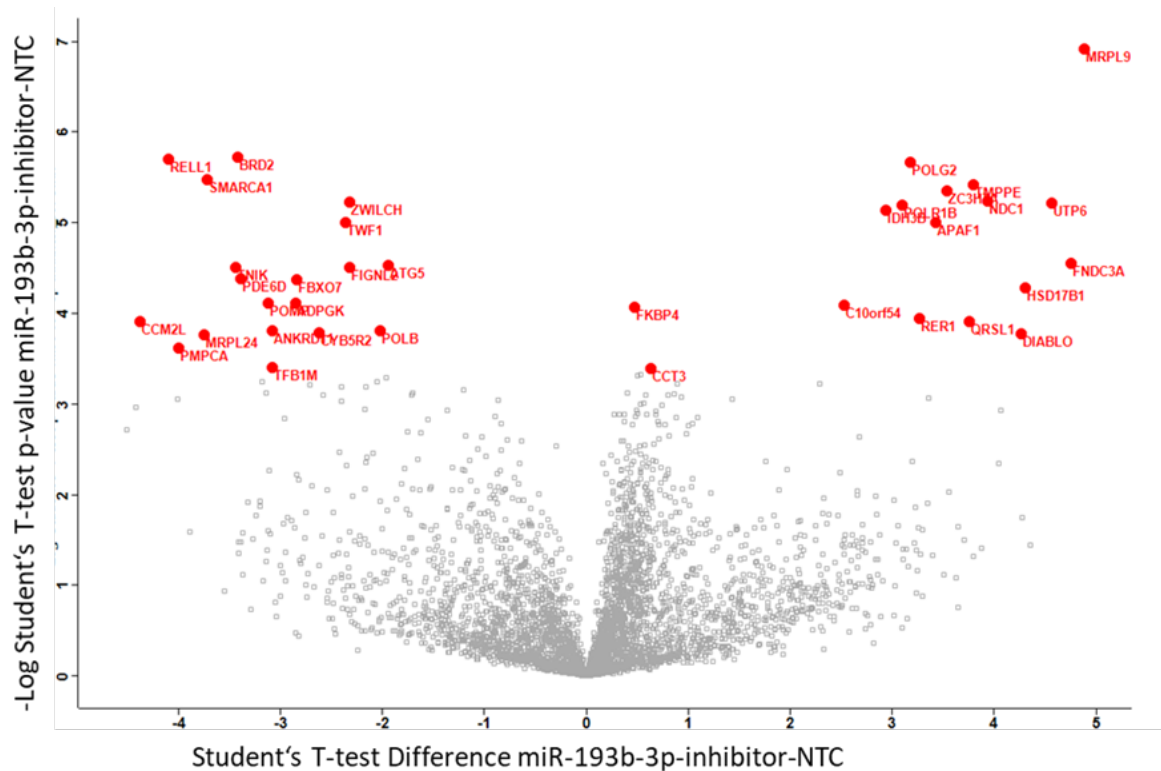


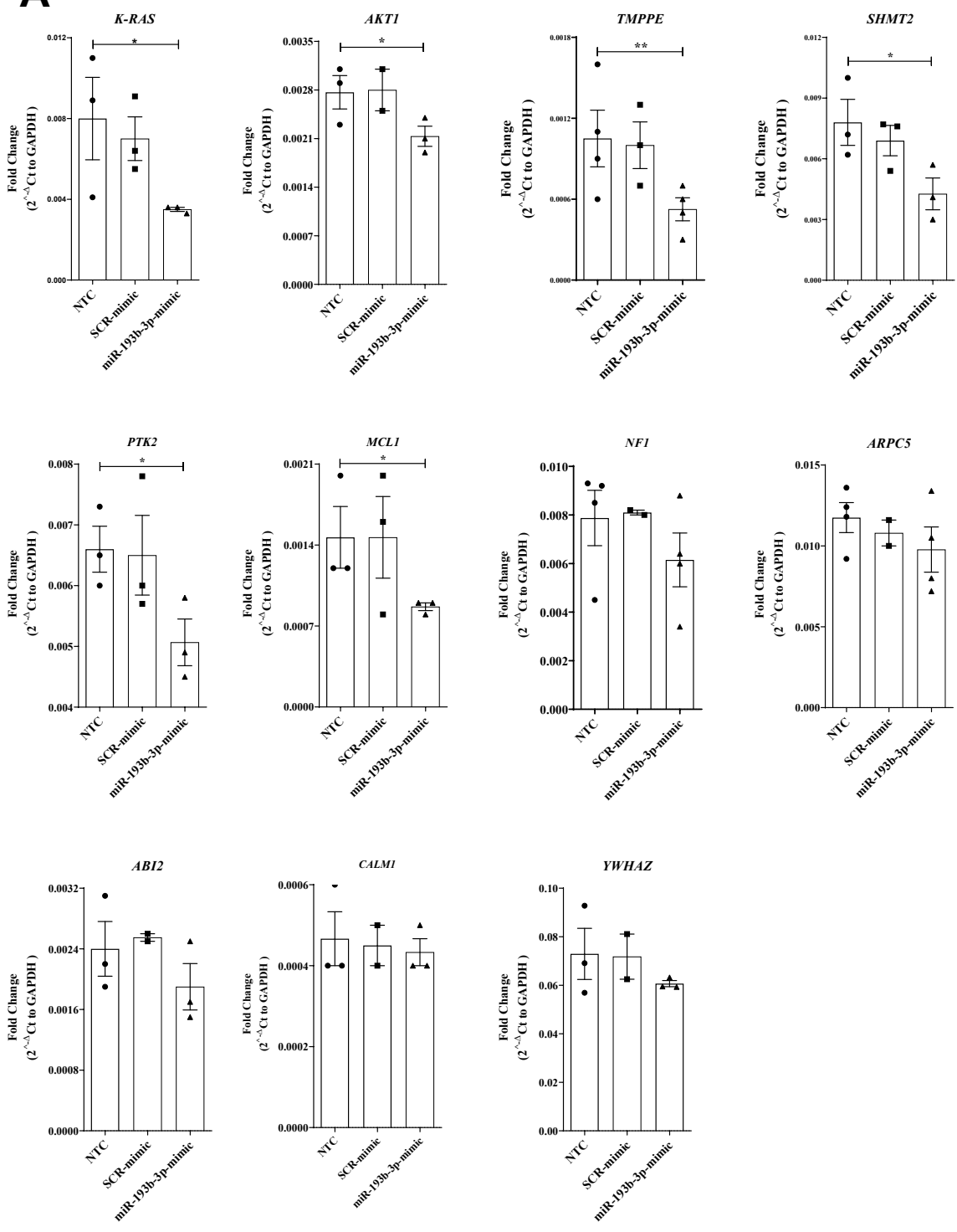
Figure 20. Graphical representation of quantitative proteomics data from JEG-3 cells transfected with or without miR-193b-3p-inhibitor. Proteins are depicted in a volcano plot of the label-free quantitative MS according to their statistical P-value (y-axis: $-\log_{10}$, p-value) and their relative abundance ratio (x-axis: \log_2 , FC) between NTC and miR-193b-3p-inhibitor transfected cells (n=5). Red spots to the left are showing the significantly downregulated protein and red spots to the right the significantly upregulated proteins in miR-193b-3p-inhibitor transfected cells. The significance thresholds were fold change ≥ 2 and p-value (Benjamini-Hochberg adjustment) ≤ 0.05 . In grey (open circles), proteins with no statistically significant abundance. NTC: non-transfected control utilized during miR-193b-3p-inhibitor transfection.

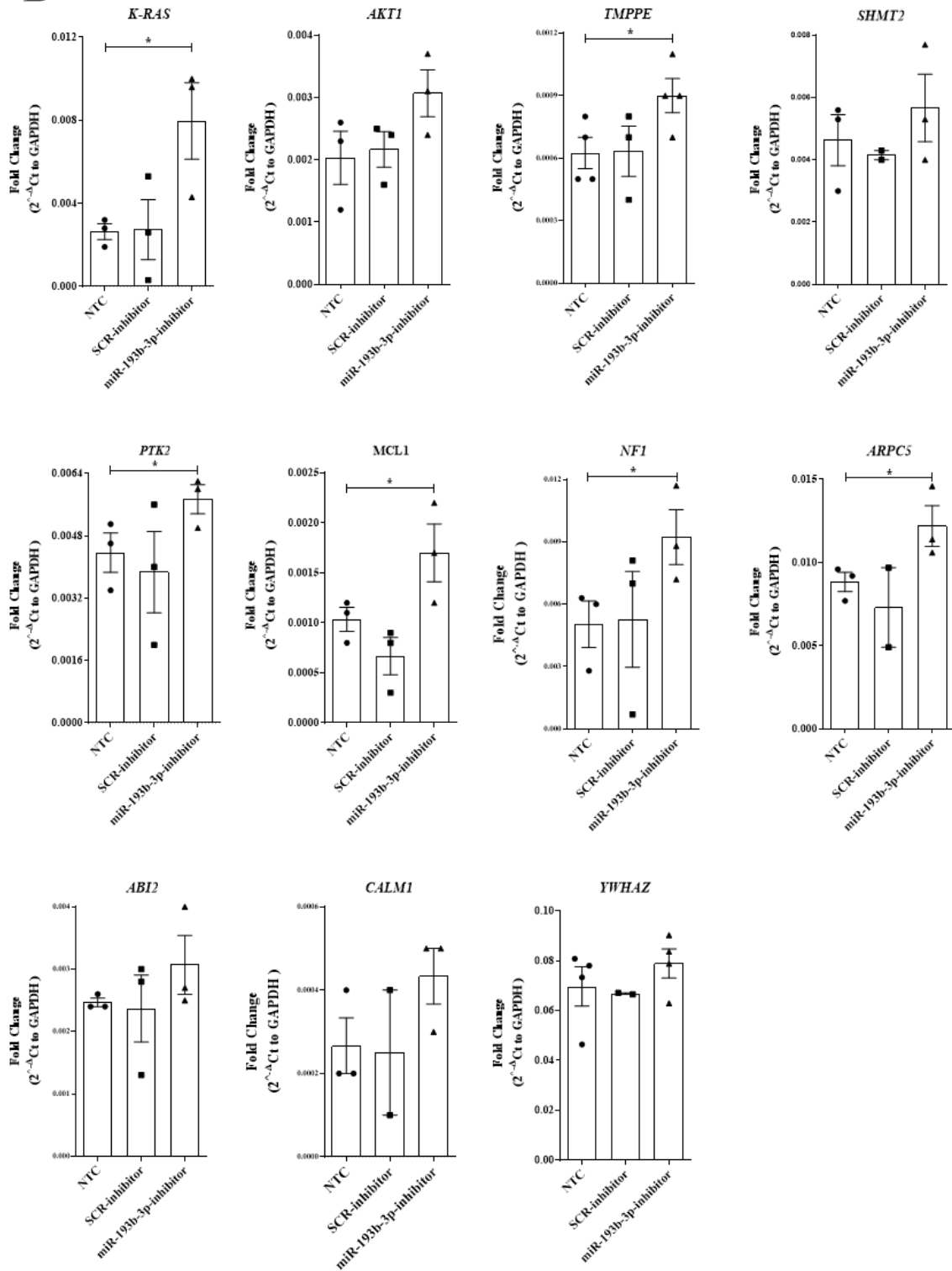
4.10. Gene and protein expression in transfected JEG-3 cell

Among the differentially expressed proteins, only one (TMPPE) was identified by bioinformatics tools as a primary target of miR-193b-3p. TMPPE and ten other potential targets of miR-193b-3p present in the proteomic dataset whose p-values were close to the B-H-adjusted significance threshold were chosen to be further evaluated at the mRNA level by qPCR in miR-193b-3p-mimic and miR-193b-3p-inhibitor transfected JEG-3 cells. The transfected and non-transfected cells were collected after 48 h of transfection. The selected targets, which were upregulated in the proteomic data set of miR-193b-3p-inhibitor transfected cells, are: *ARPC5*, *ABI2*, *PTK2*, *CALM1*, *YWHAZ*, *SHMT2*, *NF1*, *TMPPE*, *K-Ras*, *MCL1*, and *AKT1* and were further investigated by PCR. In addition, TMPPE and AKT1 were investigated by Western blot on protein level.

TMPPE was the most significantly changed protein in miR-193b-3p-inhibitor transfected JEG-3 cells which was detected by proteomics and confirmed by qPCR and Western blot. *AKT1* was significantly downregulated in miR-193b-3p-mimic transfected cells and upregulated in miR-193b-3p-inhibitor transfected cells as verified by qPCR and Western blot. In miR-193b-3p-mimic transfected cells, *K-Ras*, *SHMT2*, *PTK2*, and *MCL1* were significantly downregulated as examined by qPCR. In miR-193b-3p-inhibitor transfected cells, *K-Ras*, *PTK2*, *MCL1*, *NF1*, and *ARPC5* were significantly upregulated. *CALM1*, *YWHAZ* and *ABI2* were not significantly changed in both miR-193b-3p-mimic and -inhibitor transfected cells (Fig. 21A-C).

A



B

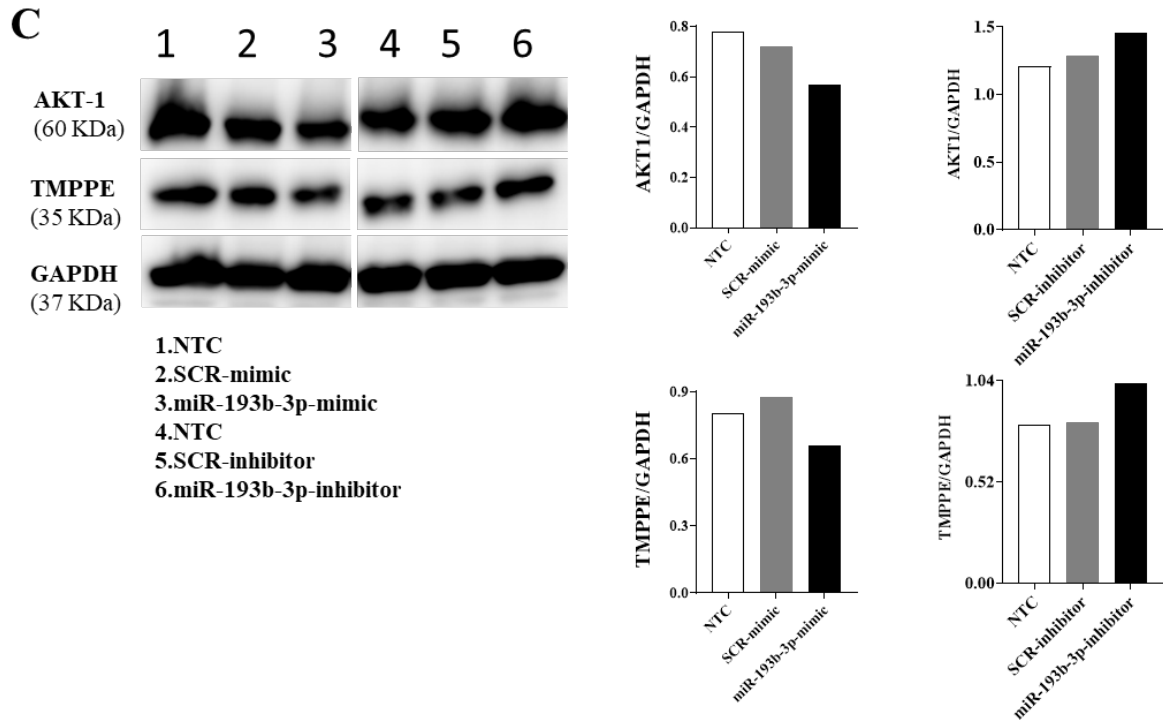


Figure 21. Validation of proteomics data for identification of potential miR-193b-3p targets. By qPCR in (A) miR-193b-3p-mimic transfected cells and (B) miR-193b-3p-inhibitor transfected cells and by Western blot in (C) for both miR-193b-3p-mimic and -inhibitor transfected cells (n=1). Bars in (A) and (B) represent means \pm SEM, n = 3. One-tailed Student t-test. * p < 0.05, ** p < 0.01.

5. DISCUSSION

The relation between pregnancy diseases and changes in miRNAs expression has increasingly received attention in recent years. Dysregulated miRNA expression was demonstrated in pregnancy complications such as preeclampsia (Zhu and Chen 2023), Gestational Diabetes Mellitus (Jiang et al. 2023), IUGR (Zhu et al. 2022), and PAS (Wang et al. 2023). miR-193b-3p is one of the pregnancy-associated miRNAs which is altered in placental diseases (Awamleh et al. 2019). This miRNA is associated with cellular processes including migration, invasion (Zhou et al. 2016), and proliferation (Zhang et al. 2017b), all of which are impaired in PAS. Nevertheless, the functions of miR-193b-3p in trophoblast cells have been poorly investigated. In this context, the aims of the current study were to investigate the role of miR-193b-3p in trophoblast cells functions that are associated with abnormal placental invasion as well as to examine the localization of this miRNA human placentas.

In functional *in vitro* assays, I found that miR-193b-3p regulated fundamental trophoblast cell processes including syncytialization, migration, proliferation, and apoptosis. TMPPE, K-Ras, PTK2, and MCL1 were found to be potential miR-193b-3p targets in trophoblast cells by using qPCR and proteomic analyses. Furthermore, trophoblast-derived EVs enriched with miR-193b-3p can be internalized by Jurkat T cells and ultimately reduce their proliferation.

5.1.1. *miR-193b-3p expression and localization in human placentas*

The human placenta expresses at least 1900 distinct miRNAs (Morales-Prieto et al. 2020); however, the localization of most of them remains unknown. qPCR is a useful tool to quantify miRNA expression; nevertheless, it does not show which cell types express the investigated miRNAs (unless cells are previously isolated). The application of miRNA-ISH to identify cell-specific miRNA expression within placental tissues has only been sporadically reported in the literature. In a study by Gu and colleagues, miR-371-5p was shown to be highly expressed in CTBs and STBs in first trimester placentas as well as in stromal cells, fetal vessel, smooth muscle cells and endothelial cells in third-trimester placentas. miR-125b-5p was mainly expressed in trophoblasts with intensive expression in third-trimester placentas (Gu et al. 2013). Zhang et al. used miRNA-ISH to localize the expression of miR-196a-5p in recurrent pregnancy loss and NP placentas. This miRNA was present in the CTBs of both. (Zhang et al. 2022). miR-193b-3p is upregulated in the STB of PAS patient assessed by miRNA-ISH (Murrieta-Coxca et al. 2023) which agrees with our expectation of its functions as it is explained below.

I performed miRNA-ISH to investigate the expression and localization of miR-193b-3p in human placentas. IHC for cytokeratine-7 was combined with miRNA-ISH to identify trophoblast cells in the decidual layer of the placenta. Our results revealed that, in the villous tree of the human placenta, miR-193b-3p was expressed by STBs and endothelial cells. In the decidual layer, miR-193b-3p is expressed in iEVTs and enEVTs. This indicates that this miRNA could have a role in EVT invasion.

The decidua constitutes a temporary stage of differentiation of the endometrium. This process is characterized by massive tissue remodeling driven by ovarian hormones, lipid mediators, and growth factors (Mori et al. 2016, Murata et al. 2022). Alterations in the interaction between decidual cells and invading trophoblasts seem to be a determinant factor in PAS. The partial or complete absence of decidua basalis is considered a histological marker of PAS. Often the decidua parietalis is absent or replaced by loose connective tissue, which does not have the same properties as the decidua (Jauniaux and Jurkovic 2012). Deeper invasion of iEVTs was reported with a significant increased number in PAS patients with missing decidua in comparison to those with existing decidua (Hannon et al. 2012). Additionally, changes in the uteroplacental vascular system have been described. It was found that the spiral arteries of PAS patients are only partially remodeled, which is related to dysregulated enEVTs function (Bartels et al. 2023).

The decidua contains decidualized endometrial stromal cells, natural killer (NK) cells, T cells, dendritic cells, and macrophages (Farine et al. 2018). Therefore, the use of cytokeratine-7 or another marker of trophoblasts is indispensable to identify invading trophoblast cells in the decidua. Cytokeratine-7 was used by several studies as a trophoblast marker (Maldonado-Estrada et al. 2004, Lee et al. 2016, Gauster et al. 2022). I observed that miR-193b-3p-positive cells present in the decidua which were not positive for cytokeratine-7 and are most likely decidual or immune cells. Further markers are required for their precise identification such as prolactin and insulin growth factor binding protein-1 (IGFBP-1), which are expressed by decidual cells (Mori et al. 2016), CD56, CD69, CD49a, integrin β 7 for decidual NK (dNK) cells identification and CD14 for macrophages (Jabrane-Ferrat 2019).

The presence of decidual and/or immune cells expressing miR-193b-3p in the decidua suggests they may play a role in controlling EVT's invasion. Further studies on decidual cells and immune cells with the manipulation of miR-193b-3p expression by transfection of miR-193b-3p-mimic/inhibitor followed by invasion and migration assays could be conducted to investigate this issue. Hannon et al. reported the absence of decidua in some cases of PAS that

coincided with more iEVTs invading the myometrium compared with NP (Hannon et al. 2012).

Taken together, these data indicate that changes in both trophoblast and decidual cells, which showed a positive expression of miR-193b-3p, are playing a vital role to have proper placental function. Moreover, the dysregulation of their differentiation due to dysregulated miR-193b-3p expression may lead to pregnancy associated disease including PAS.

5.1.2. *Syncytialization*

Human placental villi are covered by STBs which are in direct contact with maternal blood representing a fetal-maternal barrier. They are formed by the fusion of underlying mononucleated CTB cells. Several mediators of STBs formation have been identified such as *syncytin-1* and *syncytin-2* (Dubey et al. 2018, Azar et al. 2018). The STBs layer is essential for performing several placental functions such as exchange of nutrients, gases, and waste between the mother and fetus. The production of pregnancy related hormones including β hCG and release of EVs contribute to the maternal adaptations to pregnancy. STBs do not express MHC class I or II (Tsuda et al. 2019) and employ several strategies to induce maternal immune tolerance.

BeWo cells are commonly used as an *in vitro* model of trophoblast syncytialization. They display basic functional and biochemical properties of STBs, have the capacity to fuse, and produce hormones such as β hCG, progesterone, and estradiol (Schulz et al. 2023, Tossetta et al. 2023, Nashif et al. 2023). Forskolin treatment can induce BeWo cell fusion, as reported in several studies (Kudo and Boyd 2002, Gauster and Huppertz 2010, Dubey et al. 2018). In our experiments, the expression of miR-193b-3p did not change after induction of BeWo syncytialization with forskolin. Nevertheless, BeWo cells transfected with the miR-193b-3p-mimic displayed a significant reduction in syncytialization, *syncytin-1* and *syncytin-2* expression and β hCG production. Interestingly, transfection with miR-193b-3p-inhibitor caused the opposite effects and confirmed that it may play a role in syncytialization. Measurement of syncytialization as a fusion index using E-cadherin immunofluorescence was established in our lab through this study. Even though miR-193b-3p levels are not regulated by trophoblast syncytialization, the maintenance of its basal levels is required for appropriate cell function. Consequently, alterations of miR-193b-3p expression in pathological conditions could influence syncytialization. For instance, the association between syncytialization and placenta development can be observed by the knockout of *syncytin-1* in mice, a molecule that was downregulated by miR-193b-3p in our assays. Deficiencies in CTBs fusion in these

animals led to embryonic lethality between 11.5 and 13.5 days of gestation (Dupressoir et al. 2009).

Syncytin-1 (ERVW-1) and *syncytin-2 (ERVFRD-1)* are placentally expressed ERV-derived fusogens (Schust et al. 2021). ERV are human endogenous retroviruses that have evolved from ancient infections of germ cells with viral DNA which occurred numerous times resulting in 8% of the human genome being retrovirus-derived (Bannert and Kurth 2004). A few ERV-encoded genes express envelope proteins that have fusogenic functions. ERVs generally have highly conserved immunosuppressive domains integrated into the transmembrane portions of their envelope proteins. Both ERVW-1 and ERVFRD-1 contain such domains that are responsible for immune regulation at the maternal–fetal interface (Groger and Cynis 2018). Therefore, changes in the expression of miR-193b-3p and syncytins may interfere not only with trophoblast syncytialization but also immune functions of the placenta.

hCG is a hormone produced by STBs that contributes to maintaining pregnancy via stimulating progesterone synthesis by the corpus luteum. It is composed of alpha and beta (β) subunits, the latter being released into maternal circulation by proteolytic cleavage in macrophages (Cole 2010, Cai et al. 2022). β hCG promotes angiogenesis, CTBs differentiation, and regulates the phagocytosis of invading trophoblast cells making it a useful marker of placental functions (Chandra et al. 2003). In a retrospective case control study, second-trimester β hCG levels were significantly higher in PAS group compared with NP (Tomasi 1977). On the other hand, first-trimester β hCG levels showed a significant decrease in the PAS group compared with the NP and placenta previa groups (Thompson et al. 2015). Alteration in β hCG levels was also reported to be associated with preeclampsia and IUGR (Huang et al. 2022, Peris et al. 2023). In our *in vitro* experiments, upregulation of miR-193b-3p in BeWo cells led to decreased levels of β hCG. Therefore, elevated levels of this miRNA in PAS may be associated with the lower levels of circulating β hCG.

Overall, miR-193b-3p has been shown to influence syncytium formation in STBs which are not invading trophoblast suggesting their influence on EVT's via paracrine signal. Previous study documented alternation in the expression of several molecules (downregulated: miR-34a, TGF- β , E-cadherin, EGF. Upregulated: EGFR, and TIMP1) in the STBs of PAS. These findings were hard to interpret from the researchers' points of view as STBs are not invasive trophoblasts. They assumed their finding as happening secondary to a focal environmental change in uteroplacental blood flow. Particularly, the changes in oxygen concentration within the intervillous space in the invasive areas (Jauniaux and Burton 2018). Although we observed

changes in BeWo syncytialization when the levels of miR-193b-3p were modulated, there are no studies showing alterations in syncytialization in PAS placentas. Further studies are warranted to investigate whether syncytialization is affected by miR-193b-3p upregulation and if this contributes to disease in PAS placentas.

5.1.3. *Cell migration*

EVTs migration through the maternal decidua constitutes a fundamental process for proper placental development. Around day 15 of pregnancy, EVT's begin to detach from cellular columns and further differentiate into iEVTs and enEVTs (Meakin et al. 2022). The former penetrates the endometrial stroma, and the latter invades the maternal spiral arteries leading to the establishment of low resistance and high flow rate vessels that improve nutrient and oxygen transport for the fetus (Knofler et al. 2019). EVT's migration is tightly regulated by MMPs and TIMPs. MMPs facilitate EVT's migration and invasion by ECM degradation, whereas TIMPs restrict them (Zhu et al. 2012). Trophoblast migration and invasion are tightly regulated by several growth factors through ERK, AKT, PI3K and other pathways (Pollheimer and Knofler 2005). Dysregulation of these signaling pathways leads to aberrant EVT's invasion, resulting in placenta diseases and poor pregnancy outcomes. This includes preeclampsia and IUGR in which shallow invasion has been observed (Kaufmann et al. 2003), early pregnancy loss in which lack of invasion was reported (Ball et al. 2006), and PAS in which excessive invasion was documented (Tantbirojn et al. 2008). Parra-Herran et al. reported that the mean depth of trophoblast myometrial invasion was greater in PAS (47.9%) than in NP (14.5%, $P = 0.004$) (Parra-Herran and Djordjevic 2016). Aberrant increase in trophoblast migration in PAS due to increased expression of molecules that stimulate cell migration have been reported in the literature. For instance, an elevated expression of *MMP-9*, *MMP-2* (Ke et al. 2006) and *DOCK4* (Gadea and Blangy 2014) was observed in PAS placentas.

To explore the role of miR-193b-3p in trophoblast migration and other functions, JEG-3 cells were employed instead of BeWo cells because the latter were reported to have considerable limitations in migration assays (Pastuschek et al. 2021). JEG-3 cell migration was evaluated through a wound healing assay monitored via live cell imaging. In agreement with the findings obtained with HTR-8/SVneo cells (Zhou et al., 2016), migration was also diminished after miR-193b-3p upregulation in JEG-3 cells. These data indicate that the effect of miR-193b-3p on migration is not cell-line-specific but rather conserved in different trophoblastic cells. This miRNA also enhances the migration of HNSCC cells (Lenarduzzi et al. 2013). In contrast, miR-193b-3p reduces migration in other cells such as lung cancer cells

(Hu et al. 2012), epidermal squamous cell carcinoma (Gastaldi et al. 2014), and breast cancer cells (Hashemi et al. 2018). Insufficient trophoblast migration is involved in preeclampsia and IUGR (Than et al. 2018), both being placental pathologies that showed increased expression of miR-193b-3p. There is currently no direct evidence that miR-193b-3p would be involved in enhanced trophoblast migration in PAS. Although miR-193b-3p expression is elevated in PAS placentas (Murrieta-Coxca et al. 2023), our data showed that miR-193b-3p reduced trophoblast migration. PAS is a multifactorial disease with aberrant expression of several miRNAs as previously shown in **Table 3**. Thus, the aberrant increase in the EVT's migration in PAS seems to be related to other miRNAs than miR-193b-3p.

5.1.4. *Proliferation and apoptosis*

Placental morphogenesis and growth are largely determined by trophoblast proliferation and apoptosis (Smith et al. 1997). At the early stages of pregnancy, the proliferation of CTBs enables the expansion of the placental villous tree by the emergence of new villi at any segment of existing ones (Sun et al. 2020). This process results in massive linear growth of terminal villi in the second trimester of pregnancy. Following this growth, CTBs proliferation is reduced, and apoptosis increased, features that persist until the end of pregnancy (Turco and Moffett 2019, Gauster et al. 2022). Impairments in the balance between trophoblast proliferation and apoptosis ultimately result in defective placentation. For instance, decreased trophoblast numbers were reported in FGR placentas due to decreased rates of proliferation and increased apoptosis rates (Chen et al. 2002, Mayhew et al. 2003). On the other hand, increased EVT's size and quantities were reported in PAS placentas (Jauniaux and Burton 2018).

In the current study, JEG-3 cell proliferation was examined after miR-193b-3p-mimic and -inhibitor transfection. Whereas the former had increased proliferation, the latter had reduced this process. Consistent with our findings, proliferation of human auricular chondrocytes (Chen et al. 2019b) and HNSCCs was promoted by miR-193b-3p (Lenarduzzi et al. 2013). In contrast, the proliferation of keratinocytes (Huang et al. 2021), lung cancer cells (Hu et al. 2012), ovarian cancer cells (Zhang et al. 2017b), epidermal squamous cell carcinoma (Gastaldi et al. 2014), and acute Myeloid Leukemia (AML) (Wang et al. 2021) was reduced by this miRNA.

In the present study, the apoptosis of JEG-3 cells was negatively regulated by miR-193b-3p. Conversely, this miRNA was documented to elevate apoptosis in breast cancer cells (Yang et al. 2019) and in AML (Wang et al. 2021). These differences can be attributed to different targets of miR-193b-3p with distinct functions in cell proliferation and apoptosis expressed in each cell type.

Elevated proliferation and decreased apoptosis were reported in the literature as main characteristics of PAS placentas. Dysregulated proliferation in PAS was suggested to be due to impaired senescence, a permanent proliferation arrest triggered by DNA damage pathways and cell cycle regulators. A higher expression of P15, P21 (Geffen et al. 2018), p53, p16, and p21 (Duan et al. 2020) and lower expression of P16, P53 (Geffen et al. 2018), and pRb (Duan et al. 2020) in PAS compared with NP was reported. These data suggest that altered expression of cell cycle inhibitors may contribute to PAS development. Reduced apoptosis in PAS coincides with decreased expression of INSL4 (Goh et al. 2013), which reduces trophoblasts proliferation and promotes apoptosis (Millar et al. 2005). In contrast, reduced proliferation and increased apoptosis were reported to be associated with preeclampsia and fetal growth restriction. For instance, lncRNA BNIP3P1 which is upregulated in preeclampsia leads to increase the trophoblast apoptosis and reduce their proliferation by targeting miR-128-3p/BNIP3/mTOR signaling pathway (Zheng et al. 2022). miR-1227-3p was down regulated the placentas of fetal growth restriction which was associated with increased apoptosis and reduced proliferation (Cui et al. 2022). Likewise, the increase in apoptotic characteristics and decreased expression of the anti-apoptotic protein, Bcl-2, in STBs was reported in FGR and preeclampsia placentas (Farah et al. 2020).

Altogether, our functional in vitro data showed that miR-193b-3p regulates trophoblast cells growth by enhancing proliferation and repressing apoptosis, which are common features of trophoblast cells in PAS, indicating upregulation of this miRNA could contribute to the pathogenesis of PAS.

5.1.5. *The effect of miR-193b-3p-containing EV on Jurkat T cells proliferation*

Successful pregnancy relies on fetal-maternal communication and the adaptation of immune cells to avoid maternal rejection. Moreover, the immune cells at the fetomaternal interface, including T cells, dendritic cell, and NK cells, play vital roles in trophoblastic cell invasion (Li et al. 2021b). Abnormal placental immune cell function may result in abnormal increase in trophoblast invasion triggering PAS development. For instance, an elevated lymphocytic infiltrate was reported at the implantation site of PAS placentas in comparison with placentas from maternal malignancy patients with no PAS symptoms (Ernst et al. 2017). Lower amounts of immature inactivated CD209⁺ dendritic cells and CD4⁺ T cells were found in PAS, whereas FoxP3⁺ T regs cells and CD25⁺ T cells were significantly increased. Such findings suggest that the excessive trophoblast invasion in PAS is associated with immunological malfunctions of the decidua hallmarked by inhibited T cell activation (Bartels

et al. 2018). dNK cells are a subset of NK cells that produce cytokines and angiogenic factors required for healthy pregnancy and play crucial roles in trophoblast invasion and spiral artery remodeling (Jabrane-Ferrat 2019). Reduced dNK populations were reported in PAS specimen, suggesting an inverse correlation between dNK and trophoblast invasion (Laban et al. 2014).

Fetal-maternal dialogue during implantation and placentation is mediated by placental EVs (Czernek and Duchler 2020) that regulate maternal metabolism and immune reactions (Stenqvist et al. 2013). To further investigate this association, Jurkat T cells, a well-established T-lymphocyte model (Abraham and Weiss 2004), were exposed to miR-193b-3p-enriched trophoblast EV fractions. TEM (for EV morphology), NTA (for size measurements) and Western blot (for marker expression) were applied during EVs characterization. The success of EVs enrichment protocol can be noticed by the results obtained from marker expression and the size profile of both lEVs (220.5 nm) and sEVs (120 nm) fractions. sEVs collected from JEG-3 cells and placenta perfusate express both CD63 and ALIX. Conversely, CD63 and ALIX were found to be nearly absent in lEVs. CD47 was expressed by both EV fractions collected from JEG-3 cells and placenta perfusate, although Tong et al. proposed that CD47 can be used for the differentiation between small and large placental EVs (Tong et al. 2016). This discrepancy could be attributable to differences in the starting material, since they collected EVs from first trimester placental explants whereas we used EVs from term placenta and trophoblastic cell lines. Alternatively, the use of different antibodies for CD47 detection could account for this discrepancy.

Increased levels of miR-193b-3p were observed in sEV and lEV fractions after miR-193b-3p-mimic transfection, demonstrating that EVs content reflects the intracellular miRNA abundance. In agreement with a previous work, trophoblastic EVs can be taken up by Jurkat T cells (Favaro et al. 2021). Culturing Jurkat T cells with both EVs fractions concurrently led to the uptake of both with a clear preference for lEVs. The reasons for that are unknown. EV_{miR-193b-3p} elevated miR-193b-3p levels in Jurkat T cells for up to 5 days. Moreover, lEV_{miR-193b-3p} triggered an elevated expression of miR-193b-3p than sEV_{miR-193b-3p}, mirroring the fact that the former has a higher amount of miR-193b-3p than sEV_{miR-193b-3p}, as examined by qPCR, and increased uptake.

RTCA was used to assess Jurkat T cell proliferation, confirmed by BrdU incorporation assay as a reference method. As the xCELLigence system relies mainly on cell adherence, monitoring of non-adherent cells such as leukemia or lymphoma requires an adherence, for which fibronectin was used. Two methods were found in the literature for coating the

xCELLigence E-plate. The first way was reported by (Obr et al. 2013, Martinez-Serra et al. 2014). They used extracellular matrix components including fibronectin, collagen, laminin, or gelatin that facilitate cell attachment. The other way was documented by (Guan et al. 2013, Fasbender and Watzl 2018). In their approach, they used antibodies to coat the plates. These antibodies were against antigens/markers expressed by the cells they use to adhere. For example, Guan et al. coated the E-16 plate with anti-CD3 and anti-CD28 to capture Jurkat T cells (Guan et al. 2013).

In my experiments, I decided to use fibronectin instead of antibodies. This decision was based on using a cost-effective approach, which can be applied to different cell types regardless of the antigens expressed by them. Additionally, we cannot exclude the possibility of having a side effect reaction that might be elicited after the binding of the antibody in the coated plate with the target cell. In our hands, the measurements of CI after Jurkat T cells attachment to fibronectin-coated plate compared to those obtained without fibronectin coating (almost no change in CI reading) confirmed the success of our approach. The use of RTCA to measure CI for non-adherent cells was established in our lab through this study. Our results showed that miR-193b-3p-enriched EVs decreased Jurkat T cell proliferation, which was also observed when miR-193b-3p-mimic was transfected to the cells, confirming the effect was due to miR-193b-3p.

In acute lymphoblastic leukaemia (T-ALL), miR-193b-3p was demonstrated to have tumor suppression activity by binding to MYB oncogene in T cell. Suppression of miR-193b-3p enhanced T-ALL onset in a mouse model (Mets et al. 2015). Furthermore, circ_0000745 ncRNA, which functions as a sponge to miR-193b-3p in T-ALL, caused improved cell proliferation and decreased cell apoptosis (Feng et al. 2021). Along with miR-9-5p, miR-193b-3p was shown to play a role in T helper 17 (Th17) differentiation by repressing the expression of negative regulators (Shirani et al. 2020). These reports demonstrate miR-193b-3p functions in regulating immune response. Further studies are required to investigate the functions of EV-containing miR-193b-3p in immunological processes of pregnancy.

5.1.6. Influence of miR-193b-3p downregulation on trophoblast cell proteome

Bioinformatics has been widely used to predict miRNA targets based on sequence complementarity between its 5' nucleotides 2 to 8 known as the seed region and the 3'UTR of the target mRNA (Friedman et al. 2009). Empirically, potential miRNA targets can be identified by proteomics. This can be carried out through up or downregulation of the miRNA of interest and tracing the resulting effects at the protein level using proteomic approaches (Xu et al. 2011).

In our proteomics study of JEG-3 cells transfected with miR-193b-3p-inhibitor compared to controls revealed 35 differentially expressed proteins. Careful analysis of proteomics data indicated other potential proteins that have the probability to be the primary targets of this miRNA as they were computationally predicted to have miR-193b-3p binding sites. Eleven targets, whose p values were significant or close to significance, were selected to be further examined by qPCR. Six targets (*K-Ras*, *AKT1*, *TMPPE*, *SHMT2*, *PTK2* and *MCL1*) in miR-193b-3p-mimic transfected JEG-3 were found to be downregulated. In miR-193b-3p-inhibitor transfected JEG-3, 6 targets (*K-Ras*, *TMPPE*, *PTK2*, *MCL1*, *NF1* and *ARPC5*) were upregulated. Three targets (*CALM1*, *YWHAZ* and *NF1*) were not confirmed by qPCR to be upregulated in miR-193b-3p-inhibitor transfected cells as they showed a tendency to be upregulated in miR-193b-3p-inhibitor transfected cells at the protein level. This could be attributed to several reasons including variation in transcriptional rates, mRNA stability for mRNA levels, and to protein synthesis and degradation rates for protein levels (Nicolet and Wolkers 2022). Moreover, protein abundance is controlled by a complex interrelated post-transcriptional process. Protein synthesis needs more energy than mRNA transcription, therefore the tissues will produce the required level of protein in tissue specific manner whereas mRNA production does not have the same tightly controlled mechanism for its transcription (Wegler et al. 2020).

The molecules that are potentially regulated by miR-193b-3p are further discussed below in relation to their association to trophoblast cell functions examined in this study (syncytialization, migration, proliferation, and apoptosis). When there was not enough information available, data from other cell types are discussed. **Figure 22** was generated gathering results of the current thesis and data from the literature as described below.

TMPPE was the most upregulated protein in JEG-3 cells transfected with miR-193b-3p inhibitor in our proteomic data and confirmed by qPCR and Western blot. The TMPPE is a protein with predicted hydrolase activity as well as metal ion binding activities and plasma membrane localization. So far, little is known about its functions. Hydrolases include helicases, nuclease, peptidase, glycosidase and lipase (UniPort. 2022a). No published work relates TMPPE with placenta and/or trophoblast although the protein atlas database shows that it is expressed by the placenta in decidual and trophoblast cells (Atlas. 2022). Regarding pathological conditions, Hall et al. focused on major Depressive Disorder (MDD), a common disabling chronic disorder in which genetic association has become proved to play an important role. They performed genome wide meta-analysis of MDD in male subjects and found in

3p22.3, a genome locus with three genes (*CRTAP*, *GLB1*, and *TMPPE*) differentially expressed in MDD cases compared to healthy subjects (Hall et al. 2018). This is thus so far, the only instance we are aware of where *TMPPE* has been linked with disease, albeit indirectly.

K-Ras is a guanine nucleotide-binding protein that is active when bound to GTP and inactive when bound to GDP. The three common Ras protooncogenes are H-Ras, N-Ras, and K-Ras. They activate the downstream RAF-MEK-ERK signaling pathway that is important for cell cycle regulation, apoptosis, and cell differentiation. K-Ras is essential for embryonic development in mice; however, non-functional H-Ras and N-Ras do not affect the development (Liong et al. 2018). In the present study, *K-Ras* mRNA was significantly upregulated in miR-193b-3p-inhibitor transfected cells and downregulated miR-193b-3p-mimic transfected cells. K-Ras and H-Ras stimulate the production of β hCG in CC1 human choriocarcinoma cell line transfected with these oncogenes (Watari 1995). This may explain the reduced expression of β hCG in miR-193b-3p-mimic transfected cells and the increased production of β hCG after miR-193b-3p-inhibitor transfected cells. To date, alterations in K-Ras have not been described in pregnancy-associated disorders. Only one study reported that K-Ras activity was significantly increased in the placenta of obese pregnant women (Liong et al. 2018). It has been reported that non-mutated K-Ras activation is involved in endometriosis, a gynecologic disorder in which endometrial cells are present outside the uterine cavity (Yoo et al. 2017). In osteosarcoma, upregulation of miR-577 inhibits proliferation and K-Ras is its primary target that is significantly downregulated. K-Ras upregulation has the ability to rescue proliferation (Qiao et al. 2022). In colorectal cancer, K-Ras was shown to be targeted by miR-16. Downregulation of K-Ras via miR-16 resulted in proliferation and invasion inhibition and apoptosis activation (Chen et al. 2019a). In non-small cell lung cancer, miR-193a-3p is decreased. K-Ras is a target of miR-193a-3p. *In vitro* upregulation of miR-193a-3p suppressed cell proliferation and migration (Fan et al. 2017). In addition, K-Ras is positively associated with increased proliferation, migration, and invasion of breast cancer cells. miR-502-5p is downregulated in breast cancer cells and K-Ras is its primary target (Li et al. 2021a). In contrast, K-Ras promotes apoptosis via targeting the RASSF family of tumor suppressors. RASSF2 facilitates a Ras-dependent cell cycle arrest and apoptotic death (Eckfeldt et al. 2004). Overall, K-Ras was reported to increase proliferation and migration; however, it was reported by one study to increase apoptosis and decrease apoptosis by another. Such data is consistent with our finding that K-Ras was involved in regulating such processes. The pattern of regulation; however, is different due to different cells and different miRNAs investigated in the corresponding studies.

MCL1 is a Bcl-2 family protein with two isoforms 1 and 2 that are involved in the regulation of apoptosis. Isoform 1 suppresses apoptosis whereas isoform 2 induces apoptosis (Michels et al. 2005). In our investigations, MCL1 was significantly upregulated in miR-193b-3p-inhibitor transfected cells. Conversely, it was significantly downregulated in miR-193b-3p-mimic transfected cells.

MCL1 has previously been reported to be involved in various pregnancy-associated disorders including hydatidiform moles (HMs), preeclampsia, IUGR, and PAS. Fong et al. found that MCL1 is elevated in HMs (Fong et al. 2005). In preeclampsia placental tissue, the pro-apoptotic MCL1 isoform is elevated (Soleymanlou et al. 2007). On the contrary, MCL1 expression level is decreased in IUGR (Rolfo et al. 2012). MCL1 is associated with excessive defects to exit mitosis and form senescent multinucleated cells in primary human fibroblasts. This positively correlated with activated Ras expression in those cells (Dikovskaya et al. 2015). The involvement of MCL1 in preeclampsia pathogenesis was demonstrated by another study in which MCL1 expression was downregulated in preeclampsia placentas, while miR-20b was highly expressed. *In vitro* studies demonstrated that miR-20a reduces HTR-8/SVneo proliferation, invasion, and migration. Additionally, the restoration of MCL1 levels impaired miR-20b effect on HTR-8/SVneo (Zhang et al. 2020).

MCL1 was investigated in PAS and was suggested as a target of miR-125a and miR-29a/b/c. Particularly, miR-125a was reported to be downregulated in PAS tissue while MCL1 was upregulated. *In vitro* studies indicated that overexpression of miR-125a increases apoptosis in the HTR-8/SVneo trophoblast line (Gu et al. 2019b). In a second study, MCL1 was shown to be the target of miR-29a/b/c. In this study, miR-29a/b/c was downregulated in PAS tissue and shown to induce apoptosis in HTR-8/SVneo trophoblast line (Gu et al. 2016).

Such findings suggest a role for MCL1 in various pregnancy diseases, which was shown by our study as a potential target of miR-193b-3p and may indicate a disease potential mechanism linking to miR-193b-3p.

AKT1 is a serine-threonine kinase that regulates cellular proliferation, differentiation, metabolism, and survival. We found that AKT1 expression was inversely correlated with the expression of miR-193b-3p at the mRNA and protein levels. AKT1 activation was shown in a previous study to be associated with increased proliferation, decreased apoptosis, and decreased migration in HTR-8/SVneo cells (Chaiwangyen et al. 2020). In agreement with our results on trophoblast migration, Haslinger et al. found that downregulation of AKT1 reduced migration of SGHPL-5 cells. However, the proliferation of the cells was not significantly changed after

AKT1 downregulation (Haslinger et al. 2013). Another recently published study reported that AKT1 is one of the miR-1227-3p targets. In that study, miR1227-3p increased HTR-8/SVneo cell proliferation and decreased apoptosis (Cui et al. 2022). This study agrees with our findings in which AKT1 was decreased after miR-193b-3p-mimic transfection of JEG-3 cells associated with increased cell proliferation and reduced apoptosis.

ARPC5 is 1 of 7 subunits of the human Arp2/3 protein complex. The Arp2/3 complex is a multiprotein assembly that mediates actin polymerization upon stimulation by nucleation-promoting factor. It mediates the formation of branched actin networks in the cytoplasm, providing the force for cell motility (UniPort. 2022b). In our experiments, *ARPC5* mRNA was significantly upregulated in miR-193b-3p-inhibitor transfected cells and downregulated in miR-193b-3p-mimic transfected cells as assessed by qPCR. We could not identify any previous studies that associate *ARPC5* with trophoblast function and/or placental pathology. Nevertheless, it is involved in cellular growth of multiple myeloma cells and tumor growth or metastasis of HNSCC and lung squamous cell carcinoma (Xiong and Luo 2018). In a study on HNSCC, *ARPC5* was revealed as a target of miR-133a. miR-133a functions as a tumor suppressor and is commonly downregulated in HNSCC. However, *ARPC5* expression is upregulated in cancer tissue. HNSCC cell lines have reduced migration and invasion after *ARPC5* silencing (Kinoshita et al. 2012). The results in HNSCC cells are in accordance with our findings, as JEG-3 cells transfected with miR-193b-3p-mimic presented decreased expression of *ARPC5* and decreased migration.

SHMT2, a mitochondrial pyridoxal phosphate binding protein, responsible for serine cleavage to glycine associated with 5, 10-methylenetetrahydrofolate (5, 10-CH₂-THF) production, which is a key intermediary for purine biosynthesis. *SHMT2* is under the direct control of c-myc for cell survival during hypoxia, and its expression contributes to glioma cell survival in ischemia (Yang et al. 2018). In the current study, *SHMT2* was significantly downregulated after miR-193b-3p-mimic transfection and upregulated after miR-193b-3p-inhibitor transfection. To date, there are no reports relating *SHMT2* with placenta pathology and/or trophoblast functions. However, *SHMT2* was reported to suppress apoptosis, and promote tumor cell growth in bladder cancer (Zhang and Yang 2021) and hepatocellular carcinoma (Ji et al. 2019). Moreover, knockdown of *SHMT2* leads to a reduction in colorectal and prostate cancer proliferation, migration, and invasion (Liu et al. 2021, Chen et al. 2022). *SHMT2* has been shown to reduce apoptosis and increase migration as well as proliferation of breast cancer cells (Qi et al. 2020). This could explain the reduced JEG-3 cells migration after

miR-193b-3p-mimic transfection and decreased *SHMT2* expression. Nevertheless, we had decreased apoptosis and increased proliferation in miR-193b-3p-mimic transfected JEG-3 cells. This can be attributed to the distinct cell types used in different studies.

PTK2 or focal adhesion kinase (FAK) is a ubiquitously expressed non-receptor tyrosine kinase with a role in regulating the cell shape and adhesion in response to environmental signals (Zhang et al. 2014). In the present study, *PTK2* was significantly downregulated after miR-193b-3p-mimic transfection and significantly upregulated after miR-193b-3p-inhibitor transfection. Although there are no reports to date indicating that FAK has a role in placental diseases, this molecule is involved in trophoblast function. FAK activation by phosphorylation has been shown to increase EVT's migration and proliferation (MacPhee et al. 2001). Reduced FAK expression resulted in decreased migration of villous explant cultures and impaired invasion of isolated CTBs via Matrigel-coated chambers (Pollheimer and Knofler 2005). Although in our study JEG-3 proliferation was increased, their migration was decreased and potentially links back to downregulated FAK levels similar to what was described by (MacPhee et al. 2001) and (Pollheimer and Knofler 2005).

Neurofibromin is a large and multifunctional protein encoded by the tumor suppressor gene *NFI*. Inherited or de novo germline mutation in *NFI* leads to autosomal dominant disorder called Neurofibromatosis type 1 (Philpott et al. 2017). This disorder is characterized by pigmentary lesions and various types of peripheral nervous system tumors (Bergoug et al. 2020). Neurofibromin suppresses the Ras signaling pathway and the mutated form leads to abnormal Ras activity resulting in Neurofibromatosis type 1 (Agarwal et al. 2014). Mice embryonic death was detected when *NFI* functionality was lost, showing the importance of *NFI* for embryonic development (Henkemeyer et al. 1995). In the current study, *NFI* mRNA was downregulated after miR-193b-3p-mimic transfection and significantly upregulated after miR-193b-3p-inhibitor transfection. To date, there are no reports linking NF1 with placenta pathology and/or trophoblast functions.

NF1 has been reported to be inversely correlated with neural stem cell proliferation (Wegscheid et al. 2021). Additionally, increased Ras activity was noticed in *NFI*-deficient (*NFI*^{-/-}) hematopoietic cells (Zhang et al. 1998). Consistent with this observation, the absence of neurofibromin promotes CRMP2 phosphorylation, which is required for cell proliferation and survival (Moutal et al. 2017). Additionally, NF1 was reported to inhibit *MCL1* expression and decrease ovarian cells apoptosis (Su et al. 2019). Further work is needed to confirm whether the downregulation of MCL1 that we observed caused by miR-193b-3p-mimic transfection was

due its downregulation NF1 expression. A recent study showed that *NFI* downregulation via miR-27a-3p and miR-27b-3p leads to increase proliferation, migration, invasion and reduce apoptosis of human Schwann cells (Lu et al. 2021). Our finding in JEG-3 proliferation (increased) an apoptosis (decreased) together with decreased expression of *NFI*, are consistent with the aforementioned studies (Lu et al. 2021) and (Su et al. 2019). However, we observed decreased migration with *NFI* downregulation, indicating different roles of this molecule in different cell types.

HSD17B1 is a steroidogenic enzyme catalyzing the conversion of estrone to 17 β -estradiol (Peltoketo et al. 1999). In the present study, HSD17B1 was significantly upregulated in miR-193b-3p-inhibitor transfected cells. However, bioinformatics analysis did not identify HSD17B1 as a primary target of miR-193b-3p. Therefore, this molecule could be a downstream mediator of pathways regulated by miR-193b-3p. STBs and granulosa cells of the ovaries, which are involved in estrogen biosynthesis, express HSD17B1 (Luu-The et al. 1990). HSD17B1 expression is upregulated by FSH, LH, GH, and EGF (McGee and Hsueh 2000). HSD17B1 and estrogen-related receptor γ (ERR γ) are downregulated in FGR and miR-424 is upregulated. ERR γ is not a direct target of miR-424 but *in vitro* studies confirmed that ERR γ and HSD17B1 expression is inversely correlated to the expression of miR-424. This indicates that miR-424 has the possibility to mediate the expression of ERR γ via binding to sites other than mRNA 3'UTR. Additionally, upregulation of miR-424 decreased trophoblast-derived cell line invasion and proliferation (Zou et al. 2019). In another study, 22 miRNAs are significantly upregulated in preeclampsia. miR-210 and miR-518c were identified as targeting HSD17B1. HSD17B1 is significantly downregulated in preeclampsia placentas and plasma. The significant reduction in HSD17B1 is also observed in pregnant women at 20 to 23 and 27 to 30 weeks of gestation before the onset of preeclampsia. Therefore, HSD17B1 may be considered as a prognostic factor for preeclampsia development (Ishibashi et al. 2012). We found increased HSD17B1 expression after miR-193b-3p downregulation in JEG-3 cell. If HSD17B1 is also regulated by miR-193b-3p *in vivo*, dysregulation of this miRNA in placenta pathology may alter HSD17B1 levels. Therefore, HSD17B1 should be also investigated in these placenta and plasma.

Overall, qPCR and proteomic approaches after manipulating miR-193b-3p expression in combination with bioinformatics enabled identification of potential targets of this miRNA in trophoblast cells. Further analyses are required to distinguish which ones are direct targets of miR-193b-3p from those that are secondary mediators of this miRNA. This will require the

employment of additional experimental strategies, for instance, through luciferase reporter assays (Ritchie et al. 2013).

Nevertheless, there are some limitations to the current study. First, although I used two trophoblastic cell line models due to the absence of animal models, the experiments were *in vitro*. Second, the expression of miR-193b-3p should be examined in the peripheral blood of pregnant women and compare it to PAS, preeclampsia, or other pregnancy diseases to assess its use in preventing and/or monitoring pregnancy complications. Third, the western blot verification was done once for AKT1 and TMPPE as I could not get replicates. For future studies, AKT1, TMPPE, K-RAS, MCL-1 as well as other proteins should be verified with adequate number of replicates. Finally, TMPPE, K-Ras, and MCL1 should be further studied in the trophoblastic functions which are related to pregnancy disorder development to reveal their biological roles and explore their potential as diagnostic markers or targets for therapeutic intervention.

6. CONCLUSIONS

Due to their ability to fine-tune the expression of genes, miRNAs are critical players in regulating cellular processes that are fundamental for placenta development and function. In the current study, miR-193b-3p is expressed by trophoblast cells present in the villi (STBs) and decidua (enEVT and iEVT) and in non-trophoblast cells (cytokeratin-7 negative) present in the decidua of human placentas. These results reinforce the current concepts in which alterations in both trophoblast and decidua contribute to potential complication during pregnancy.

Using trophoblastic cell lines in which the expression of miR-193b-3p was manipulated, it was demonstrated that this miRNA regulates main trophoblastic cell functions. miR-193b-3p upregulation reduced trophoblast migration, apoptosis, and syncytialization as well as increased proliferation. Accordingly, the downregulation of this miRNA had the opposite effects. Analyses by qPCR, proteomics, and bioinformatics found eight potential targets of miR-193b-3p in JEG-3 trophoblastic cells. Their influence on cellular processes were predicted from the literature and shown in **Fig. 22**. *MCL1*, *K-Ras*, *PTK2*, and *TMPPE* were significantly upregulated in miR-193b-3p-inhibitor transfected cells and significantly downregulated in miR-193b-3p-mimic transfected cells indicating a correlation between them. These molecules may mediate the effects of miR-193b-3p on trophoblast cells.

The content of EVs produced by trophoblast cells transfected with miR-193b-3p-mimic reflected the elevated cytoplasmic levels of this miRNA. Jurkat T cells were able to incorporate both IEVs and sEVs, with a clear preference to the former, leading to elevated levels of miR-193b-3p that lasted for 5 days. miR-193b-3p-enriched EVs reduced Jurkat T cell proliferation, indicating the role of this miRNA in mediating the communication between the placenta and maternal immune cells. If elevated levels of placental miR-193b-3p can be detected in maternal plasma, it may be used as a biomarker of pregnancy related diseases and benefits from the sensitivity of qPCR-based detection methods.

Collectively, the results from this study demonstrated that miR-193b-3p regulates trophoblast cell functions. Therefore, the dysregulation of miR-193b-3p in placenta may contribute to its pathogenesis through changes in trophoblast cell functions. Further studies are warranted to deepen our knowledge of miR-193b-3p functions in trophoblast cells and its association with various pregnancy disorders.

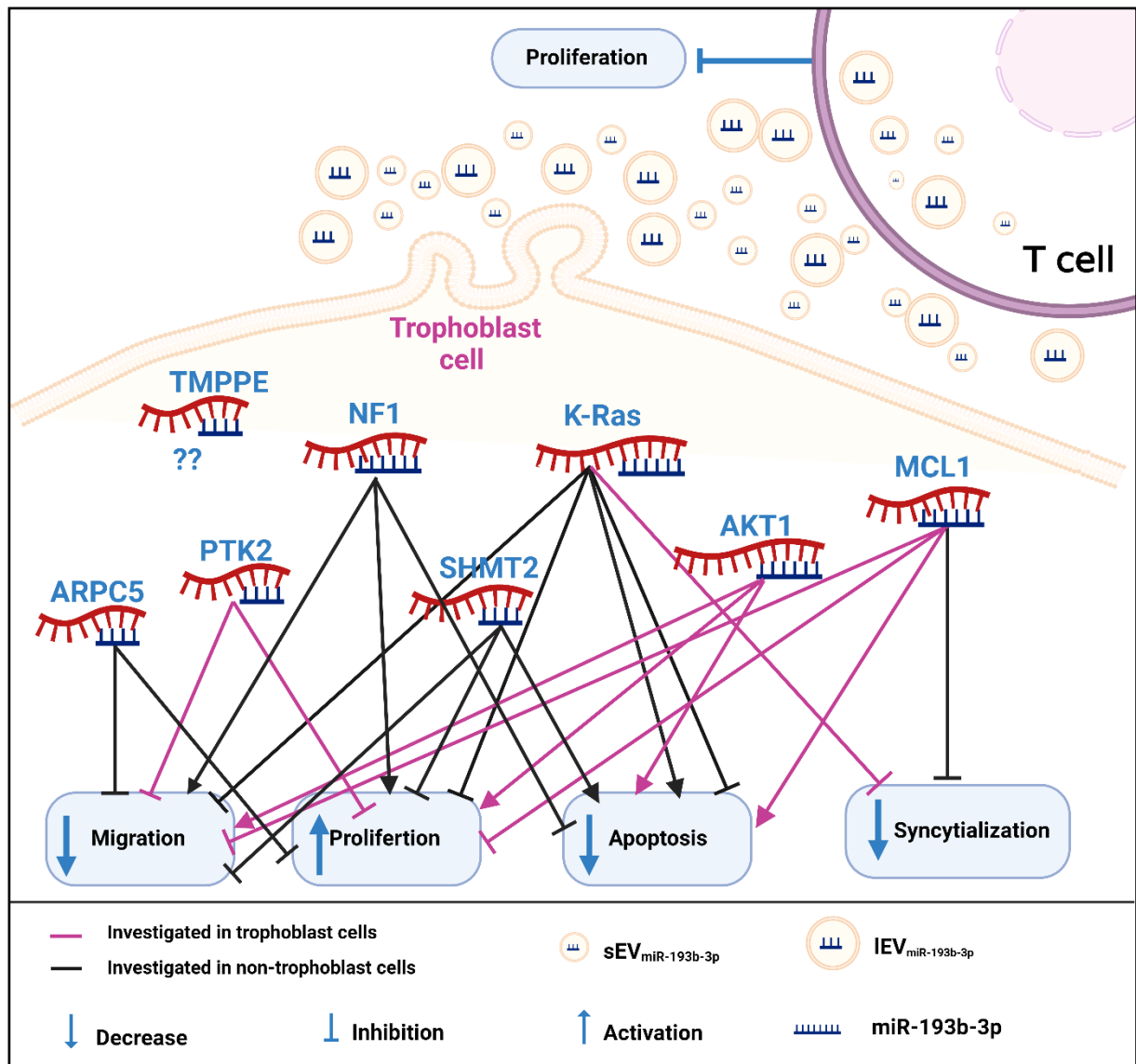


Figure 22. Potential targets of miR-193b-3p and their effects on cellular processes. This schematic model was produced using data generated in this thesis and from the literature. miR-193b-3p reduced migration, apoptosis, and syncytialization as well as enhanced proliferation in trophoblast cells. The potential mRNA targets of miR-193b-3p were identified by qPCR, proteomics, and bioinformatics tools. Their influence on cellular processes was extracted from published research on trophoblast (pink lines) and non-trophoblast cells (black lines). No functional studies were found to be related to TMPPE. sEV_{miR-193b-3p} and lEV_{miR-193b-3p} produced from miR-193b-3p-mimic transfected trophoblast cells are taken up by Jurkat T cells resulting in a decrease in their proliferation. sEV_{miR-193b-3p}: miR-193b-3p-enriched small extracellular vesicles and lEV_{miR-193b-3p}: miR-193b-3p-enriched large extracellular vesicles (Created with BioRender.com).

REFERENCES

- Abels ER, Breakefield XO. 2016. Introduction to Extracellular Vesicles: Biogenesis, RNA Cargo Selection, Content, Release, and Uptake. *Cell Mol Neurobiol*, 36 (3):301-312.
- Abou-Kheir W, Eid A, El-Merahbi R, Assaf R, Daoud G. 2015. A Unique Expression of Keratin 14 in a Subset of Trophoblast Cells. *PLoS One*, 10 (10):e0139939.
- Abraham RT, Weiss A. 2004. Jurkat T cells and development of the T-cell receptor signalling paradigm. *Nat Rev Immunol*, 4 (4):301-308.
- Adamczyk K. 2017. *Epidemiologische Untersuchungen zu Trophoblastinvasionsstörungen* Jena: Jena University Hospital.
- Addo KA, Palakodety N, Hartwell HJ, Tingare A, Fry RC. 2020. Placental microRNAs: Responders to environmental chemicals and mediators of pathophysiology of the human placenta. *Toxicol Rep*, 7:1046-1056.
- Agarwal R, Liebe S, Turski ML, Vidwans SJ, Janku F, Garrido-Laguna I, Munoz J, Schwab R, Rodon J, Kurzrock R, Subbiah V, Pan-Cancer Working G. 2014. Targeted therapy for hereditary cancer syndromes: neurofibromatosis type 1, neurofibromatosis type 2, and Gorlin syndrome. *Discov Med*, 18 (101):323-330.
- Aplin JD, Jones CJP. 2021. Cell dynamics in human villous trophoblast. *Hum Reprod Update*, 27 (5):904-922.
- Arakaza A, Zou L, Zhu J. 2023. Placenta Accreta Spectrum Diagnosis Challenges and Controversies in Current Obstetrics: A Review. *Int J Womens Health*, 15:635-654.
- Armstrong CA, Harding S, Matthews T, Dickinson JE. 2004. Is placenta accreta catching up with us? *Australian & New Zealand Journal of Obstetrics & Gynaecology*, 44 (3):210-213.
- Atlas. THP 2022. TMPPE Retrieved from <https://www.proteinatlas.org/ENSG00000188167-TMPPE/tissue/placenta#>.
- Awamleh Z, Gloor GB, Han VKM. 2019. Placental microRNAs in pregnancies with early onset intrauterine growth restriction and preeclampsia: potential impact on gene expression and pathophysiology. *BMC Med Genomics*, 12 (1):91.
- Azar C, Valentine M, Trausch-Azar J, Druley T, Nelson DM, Schwartz AL. 2018. RNA-Seq identifies genes whose proteins are transformative in the differentiation of cytotrophoblast to syncytiotrophoblast, in human primary villous and BeWo trophoblasts. *Sci Rep*, 8 (1):5142.
- Bahar A, Abusham A, Eskandar M, Sobande A, Alsunaidi M. 2009. Risk factors and pregnancy outcome in different types of placenta previa. *J Obstet Gynaecol Can*, 31 (2):126-131.
- Bailit JL, Grobman WA, Rice MM, Reddy UM, Wapner RJ, Varner MW, Leveno KJ, Iams JD, Tita ATN, Saade G, Rouse DJ, Blackwell SC, Eunice Kennedy Shriver National Institute of Child H, Human Development Maternal-Fetal Medicine Units N. 2015. Morbidly adherent placenta treatments and outcomes. *Obstet Gynecol*, 125 (3):683-689.
- Baldwin HJ, Patterson JA, Nippita TA, Torvaldsen S, Ibiebele I, Simpson JM, Ford JB. 2017. Maternal and neonatal outcomes following abnormally invasive placenta: a population-based record linkage study. *Acta Obstet Gynecol Scand*, 96 (11):1373-1381.
- Ball E, Bulmer JN, Ayis S, Lyall F, Robson SC. 2006. Late sporadic miscarriage is associated with abnormalities in spiral artery transformation and trophoblast invasion. *Journal of Pathology*, 208 (4):535-542.
- Banfalvi G. 2017. Methods to detect apoptotic cell death. *Apoptosis*, 22 (2):306-323.
- Bannert N, Kurth R. 2004. Retroelements and the human genome: new perspectives on an old relation. *Proc Natl Acad Sci U S A*, 101 Suppl 2:14572-14579.
- Bartels HC, Postle JD, Downey P, Brennan DJ. 2018. Placenta Accreta Spectrum: A Review of Pathology, Molecular Biology, and Biomarkers. *Dis Markers*, 2018:1507674.
- Bartels HC, Walsh JM, O'Connor C, McParland P, Carroll S, Higgins S, Mulligan KM, Downey P, Brophy D, Colleran G, Thompson C, Walsh T, O'Brien DJ, Brennan DJ, McVey R,

- McAuliffe FM, Donnelly J, Corcoran SM. 2023. Placenta accreta spectrum ultrasound stage and fetal growth. *Int J Gynaecol Obstet*, 160 (3):955-961.
- Bass-Stringer S, Ooi JYY, McMullen JR. 2020. Clusterin is regulated by IGF1-PI3K signaling in the heart: implications for biomarker and drug target discovery, and cardiotoxicity. *Archives of Toxicology*, 94 (5):1763-1768.
- Bassetty KC, Vijayaselvi R, Yadav B, David LS, Beck MM. 2021. Placenta accreta spectrum: Management and outcomes in a tertiary centre in India: An observational cross-sectional study. *Trop Doct*, 51 (3):398-403.
- Basu J, Agamasu E, Bendek B, Salafia CM, Mishra A, Lopez JV, Kroes J, Dragich SC, Thakur A, Mikhail M. 2018. Correlation Between Placental Matrix Metalloproteinase 9 and Tumor Necrosis Factor-alpha Protein Expression Throughout Gestation in Normal Human Pregnancy. *Reprod Sci*, 25 (4):621-627.
- Bencaiova G, Burkhardt T, Beinder E. 2007. Abnormal placental invasion experience at 1 center. *J Reprod Med*, 52 (8):709-714.
- Bergoug M, Doudeau M, Godin F, Mosrin C, Vallee B, Benedetti H. 2020. Neurofibromin Structure, Functions and Regulation. *Cells*, 9 (11):2365.
- Bloomfield G, Kay RR. 2016. Uses and abuses of macropinocytosis. *J Cell Sci*, 129 (14):2697-2705.
- Bobadilla AVP, Arevalo J, Sarro E, Byrne HM, Maini PK, Carraro T, Balocco S, Meseguer A, Alarcon T. 2019. In vitro cell migration quantification method for scratch assays. *J R Soc Interface*, 16 (151):20180709.
- Breen JL, Neubecker R, Gregori CA, Franklin JE, Jr. 1977. Placenta accreta, increta, and percreta. A survey of 40 cases. *Obstet Gynecol*, 49 (1):43-47.
- Budhu A, Ji J, Wang XW. 2010. The clinical potential of microRNAs. *J Hematol Oncol*, 3:37.
- Burandt E, Lubbersmeyer F, Gorbokon N, Buscheck F, Luebke AM, Menz A, Kluth M, Hube-Magg C, Hinsch A, Hoflmayer D, Weidemann S, Fraune C, Moller K, Jacobsen F, Lebok P, Clauditz TS, Sauter G, Simon R, Uhlig R, Wilczak W, Steurer S, Minner S, Krech R, Dum D, Krech T, Marx AH, Bernreuther C. 2021. E-Cadherin expression in human tumors: a tissue microarray study on 10,851 tumors. *Biomark Res*, 9 (1):1-17.
- Burton GJ, Cindrova-Davies T, Turco MY. 2020. Review: Histotrophic nutrition and the placental-endometrial dialogue during human early pregnancy. *Placenta*, 102:21-26.
- Burton GJ, Jauniaux E. 2015. What is the placenta? *Am J Obstet Gynecol*, 213 (4 Suppl):S6 e1, S6-8.
- Butler TM, Elustondo PA, Hannigan GE, MacPhee DJ. 2009. Integrin-linked kinase can facilitate syncytialization and hormonal differentiation of the human trophoblast-derived BeWo cell line. *Reprod Biol Endocrinol*, 7 (1):1-14.
- Cai S, Lin R, Liu S, Wang X, Wei H, Huang C, Li Y, Chen X, Li L, Zeng Y, Lian R, Diao L. 2022. Intrauterine infusion of human chorionic gonadotropin improves the endometrial FoxP3(+) Tregs level and pregnancy outcomes in patients with lower endometrial FoxP3(+) Tregs. *J Reprod Immunol*, 153:103678.
- Cai X, Hagedorn C, Cullen B. 2004. Human microRNAs are processed from capped, polyadenylated transcripts that can also function as mRNAs. *RNA*, 10:1957-1966.
- Carusi D. 2017. Placenta Accreta: Epidemiology and Risk Factors In: Silver R, Hrsg. *Placenta Accreta Syndrom*. Taylor & Francis Group, LLC.
- Cha J, Sun X, Dey SK. 2012a. Mechanisms of implantation: strategies for successful pregnancy. *Nat Med*, 18 (12):1754-1767.
- Cha JY, Sun XF, Dey SK. 2012b. Mechanisms of implantation: strategies for successful pregnancy. *Nature Medicine*, 18 (12):1754-1767.
- Chaiwangyen W, Murrieta-Coxca JM, Favaro RR, Photini SM, Gutierrez-Samudio RN, Schleussner E, Markert UR, Morales-Prieto DM. 2020. MiR-519d-3p in Trophoblastic

- Cells: Effects, Targets and Transfer to Allogeneic Immune Cells via Extracellular Vesicles. *Int J Mol Sci*, 21 (10).
- Chandra S, Scott H, Dodds L, Watts C, Blight C, Van Den Hof M. 2003. Unexplained elevated maternal serum alpha-fetoprotein and/or human chorionic gonadotropin and the risk of adverse outcomes. *Am J Obstet Gynecol*, 189 (3):775-781.
- Chang ZK, Meng FG, Zhang ZQ, Mao GP, Huang ZY, Liao WM, He AS. 2018. MicroRNA-193b-3p regulates matrix metalloproteinase 19 expression in interleukin-1beta-induced human chondrocytes. *J Cell Biochem*, 119 (6):4775-4782.
- Chen CP, Bajoria R, Aplin JD. 2002. Decreased vascularization and cell proliferation in placentas of intrauterine growth-restricted fetuses with abnormal umbilical artery flow velocity waveforms. *Am J Obstet Gynecol*, 187 (3):764-769.
- Chen CP, Chen LF, Yang SR, Chen CY, Ko CC, Chang GD, Chen H. 2008. Functional characterization of the human placental fusogenic membrane protein syncytin 2. *Biol Reprod*, 79 (5):815-823.
- Chen JH, Yan CN, Yu HH, Zhen SH, Yuan Q. 2019a. miR-548d-3p inhibits osteosarcoma by downregulating KRAS. *Aging-Us*, 11 (14):5058-5069.
- Chen K, Rajewsky N. 2007. The evolution of gene regulation by transcription factors and microRNAs. *Nature Reviews | Genetics*, 8:93-103.
- Chen L, Liu H, Ji Y, Ma Z, Shen K, Shangguan X, Qian H, Zhao Y, Pan CW, Xue W. 2022. Downregulation of SHMT2 promotes the prostate cancer proliferation and metastasis by inducing epithelial-mesenchymal transition. *Exp Cell Res*, 415 (2):113138.
- Chen S, Pang D, Li Y, Zhou J, Liu Y, Yang S, Liang K, Yu B. 2020. Serum miRNA biomarker discovery for placenta accreta spectrum. *Placenta*, 101:215-220.
- Chen X, Zhang RH, Zhang Q, Xu ZC, Xu F, Li DT, Li YY. 2019b. Chondrocyte sheet in vivo cartilage regeneration technique using miR-193b-3p to target MMP16. *Aging-Us*, 11 (17):7070-7082.
- Cheong ML, Wang LJ, Chuang PY, Chang CW, Lee YS, Lo HF, Tsai MS, Chen HW. 2016. A Positive Feedback Loop between Glial Cells Missing 1 and Human Chorionic Gonadotropin (hCG) Regulates Placental hCG beta Expression and Cell Differentiation. *Molecular and Cellular Biology*, 36 (1):197-209.
- Chew SY. 1980. Placental accreta. *Singapore Med J*, 21 (5):699-702.
- Chiu RW, Lo YM. 2010. Pregnancy-associated microRNAs in maternal plasma: a channel for fetal-maternal communication? *Clin Chem*, 56 (11):1656-1657.
- Chiu RW, Lo YM. 2013. Clinical applications of maternal plasma fetal DNA analysis: translating the fruits of 15 years of research. *Clin Chem Lab Med*, 51 (1):197-204.
- Choi WY, Giraldez AJ, Schier AF. 2007. Target protectors reveal dampening and balancing of Nodal agonist and antagonist by miR-430. *Science*, 318 (5848):271-274.
- Cole LA. 2010. Biological functions of hCG and hCG-related molecules. *Reprod Biol Endocrinol*, 8 (1):1-14.
- Conturie CL, Lyell DJ. 2022. Prenatal diagnosis of placenta accreta spectrum. *Curr Opin Obstet Gynecol*, 34 (2):90-99.
- Cortina ME, Litwin S, Rial Hawila MR, Miranda S. 2017. Multiparity upregulates placental plasminogen and urokinase-type plasminogen activator. *Am J Reprod Immunol*, 77 (4):e12633.
- Crha K, Ventruba P, Zakova J, Jeseta M, Pilka R, Vodicka J, Serpa P. 2019. The role of mesenchymal-epithelial transition in endometrial function and receptivity. *Ceska Gynekologie-Czech Gynaecology*, 84 (5):371-375.
- Cui J, Kang X, Shan Y, Zhang M, Gao Y, Wu W, Chen L. 2022. miR-1227-3p participates in the development of fetal growth restriction via regulating trophoblast cell proliferation and apoptosis. *Sci Rep*, 12 (1):6374.

- Czernek L, Duchler M. 2020. Exosomes as Messengers between Mother and Fetus in Pregnancy. *Int J Mol Sci*, 21 (12): 4264-4281.
- Daltveit AK, Tollanes MC, Pihlstrom H, Irgens LM. 2008. Cesarean delivery and subsequent pregnancies. *Obstet Gynecol*, 111 (6):1327-1334.
- Daskalakis G, Anastasakis E, Papantoniou N, Mesogitis S, Theodora M, Antsaklis A. 2007. Emergency obstetric hysterectomy. *Acta Obstet Gynecol Scand*, 86 (2):223-227.
- Dikovskaya D, Cole JJ, Mason SM, Nixon C, Karim SA, McGarry L, Clark W, Hewitt RN, Sammons MA, Zhu JJ, Athineos D, Leach JDG, Marchesi F, van Tuyn J, Tait SW, Brock C, Morton JP, Wu H, Berger SL, Blyth K, Adams PD. 2015. Mitotic Stress Is an Integral Part of the Oncogene-Induced Senescence Program that Promotes Multinucleation and Cell Cycle Arrest. *Cell Reports*, 12 (9):1483-1496.
- Dini P, Daels P, Loux SC, Esteller-Vico A, Carossino M, Scoggin KE, Ball BA. 2018. Kinetics of the chromosome 14 microRNA cluster ortholog and its potential role during placental development in the pregnant mare. *BMC Genomics*, 19 (1):1-21.
- Dini P, El-Sheikh Ali H, Carossino M, S CL, Esteller-Vico A, K ES, Daels P, B AB. 2019. Expression Profile of the Chromosome 14 MicroRNA Cluster (C14MC) Ortholog in Equine Maternal Circulation throughout Pregnancy and Its Potential Implications. *Int J Mol Sci*, 20 (24):6285.
- Donker RB, Mouillet JF, Chu T, Hubel CA, Stolz DB, Morelli AE, Sadovsky Y. 2012. The expression profile of C19MC microRNAs in primary human trophoblast cells and exosomes. *Mol Hum Reprod*, 18 (8):417-424.
- Doyle LM, Wang MZ. 2019. Overview of Extracellular Vesicles, Their Origin, Composition, Purpose, and Methods for Exosome Isolation and Analysis. *Cells*, 8 (7):727.
- Duan LY, Schimmelmann M, Wu YQ, Reisch B, Faas M, Kimmig R, Winterhager E, Koninger A, Gellhaus A. 2020. CCN3 Signaling Is Differently Regulated in Placental Diseases Preeclampsia and Abnormally Invasive Placenta. *Frontiers in Endocrinology*, 11:597549.
- Dubey R, Malhotra SS, Gupta SK. 2018. Forskolin-mediated BeWo cell fusion involves down-regulation of miR-92a-1-5p that targets dysferlin and protein kinase cAMP-activated catalytic subunit alpha. *American Journal of Reproductive Immunology*, 79 (6):e12834.
- Dupressoir A, Vernochet C, Bawa O, Harper F, Pierron G, Opolon P, Heidmann T. 2009. Syncytin-A knockout mice demonstrate the critical role in placentation of a fusogenic, endogenous retrovirus-derived, envelope gene. *Proc Natl Acad Sci U S A*, 106 (29):12127-12132.
- Durnaoglu S, Lee SK, Ahn J. 2021. Syncytin, envelope protein of human endogenous retrovirus (HERV): no longer 'fossil' in human genome. *Animal Cells and Systems*, 25 (6):358-368.
- Dyer I, Miller HK, Mc LJ, Jr. 1954. Placenta accreta; a 15 year study at Charity Hospital and Touro Infirmary in New Orleans. *J La State Med Soc*, 106 (1):12-18.
- Eckfeld K, Hesson L, Vos MD, Bieche I, Latif F, Clark GJ. 2004. RASSF4/AD037 is a potential ras effector/tumor suppressor of the RASSF family. *Cancer Res*, 64 (23):8688-8693.
- Einerson BD, Comstock J, Silver RM, Branch DW, Woodward PJ, Kennedy A. 2020. Placenta Accreta Spectrum Disorder: Uterine Dehiscence, Not Placental Invasion. *Obstet Gynecol*, 135 (5):1104-1111.
- El Gelany S, Mosbeh MH, Ibrahim EM, Mohammed M, Khalifa EM, Abdelhakium AK, Yousef AM, Hassan H, Goma K, Alghany AA, Mohammed HF, Azmy AM, Ali WA, Abdelraheim AR. 2019. Placenta Accreta Spectrum (PAS) disorders: incidence, risk factors and outcomes of different management strategies in a tertiary referral hospital in Minia, Egypt: a prospective study. *BMC Pregnancy Childbirth*, 19 (1):1-8.
- Eller AG, Porter TF, Soisson P, Silver RM. 2009. Optimal management strategies for placenta accreta. *BJOG*, 116 (5):648-654.

- Ernst LM, Linn RL, Minturn L, Miller ES. 2017. Placental Pathologic Associations With Morbidly Adherent Placenta: Potential Insights Into Pathogenesis. *Pediatric and Developmental Pathology*, 20 (5):387-393.
- Esau C, Davis S, Murray SF, Yu XX, Pandey SK, Pear M, Watts L, Booten SL, Graham M, McKay R, Subramaniam A, Propp S, Lollo BA, Freier S, Bennett CF, Bhanot S, Monia BP. 2006. miR-122 regulation of lipid metabolism revealed by in vivo antisense targeting. *Cell Metab*, 3 (2):87-98.
- Escudero CA, Herlitz K, Troncoso F, Acurio J, Aguayo C, Roberts JM, Truong G, Duncombe G, Rice G, Salomon C. 2016. Role of Extracellular Vesicles and microRNAs on Dysfunctional Angiogenesis during Preeclamptic Pregnancies. *Front Physiol*, 7:98.
- Esh-Broder E, Ariel I, Abas-Bashir N, Bdolah Y, Celnikier DH. 2011. Placenta accreta is associated with IVF pregnancies: a retrospective chart review. *BJOG*, 118 (9):1084-1089.
- Eshkoli T, Weintraub AY, Sergienko R, Sheiner E. 2013. Placenta accreta: risk factors, perinatal outcomes, and consequences for subsequent births. *Am J Obstet Gynecol*, 208 (3):219 e211-217.
- Ewert KK, Zidovska A, Ahmad A, Bouxsein NF, Evans HM, McAllister CS, Samuel CE, Safinya CR. 2010. Cationic liposome-nucleic acid complexes for gene delivery and silencing: pathways and mechanisms for plasmid DNA and siRNA. *Top Curr Chem*, 296:191-226.
- Fan Q, Hu XT, Zhang HY, Wang SG, Zhang HL, You CY, Zhang CY, Liang HW, Chen X, Ba Y. 2017. MiR-193a-3p is an Important Tumour Suppressor in Lung Cancer and Directly Targets KRAS. *Cellular Physiology and Biochemistry*, 44 (4):1311-1324.
- Farah O, Nguyen C, Tekkotte C, Parast MM. 2020. Trophoblast lineage-specific differentiation and associated alterations in preeclampsia and fetal growth restriction. *Placenta*, 102:4-9.
- Farine T, Parsons M, Lye S, Shynlova O. 2018. Isolation of Primary Human Decidual Cells from the Fetal Membranes of Term Placentae. *J Vis Exp*, (134):e57443.
- Farquhar CM, Li Z, Lensen S, McLintock C, Pollock W, Peek MJ, Ellwood D, Knight M, Homer CS, Vaughan G, Wang A, Sullivan E. 2017. Incidence, risk factors and perinatal outcomes for placenta accreta in Australia and New Zealand: a case-control study. *BMJ Open*, 7 (10):e017713.
- Fasbender F, Watzl C. 2018. Impedance-based analysis of Natural Killer cell stimulation. *Sci Rep*, 8 (1):1-9.
- Favaro RR, Murrieta-Coxca JM, Gutierrez-Samudio RN, Morales-Prieto DM, Markert UR. 2021. Immunomodulatory properties of extracellular vesicles in the dialogue between placental and immune cells. *American Journal of Reproductive Immunology*, 85 (2):e13383.
- Feng HH, Li F, Tang P. 2021. Circ_0000745 regulates NOTCH1-mediated cell proliferation and apoptosis in pediatric T-cell acute lymphoblastic leukemia through adsorbing miR-193b-3p. *Hematology*, 26 (1):885-895.
- Fischer I, Redel S, Hofmann S, Kuhn C, Friese K, Walzel H, Jeschke U. 2010. Stimulation of syncytium formation in vitro in human trophoblast cells by galectin-1. *Placenta*, 31 (9):825-832.
- Fischer I, Weber M, Kuhn C, Fitzgerald JS, Schulze S, Friese K, Walzel H, Markert UR, Jeschke U. 2011. Is galectin-1 a trigger for trophoblast cell fusion?: the MAP-kinase pathway and syncytium formation in trophoblast tumour cells BeWo. *Mol Hum Reprod*, 17 (12):747-757.
- Fitzgerald JS, Poehlmann TG, Schleussner E, Markert UR. 2008. Trophoblast invasion: the role of intracellular cytokine signalling via signal transducer and activator of transcription 3 (STAT3). *Hum Reprod Update*, 14 (4):335-344.

- Fitzpatrick KE, Sellers S, Spark P, Kurinczuk JJ, Brocklehurst P, Knight M. 2012. Incidence and risk factors for placenta accreta/increta/percreta in the UK: a national case-control study. *PLoS One*, 7 (12):e52893.
- Floridon C, Nielsen O, Holund B, Sunde L, Westergaard JG, Thomsen SG, Teisner B. 2000. Localization of E-cadherin in villous, extravillous and vascular trophoblasts during intrauterine, ectopic and molar pregnancy. *Mol Hum Reprod*, 6 (10):943-950.
- Fong PY, Xue WC, Ngan HY, Chan KY, Khoo US, Tsao SW, Chiu PM, Man LS, Cheung AN. 2005. Mcl-1 expression in gestational trophoblastic disease correlates with clinical outcome: a differential expression study. *Cancer*, 103 (2):268-276.
- FOX H. 1972. PLACENTA ACCRETA, 1945–1969. *Obstetrical & Gynecological Survey*, 27 (7):475-490.
- Friedman RC, Farh KKH, Burge CB, Bartel DP. 2009. Most mammalian mRNAs are conserved targets of microRNAs. *Genome Research*, 19 (1):92-105.
- Fu G, Brkic J, Hayder H, Peng C. 2013. MicroRNAs in Human Placental Development and Pregnancy Complications. *Int J Mol Sci*, 14 (3):5519-5544.
- Fuhrmans M, Marelli G, Smirnova YG, Muller M. 2015. Mechanics of membrane fusion/pore formation. *Chem Phys Lipids*, 185:109-128.
- Fus-Kujawa A, Prus P, Bajdak-Rusinek K, Teper P, Gawron K, Kowalczyk A, Sieron AL. 2021. An Overview of Methods and Tools for Transfection of Eukaryotic Cells in vitro. *Front Bioeng Biotechnol*, 9:701031.
- Gadea G, Blangy A. 2014. Dock-family exchange factors in cell migration and disease. *Eur J Cell Biol*, 93 (10-12):466-477.
- Gao XN, Lin J, Gao L, Li YH, Wang LL, Yu L. 2011. MicroRNA-193b regulates c-Kit proto-oncogene and represses cell proliferation in acute myeloid leukemia. *Leuk Res*, 35 (9):1226-1232.
- Gardiner C, Ferreira YJ, Dragovic RA, Redman CW, Sargent IL. 2013. Extracellular vesicle sizing and enumeration by nanoparticle tracking analysis. *J Extracell Vesicles*, 2(1):19671-19682.
- Garmi G, Salim R. 2012. Epidemiology, etiology, diagnosis, and management of placenta accreta. *Obstet Gynecol Int*, 2012:873929.
- Gastaldi C, Bertero T, Xu N, Bourget-Ponzio I, Lebrigand K, Fourre S, Popa A, Cardot-Leccia N, Meneguzzi G, Sonkoly E, Pivarsci A, Mari B, Barbry P, Ponzio G, Rezzonico R. 2014. miR-193b/365a cluster controls progression of epidermal squamous cell carcinoma. *Carcinogenesis*, 35 (5):1110-1120.
- Gauster M, Blaschitz A, Siwetz M, Huppertz B. 2013. Keratins in the human trophoblast. *Histol Histopathol*, 28 (7):817-825.
- Gauster M, Huppertz B. 2010. The paradox of caspase 8 in human villous trophoblast fusion. *Placenta*, 31 (2):82-88.
- Gauster M, Moser G, Wernitznig S, Kupper N, Huppertz B. 2022. Early human trophoblast development: from morphology to function. *Cell Mol Life Sci*, 79 (6):345.
- Gauster M, Siwetz M, Orendi K, Moser G, Desoye G, Huppertz B. 2010. Caspases rather than calpains mediate remodelling of the fodrin skeleton during human placental trophoblast fusion. *Cell Death Differ*, 17 (2):336-345.
- Geffen KT, Gal H, Vainer I, Markovitch O, Amiel A, Krizhanovsky V, Biron-Shental T. 2018. Senescence and Telomere Homeostasis Might Be Involved in Placenta Percreta-Preliminary Investigation. *Reproductive Sciences*, 25 (8):1254-1260.
- Gielchinsky Y, Rojansky N, Fasouliotis SJ, Ezra Y. 2002. Placenta accreta--summary of 10 years: a survey of 310 cases. *Placenta*, 23 (2-3):210-214.
- Gioia L, Siddique A, Head SR, Salomon DR, Su AI. 2018. A genome-wide survey of mutations in the Jurkat cell line. *BMC Genomics*, 19 (1):334.

- Goh W, Yamamoto SY, Thompson KS, Bryant-Greenwood GD. 2013. Relaxin, Its Receptor (RXFP1), and Insulin-Like Peptide 4 Expression Through Gestation and in Placenta Accreta. *Reproductive Sciences*, 20 (8):968-980.
- Gottlieb A, Flor I, Nimzyk R, Burchardt L, Helmke B, Langenbuch M, Spiekermann M, Feidicker S, Bullerdiek J. 2021. The expression of miRNA encoded by C19MC and miR-371-3 strongly varies among individual placentas but does not differ between spontaneous and induced abortions. *Protoplasma*, 258 (1):209-218.
- Grobman WA, Gersnoviez R, Landon MB, Spong CY, Leveno KJ, Rouse DJ, Varner MW, Moawad AH, Caritis SN, Harper M, Wapner RJ, Sorokin Y, Miodovnik M, Carpenter M, O'Sullivan MJ, Sibai BM, Langer O, Thorp JM, Ramin SM, Mercer BM, National Institute of Child H, Human Development Maternal-Fetal Medicine Units N. 2007. Pregnancy outcomes for women with placenta previa in relation to the number of prior cesarean deliveries. *Obstet Gynecol*, 110 (6):1249-1255.
- Groger V, Cynis H. 2018. Human Endogenous Retroviruses and Their Putative Role in the Development of Autoimmune Disorders Such as Multiple Sclerosis. *Front Microbiol*, 9:265.
- Gu Y, Bian Y, Xu X, Wang X, Zuo C, Meng J, Li H, Zhao S, Ning Y, Cao Y, Huang T, Yan J, Chen ZJ. 2016. Downregulation of miR-29a/b/c in placenta accreta inhibits apoptosis of implantation site intermediate trophoblast cells by targeting MCL1. *Placenta*, 48:13-19.
- Gu Y, Meng J, Zuo C, Wang S, Li H, Zhao S, Huang T, Wang X, Yan J. 2019a. Downregulation of MicroRNA-125a in Placenta Accreta Spectrum Disorders Contributes Antiapoptosis of Implantation Site Intermediate Trophoblasts by Targeting MCL1. *Reprod Sci*, 26 (12):1582-1589.
- Gu Y, Sun JX, Groome LJ, Wang YP. 2013. Differential miRNA expression profiles between the first and third trimester human placentas. *American Journal of Physiology-Endocrinology and Metabolism*, 304 (8):E836-E843.
- Gu YZ, Meng JL, Zuo CT, Wang S, Li HY, Zhao SG, Huang T, Wang XT, Yan JH. 2019b. Downregulation of MicroRNA-125a in Placenta Accreta Spectrum Disorders Contributes Antiapoptosis of Implantation Site Intermediate Trophoblasts by Targeting MCL1. *Reproductive Sciences*, 26 (12):1582-1589.
- Guan N, Deng J, Li T, Xu X, Irelan JT, Wang MW. 2013. Label-free monitoring of T cell activation by the impedance-based xCELLigence system. *Mol Biosyst*, 9 (5):1035-1043.
- Guo L, Zhao Y, Zhang H, Yang S, Chen F. 2014. Integrated evolutionary analysis of human miRNA gene clusters and families implicates evolutionary relationships. *Gene*, 534 (1):24-32.
- Gurung S, Perocheau D, Touramanidou L, Baruteau J. 2021. The exosome journey: from biogenesis to uptake and intracellular signalling. *Cell Commun Signal*, 19 (1):47.
- Hall LS, Adams MJ, Arnau-Soler A, Clarke TK, Howard DM, Zeng Y, Davies G, Hagensars SP, Maria Fernandez-Pujals A, Gibson J, Wigmore EM, Boutin TS, Hayward C, Scotland G, Major Depressive Disorder Working Group of the Psychiatric Genomics C, Porteous DJ, Deary IJ, Thomson PA, Haley CS, McIntosh AM. 2018. Genome-wide meta-analyses of stratified depression in Generation Scotland and UK Biobank. *Transl Psychiatry*, 8 (1):9.
- Hannon T, Innes BA, Lash GE, Bulmer JN, Robson SC. 2012. Effects of local decidua on trophoblast invasion and spiral artery remodeling in focal placenta creta - an immunohistochemical study. *Placenta*, 33 (12):998-1004.
- Harer WB. 1956. Placenta accreta; report of eight cases. *Am J Obstet Gynecol*, 72 (6):1309-1314.

- Hasegawa K, Ikenoue S, Tanaka Y, Oishi M, Endo T, Sato Y, Ishii R, Kasuga Y, Ochiai D, Tanaka M. 2023. Ultrasonographic Prediction of Placental Invasion in Placenta Previa by Placenta Accreta Index. *J Clin Med*, 12(3):1090-1097.
- Hashemi ZS, Moghadam MF, Farokhimanesh S, Rajabibazl M, Sadroddiny E. 2018. Inhibition of breast cancer metastasis by co-transfection of miR-31/193b-mimics. *Iran J Basic Med Sci*, 21 (4):427-433.
- Haslinger P, Haider S, Sonderegger S, Otten JV, Pollheimer J, Whitley G, Knofler M. 2013. AKT isoforms 1 and 3 regulate basal and epidermal growth factor-stimulated SGHPL-5 trophoblast cell migration in humans. *Biol Reprod*, 88 (3):54.
- Hayder H, O'Brien J, Nadeem U, Peng C. 2018. MicroRNAs: crucial regulators of placental development. *Reproduction*, 155 (6):R259-R271.
- Heaton SJ, Eady JJ, Parker ML, Gotts KL, Dainty JR, Fairweather-Tait SJ, McArdle HJ, Srai KS, Elliott RM. 2008. The use of BeWo cells as an in vitro model for placental iron transport. *Am J Physiol Cell Physiol*, 295 (5):C1445-1453.
- Henkemeyer M, Rossi DJ, Holmyard DP, Puri MC, Mbamalu G, Harpal K, Shih TS, Jacks T, Pawson T. 1995. Vascular system defects and neuronal apoptosis in mice lacking ras GTPase-activating protein. *Nature*, 377 (6551):695-701.
- Hertig AT, Rock J, Adams EC. 1956. A description of 34 human ova within the first 17 days of development. *Am J Anat*, 98 (3):435-493.
- Hildebrand J, Rutze M, Walz N, Gallinat S, Wenck H, Deppert W, Grundhoff A, Knott A. 2011. A comprehensive analysis of microRNA expression during human keratinocyte differentiation in vitro and in vivo. *J Invest Dermatol*, 131 (1):20-29.
- Horgan R, Abuhamad A. 2022. Placenta Accreta Spectrum: Prenatal Diagnosis and Management. *Obstet Gynecol Clin North Am*, 49 (3):423-438.
- Hu H, Li S, Liu J, Ni B. 2012. MicroRNA-193b modulates proliferation, migration, and invasion of non-small cell lung cancer cells. *Acta Biochim Biophys Sin (Shanghai)*, 44 (5):424-430.
- Huang C, Zhong W, Ren X, Huang X, Li Z, Chen C, Jiang B, Chen Z, Jian X, Yang L, Liu X, Huang H, Shen C, Chen X, Dou X, Yu B. 2021. Correction: MiR-193b-3p-ERBB4 axis regulates psoriasis pathogenesis via modulating cellular proliferation and inflammatory-mediator production of keratinocytes. *Cell Death Dis*, 12 (11):1072.
- Huang J, Liu Y, Yang H, Xu Y, Lv W. 2022. The Effect of Serum beta-Human Chorionic Gonadotropin on Pregnancy Complications and Adverse Pregnancy Outcomes: A Systematic Review and Meta-Analysis. *Comput Math Methods Med*, 2022:8315519.
- Hung TH, Shau WY, Hsieh CC, Chiu TH, Hsu JJ, Hsieh TT. 1999. Risk factors for placenta accreta. *Obstet Gynecol*, 93 (4):545-550.
- Huppertz B. 2007. The feto-maternal interface: setting the stage for potential immune interactions. *Semin Immunopathol*, 29 (2):83-94.
- Huppertz B, Gauster M. 2011. Trophoblast Fusion. *Cell Fusion in Health and Disease: I: Cell Fusion in Health*, 713:81-95.
- Huppertz B, Weiss G, Moser G. 2014. Trophoblast invasion and oxygenation of the placenta: measurements versus presumptions. *J Reprod Immunol*, 101-102:74-79.
- Iacovelli A, Liberati M, Khalil A, Timor-Trisch I, Leombroni M, Buca D, Milani M, Flacco ME, Manzoli L, Fanfani F, Cali G, Familiari A, Scambia G, D'Antonio F. 2020. Risk factors for abnormally invasive placenta: a systematic review and meta-analysis. *J Matern Fetal Neonatal Med*, 33 (3):471-481.
- Ishibashi O, Ohkuchi A, Ali MM, Kurashina R, Luo SS, Ishikawa T, Takizawa T, Hirashima C, Takahashi K, Migita M, Ishikawa G, Yoneyama K, Asakura H, Izumi A, Matsubara S, Takeshita T, Takizawa T. 2012. Hydroxysteroid (17-beta) Dehydrogenase 1 Is Dysregulated by Mir-210 and Mir-518c That Are Aberrantly Expressed in Preeclamptic Placentas A Novel Marker for Predicting Preeclampsia. *Hypertension*, 59 (2):265-273.

- Jabrane-Ferrat N. 2019. Features of Human Decidual NK Cells in Healthy Pregnancy and During Viral Infection. *Front Immunol*, 10:1397.
- Jain V, Bos H, Bujold E. 2020. Guideline No. 402: Diagnosis and Management of Placenta Previa. *J Obstet Gynaecol Can*, 42 (7):906-917.
- James JL, Boss AL, Sun C, Allerkamp HH, Clark AR. 2022. From stem cells to spiral arteries: A journey through early placental development. *Placenta*, 125:68-77.
- Janaiah Kota RRC, Kathryn A. O'Donnell, Erik A. Wentzel, Chrystal L. Montgomery, Hun-Way Hwang, Tsung-Cheng Chang, Perumal Vivekanandan, Michael Torbenson, K. Reed Clark, Jerry R. Mendell, Joshua T. Mendell. 2009. Therapeutic delivery of miR-26a inhibits cancer cell proliferation and induces tumor-specific apoptosis. *Cell*, 137 (6):1005–1017.
- Jankovicova J, Secova P, Michalkova K, Antalikova J. 2020. Tetraspanins, More than Markers of Extracellular Vesicles in Reproduction. *Int J Mol Sci*, 21 (20):7568.
- Jauniaux E, Burton GJ. 2018. Pathophysiology of Placenta Accreta Spectrum Disorders: A Review of Current Findings. *Clin Obstet Gynecol*, 61 (4):743-754.
- Jauniaux E, Jurkovic D. 2012. Placenta accreta: pathogenesis of a 20th century iatrogenic uterine disease. *Placenta*, 33 (4):244-251.
- Ji L, Brkic J, Liu M, Fu G, Peng C, Wang YL. 2013. Placental trophoblast cell differentiation: physiological regulation and pathological relevance to preeclampsia. *Mol Aspects Med*, 34 (5):981-1023.
- Ji LJ, Tang YY, Pang XM, Zhang YC. 2019. Increased Expression of Serine Hydroxymethyltransferase 2 (SHMT2) is a Negative Prognostic Marker in Patients with Hepatocellular Carcinoma and is Associated with Proliferation of HepG2 Cells. *Medical Science Monitor*, 25:5823-5832.
- Jiang J, Gao H, Zhou W, Cai H, Liao L, Wang C. 2023. Circular RNA HIPK3 facilitates ferroptosis in gestational diabetes mellitus by regulating glutathione peroxidase 4 DNA methylation. *J Gene Med*:e3526.
- Jin G, Howe PH. 1999. Transforming growth factor beta regulates clusterin gene expression via modulation of transcription factor c-Fos. *Eur J Biochem*, 263 (2):534-542.
- Kabekkodu SP, Shukla V, Varghese VK, Adiga D, Vethil Jishnu P, Chakrabarty S, Satyamoorthy K. 2020. Cluster miRNAs and cancer: Diagnostic, prognostic and therapeutic opportunities. *Wiley Interdiscip Rev RNA*, 11 (2):e1563.
- Kabekkodu SP, Shukla V, Varghese VK, J DS, Chakrabarty S, Satyamoorthy K. 2018. Clustered miRNAs and their role in biological functions and diseases. *Biol Rev Camb Philos Soc*, 93 (4):1955-1986.
- Kaksonen M, Roux A. 2018. Mechanisms of clathrin-mediated endocytosis. *Nat Rev Mol Cell Biol*, 19 (5):313-326.
- Kamara M, Henderson JJ, Doherty DA, Dickinson JE, Pennell CE. 2013. The risk of placenta accreta following primary elective caesarean delivery: a case-control study. *BJOG*, 120 (7):879-886.
- Kariya Y, Oyama M, Kariya Y, Hashimoto Y. 2021. Phosphorylated Osteopontin Secreted from Cancer Cells Induces Cancer Cell Motility. *Biomolecules*, 11 (9):1323.
- Kaufmann P, Black S, Huppertz B. 2003. Endovascular trophoblast invasion: implications for the pathogenesis of intrauterine growth retardation and preeclampsia. *Biol Reprod*, 69 (1):1-7.
- Ke Y, Lu JH, Yang BL, Guo HQ, Ma QY, Zhu H, Shu HM, Li DJ. 2006. [Involvement of matrix metalloproteinase-2, -9, and tissue inhibitors of metalloproteinase-1, 2 in occurrence of the accrete placenta]. *Zhonghua Fu Chan Ke Za Zhi*, 41 (5):311-314.
- Kemp B, Kertschanska S, Kadyrov M, Rath W, Kaufmann P, Huppertz B. 2002. Invasive depth of extravillous trophoblast correlates with cellular phenotype: a comparison of intra- and extrauterine implantation sites. *Histochem Cell Biol*, 117 (5):401-414.

- Kennare R, Tucker G, Heard A, Chan A. 2007. Risks of adverse outcomes in the next birth after a first cesarean delivery. *Obstet Gynecol*, 109 (2 Pt 1):270-276.
- Khankin EV, Royle C, Karumanchi SA. 2010. Placental vasculature in health and disease. *Semin Thromb Hemost*, 36 (3):309-320.
- Khashoggi TY. 2003. Higher order multiple repeat cesarean sections: maternal and fetal outcome. *Ann Saudi Med*, 23 (5):278-282.
- Khordadmehr M, Shahbazi R, Sadreddini S, Baradaran B. 2019. miR-193: A new weapon against cancer. *Journal of Cellular Physiology*, 234 (10):16861-16872.
- Kidron D, Vainer I, Fisher Y, Sharony R. 2017. Automated image analysis of placental villi and syncytial knots in histological sections. *Placenta*, 53:113-118.
- Kim VN. 2005. MicroRNA biogenesis: coordinated cropping and dicing. *Nat Rev Mol Cell Biol*, 6 (5):376-385.
- Kim VN, Nam JW. 2006. Genomics of microRNA. *Trends Genet*, 22 (3):165-173.
- Kinoshita T, Nohata N, Watanabe-Takano H, Yoshino H, Hidaka H, Fujimura L, Fuse M, Yamasaki T, Enokida H, Nakagawa M, Hanazawa T, Okamoto Y, Seki N. 2012. Actin-related protein 2/3 complex subunit 5 (ARPC5) contributes to cell migration and invasion and is directly regulated by tumor-suppressive microRNA-133a in head and neck squamous cell carcinoma. *Int J Oncol*, 40 (6):1770-1778.
- Knight SW, Bass BL. 2001. A role for the RNase III enzyme DCR-1 in RNA interference and germ line development in *Caenorhabditis elegans*. *Science*, 293 (5538):2269-2271.
- Knofler M, Haider S, Saleh L, Pollheimer J, Gamage T, James J. 2019. Human placenta and trophoblast development: key molecular mechanisms and model systems. *Cell Mol Life Sci*, 76 (18):3479-3496.
- Kocherova I, Bryja A, Mozdziak P, Angelova Volponi A, Dyszkiewicz-Konwinska M, Piotrowska-Kempisty H, Antosik P, Bukowska D, Bruska M, Izycki D, Zabel M, Nowicki M, Kempisty B. 2019. Human Umbilical Vein Endothelial Cells (HUVECs) Co-Culture with Osteogenic Cells: From Molecular Communication to Engineering Prevascularised Bone Grafts. *J Clin Med*, 8 (10):1602.
- Kudo Y, Boyd CAR. 2002. Changes in expression and function of syncytin and its receptor, amino acid transport system B-o (ASCT2), in human placental choriocarcinoma BeWo cells during syncytialization. *Placenta*, 23 (7):536-541.
- Kwee A, Bots ML, Visser GH, Bruinse HW. 2006. Emergency peripartum hysterectomy: A prospective study in The Netherlands. *Eur J Obstet Gynecol Reprod Biol*, 124 (2):187-192.
- Laban M, Ibrahim EAS, Elsafty MSE, Hassanin AS. 2014. Placenta accreta is associated with decreased decidual natural killer (dNK) cells population: a comparative pilot study. *European Journal of Obstetrics & Gynecology and Reproductive Biology*, 181:284-288.
- Larios J, Mercier V, Roux A, Gruenberg J. 2020. ALIX- and ESCRT-III-dependent sorting of tetraspanins to exosomes. *Journal of Cell Biology*, 219 (3).
- Lau WC, Fung HY, Rogers MS. 1997. Ten years experience of caesarean and postpartum hysterectomy in a teaching hospital in Hong Kong. *Eur J Obstet Gynecol Reprod Biol*, 74 (2):133-137.
- Lee CQ, Gardner L, Turco M, Zhao N, Murray MJ, Coleman N, Rossant J, Hemberger M, Moffett A. 2016. What Is Trophoblast? A Combination of Criteria Define Human First-Trimester Trophoblast. *Stem Cell Reports*, 6 (2):257-272.
- Lee Y, Jeon K, Lee JT, Kim S, Kim VN. 2002. MicroRNA maturation: stepwise processing and subcellular localization. *EMBO J*, 21 (17):4663-4670.
- Lenarduzzi M, Hui AB, Alajez NM, Shi W, Williams J, Yue S, O'Sullivan B, Liu FF. 2013. MicroRNA-193b enhances tumor progression via down regulation of neurofibromin 1. *PLoS One*, 8 (1):e53765.

- Lewis BP, Burge CB, Bartel DP. 2005. Conserved seed pairing, often flanked by adenosines, indicates that thousands of human genes are microRNA targets. *Cell*, 120 (1):15-20.
- Li J, Gao X, Zhang Z, Lai Y, Lin X, Lin B, Ma M, Liang X, Li X, Lv W, Lin Y, Zhang N. 2021a. CircCD44 plays oncogenic roles in triple-negative breast cancer by modulating the miR-502-5p/KRAS and IGF2BP2/Myc axes. *Mol Cancer*, 20 (1):138.
- Li N, Hou R, Liu CX, Yang T, Qiao C, Wei J. 2021b. Integration of transcriptome and proteome profiles in placenta accreta reveals trophoblast over-migration as the underlying pathogenesis. *Clinical Proteomics*, 18 (1):1-12.
- Li N, Hou R, Yang T, Liu C, Wei J. 2020. miR-193a-3p Mediates Placenta Accreta Spectrum Development by Targeting EFNB2 via Epithelial-Mesenchymal Transition Pathway Under Decidua Defect Conditions. *Front Mol Biosci*, 7:613802.
- Li S, Winuthayanon W. 2017. Oviduct: roles in fertilization and early embryo development. *J Endocrinol*, 232 (1):R1-R26.
- Lima JF, Cerqueira L, Figueiredo C, Oliveira C, Azevedo NF. 2018. Anti-miRNA oligonucleotides: A comprehensive guide for design. *RNA Biol*, 15 (3):338-352.
- Lin L, Xu B, Rote NS. 1999. Expression of endogenous retrovirus ERV-3 induces differentiation in BeWo, a choriocarcinoma model of human placental trophoblast. *Placenta*, 20 (1):109-118.
- Liong S, Barker G, Lappas M. 2018. Placental Ras Regulates Inflammation Associated with Maternal Obesity. *Mediators Inflamm*, 2018:3645386.
- Liu C, Wang L, Liu X, Tan Y, Tao L, Xiao Y, Deng P, Wang H, Deng Q, Lin Y, Jie H, Zhang H, Zhang J, Peng Y, Zhang H, Zhou Z, Sun Q, Cen X, Zhao Y. 2021. Cytoplasmic SHMT2 drives the progression and metastasis of colorectal cancer by inhibiting beta-catenin degradation. *Theranostics*, 11 (6):2966-2986.
- Liu M, Su C, Zhu L, Dong F, Shu H, Zhang H, Wang M, Wang F, Man D. 2023. Highly expressed FYN promotes the progression of placenta accreta by activating STAT3, p38, and JNK signaling pathways. *Acta Histochem*, 125 (1):151991.
- Long Y, Chen Y, Fu XQ, Yang F, Chen ZW, Mo GL, Lao DY, Li MJ. 2019. Research on the expression of MRNA-518b in the pathogenesis of placenta accreta. *Eur Rev Med Pharmacol Sci*, 23 (1):23-28.
- Lu H, Liu P, Pang Q. 2021. MiR-27a-3p/miR-27b-3p Promotes Neurofibromatosis Type 1 via Targeting of NF1. *J Mol Neurosci*, 71 (11):2353-2363.
- Lu TX, Rothenberg ME. 2018. MicroRNA. *J Allergy Clin Immunol*, 141 (4):1202-1207.
- Lunghi L, Ferretti ME, Medici S, Biondi C, Vesce F. 2007. Control of human trophoblast function. *Reprod Biol Endocrinol*, 5 (6):1-14.
- Luu-The V, Labrie C, Simard J, Lachance Y, Zhao HF, Couet J, Leblanc G, Labrie F. 1990. Structure of two in tandem human 17 beta-hydroxysteroid dehydrogenase genes. *Mol Endocrinol*, 4 (2):268-275.
- MacPhee DJ, Mostachfi H, Han R, Lye SJ, Post M, Caniggia I. 2001. Focal adhesion kinase is a key mediator of human trophoblast development. *Lab Invest*, 81 (11):1469-1483.
- Makhseed M, Moussa MA. 1999. Placenta accreta in Kuwait: does a discrepancy exist between fundal and praevia accreta? *Eur J Obstet Gynecol Reprod Biol*, 86 (2):159-163.
- Makoha FW, Felimban HM, Fathuddien MA, Roomi F, Ghabra T. 2004. Multiple cesarean section morbidity. *Int J Gynaecol Obstet*, 87 (3):227-232.
- Malassine A, Frendo JL, Blaise S, Handschuh K, Gerbaud P, Tsatsaris V, Heidmann T, Evain-Brion D. 2008. Human endogenous retrovirus-FRD envelope protein (syncytin 2) expression in normal and trisomy 21-affected placenta. *Retrovirology*, 5 (6):1-10.
- Maldonado-Estrada J, Menu E, Roques P, Barre-Sinoussi F, Chaouat G. 2004. Evaluation of Cytokeratin 7 as an accurate intracellular marker with which to assess the purity of human placental villous trophoblast cells by flow cytometry. *J Immunol Methods*, 286 (1-2):21-34.

- Maqueo-Topete M, Chavez-Azuela J, Valenzuela-Lopez S, Espinosa-Hernandez J. 1968. Placenta accreta and circumvallate (extrachorialis). *Obstet Gynecol*, 32 (3):397-401.
- Martinez-Serra J, Gutierrez A, Munoz-Capo S, Navarro-Palou M, Ros T, Amat JC, Lopez B, Marcus TF, Fueyo L, Suquia AG, Gines J, Rubio F, Ramos R, Besalduch J. 2014. xCELLigence system for real-time label-free monitoring of growth and viability of cell lines from hematological malignancies. *Onco Targets Ther*, 7:985-994.
- Martinez J, Patkaniowska A, Urlaub H, Luhrmann R, Tuschl T. 2002. Single-stranded antisense siRNAs guide target RNA cleavage in RNAi. *Cell*, 110 (5):563-574.
- Matsuyama H, Suzuki HI. 2019. Systems and Synthetic microRNA Biology: From Biogenesis to Disease Pathogenesis. *Int J Mol Sci*, 21 (1):132.
- Matsuzaki S, Mandelbaum RS, Sangara RN, McCarthy LE, Vestal NL, Klar M, Matsushima K, Amaya R, Ouzounian JG, Matsuo K. 2021. Trends, characteristics, and outcomes of placenta accreta spectrum: a national study in the United States. *Am J Obstet Gynecol*, 225 (5):534 e531-534 e538.
- Matthews KC, Quinn AS, Chasen ST. 2022. Potentially Preventable Primary Cesarean Sections in Future Placenta Accreta Spectrum. *Am J Perinatol*, 39 (2):120-124.
- Mayhew TM, Ohadike C, Baker PN, Crocker IP, Mitchell C, Ong SS. 2003. Stereological investigation of placental morphology in pregnancies complicated by pre-eclampsia with and without intrauterine growth restriction. *Placenta*, 24 (2-3):219-226.
- McGee EA, Hsueh AJ. 2000. Initial and cyclic recruitment of ovarian follicles. *Endocr Rev*, 21 (2):200-214.
- Meakin C, Barrett ES, Aleksunes LM. 2022. Extravillous trophoblast migration and invasion: Impact of environmental chemicals and pharmaceuticals. *Reprod Toxicol*, 107:60-68.
- Mets E, Van der Meulen J, Van Peer G, Boice M, Mestdagh P, Van de Walle I, Lammens T, Goossens S, De Moerloose B, Benoit Y, Van Roy N, Clappier E, Poppe B, Vandesompele J, Wendel HG, Taghon T, Rondou P, Soulier J, Van Vlierberghe P, Speleman F. 2015. MicroRNA-193b-3p acts as a tumor suppressor by targeting the MYB oncogene in T-cell acute lymphoblastic leukemia. *Leukemia*, 29 (4):798-806.
- Mi S, Lee X, Li X, Veldman GM, Finnerty H, Racie L, LaVallie E, Tang XY, Edouard P, Howes S, Keith JC, Jr., McCoy JM. 2000. Syncytin is a captive retroviral envelope protein involved in human placental morphogenesis. *Nature*, 403 (6771):785-789.
- Michels J, Johnson PW, Packham G. 2005. Mcl-1. *Int J Biochem Cell Biol*, 37 (2):267-271.
- Millar L, Streiner N, Webster L, Yamamoto S, Okabe R, Kawamata T, Shimoda J, Bullesbach E, Schwabe C, Bryant-Greenwood G. 2005. Early placental insulin-like protein (INSL4 or EPIL) in placental and fetal membrane growth. *Biol Reprod*, 73 (4):695-702.
- Millar WG. 1959. A clinical and pathological study of placenta accreta. *J Obstet Gynaecol Br Emp*, 66:353-364.
- Miller DA, Chollet JA, Goodwin TM. 1997. Clinical risk factors for placenta previa-placenta accreta. *Am J Obstet Gynecol*, 177 (1):210-214.
- miRBase. 2022. Stem-loop sequence hsa-mir-193b. Retrieved from https://www.mirbase.org/cgi-bin/mirna_entry.pl?acc=MI0003137.
- Morales-Prieto DM, Favaro RR, Markert UR. 2020. Placental miRNAs in fetomaternal communication mediated by extracellular vesicles. *Placenta*, 102:27-33.
- Morales-Prieto DM, Ospina-Prieto S, Chaiwangyen W, Schoenleben M, Markert UR. 2013. Pregnancy-associated miRNA-clusters. *J Reprod Immunol*, 97 (1):51-61.
- Mori M, Bogdan A, Balassa T, Csabai T, Szekeres-Bartho J. 2016. The decidua-the maternal bed embracing the embryo-maintains the pregnancy. *Semin Immunopathol*, 38 (6):635-649.
- Morlando M, Sarno L, Napolitano R, Capone A, Tessitore G, Maruotti GM, Martinelli P. 2013. Placenta accreta: incidence and risk factors in an area with a particularly high rate of cesarean section. *Acta Obstet Gynecol Scand*, 92 (4):457-460.

- Moser G, Weiss G, Gauster M, Sundl M, Huppertz B. 2015. Evidence from the very beginning: endoglandular trophoblasts penetrate and replace uterine glands in situ and in vitro. *Hum Reprod*, 30 (12):2747-2757.
- Moutal A, Yang XF, Li WN, Gilbraith KB, Luo SZ, Cai S, Francois-Moutal L, Chew LA, Yeon SK, Bellampalli SS, Qu CLL, Xie JY, Ibrahim MM, Khanna M, Park KD, Porreca F, Khanna R. 2017. CRISPR/Cas9 editing of Nf1 gene identifies CRMP2 as a therapeutic target in neurofibromatosis type 1-related pain that is reversed by (S)-Lacosamide. *Pain*, 158 (12):2301-2319.
- Msheik H, Azar J, El Sabeh M, Abou-Kheir W, Daoud G. 2020. HTR-8/SVneo: A model for epithelial to mesenchymal transition in the human placenta. *Placenta*, 90:90-97.
- Mulcahy LA, Pink RC, Carter DR. 2014. Routes and mechanisms of extracellular vesicle uptake. *J Extracell Vesicles*, 3 (1):24641.
- Mullen C, Battarbee AN, Ernst LM, Peaceman AM. 2019. Occult Placenta Accreta: Risk Factors, Adverse Obstetrical Outcomes, and Recurrence in Subsequent Pregnancies. *Am J Perinatol*, 36 (5):472-475.
- Murata H, Tanaka S, Okada H. 2022. The Regulators of Human Endometrial Stromal Cell Decidualization. *Biomolecules*, 12 (9):1275.
- Murrieta-Coxca JM, Barth E, Fuentes-Zacarias P, Gutierrez-Samudio RN, Groten T, Gellhaus A, Koninger A, Marz M, Markert UR, Morales-Prieto DM. 2023. Identification of altered miRNAs and their targets in placenta accreta. *Front Endocrinol (Lausanne)*, 14:1021640.
- Murrieta-Coxca JM, Gutierrez-Samudio RN, El-Shorafa HM, Groten T, Rodriguez-Martinez S, Cancino-Diaz ME, Cancino-Diaz JC, Favaro RR, Markert UR, Morales-Prieto DM. 2020. Role of IL-36 Cytokines in the Regulation of Angiogenesis Potential of Trophoblast Cells. *Int J Mol Sci*, 22 (1):285.
- Nakamura O. 2009. Children's Immunology, what can we learn from animal studies (1): Decidual cells induce specific immune system of feto-maternal interface. *Journal of Toxicological Sciences*, 34:Sp331-Sp339.
- Nakashima A, Shima T, Aoki A, Kawaguchi M, Yasuda I, Tsuda S, Yoneda S, Yamaki-Ushijima A, Cheng SB, Sharma S, Saito S. 2021. Molecular and immunological developments in placentas. *Hum Immunol*, 82 (5):317-324.
- Nashif SK, Mahr RM, Jena S, Jo S, Nelson AB, Sadowski D, Crawford PA, Puchalska P, Alejandro EU, Gearhart MD, Wernimont SA. 2023. Metformin impairs trophoblast metabolism and differentiation in a dose-dependent manner. *Front Cell Dev Biol*, 11:1167097.
- Nicolet BP, Wolkers MC. 2022. The relationship of mRNA with protein expression in CD8+ T cells associates with gene class and gene characteristics. *PLoS One*, 17 (10):e0276294.
- Nisenblat V, Barak S, Griness OB, Degani S, Ohel G, Gonen R. 2006. Maternal complications associated with multiple cesarean deliveries. *Obstet Gynecol*, 108 (1):21-26.
- O'Brien J, Hayder H, Zayed Y, Peng C. 2018. Overview of MicroRNA Biogenesis, Mechanisms of Actions, and Circulation. *Front Endocrinol (Lausanne)*, 9:402.
- O'Brien K, Breyne K, Ughetto S, Laurent LC, Breakefield XO. 2020. RNA delivery by extracellular vesicles in mammalian cells and its applications. *Nat Rev Mol Cell Biol*, 21 (10):585-606.
- O'Rinn SE, Barrett JFR, Parsons JA, Kingdom JC, D'Souza R. 2023. Engaging pregnant individuals and healthcare professionals in an international mixed methods study to develop a core outcome set for studies on placenta accreta spectrum disorder (COPAS): a study protocol. *BMJ Open*, 13 (4):e060699.

- Obr A, Roselova P, Grebenova D, Kuzelova K. 2013. Real-time monitoring of hematopoietic cell interaction with fibronectin fragment: the effect of histone deacetylase inhibitors. *Cell Adh Migr*, 7 (3):275-282.
- Okahara G, Matsubara S, Oda T, Sugimoto J, Jinno Y, Kanaya F. 2004. Expression analyses of human endogenous retroviruses (HERVs): tissue-specific and developmental stage-dependent expression of HERVs. *Genomics*, 84 (6):982-990.
- Olivier E, Wakx A, Fouyet S, Dutot M, Rat P. 2021. JEG-3 placental cells in toxicology studies: a promising tool to reveal pregnancy disorders. *Anat Cell Biol*, 54 (1):83-92.
- Ospina-Prieto S, Chaiwangyen W, Herrmann J, Groten T, Schleussner E, Markert UR, Morales-Prieto DM. 2016. MicroRNA-141 is upregulated in preeclamptic placentae and regulates trophoblast invasion and intercellular communication. *Translational Research*, 172:61-72.
- Ostling H, Kruse R, Helenius G, Lodefalk M. 2019. Placental expression of microRNAs in infants born small for gestational age. *Placenta*, 81:46-53.
- Ota Y, Watanabe H, Fukasawa I, Tanaka S, Kawatsu T, Oishi A, Yasuda S, Inaba N. 1999. Placenta accreta/increta. Review of 10 cases and a case report. *Arch Gynecol Obstet*, 263 (1-2):69-72.
- Palova E, Redecha M, Malova A, Hammerova L, Kosibova Z. 2016. Placenta accreta as a cause of peripartum hysterectomy. *Bratisl Lek Listy*, 117 (4):212-216.
- Parra-Herran C, Djordjevic B. 2016. Histopathology of Placenta Creta: Chorionic Villi Intrusion into Myometrial Vascular Spaces and Extravillous Trophoblast Proliferation are Frequent and Specific Findings With Implications for Diagnosis and Pathogenesis. *Int J Gynecol Pathol*, 35 (6):497-508.
- Pastuschek J, Nonn O, Gutierrez-Samudio RN, Murrieta-Coxca JM, Muller J, Sanft J, Huppertz B, Markert UR, Groten T, Morales-Prieto DM. 2021. Molecular characteristics of established trophoblast-derived cell lines. *Placenta*, 108:122-133.
- Peltoketo H, Vihko P, Vihko R. 1999. Regulation of estrogen action: role of 17 beta-hydroxysteroid dehydrogenases. *Vitam Horm*, 55:353-398.
- Pereira RM, Mekary RA, da Cruz Rodrigues KC, Anaruma CP, Ropelle ER, da Silva ASR, Cintra DE, Pauli JR, de Moura LP. 2018. Protective molecular mechanisms of clusterin against apoptosis in cardiomyocytes. *Heart Fail Rev*, 23 (1):123-129.
- Peris M, Crompton K, Shepherd DA, Amor DJ. 2023. The association between hCG and adverse pregnancy outcomes: a systematic review and meta-analysis. *Am J Obstet Gynecol*.
- Philpott C, Tovell H, Frayling IM, Cooper DN, Upadhyaya M. 2017. The NF1 somatic mutational landscape in sporadic human cancers. *Human Genomics*, 11 (1):1-19.
- Pidikova P, Reis R, Herichova I. 2020. miRNA Clusters with Down-Regulated Expression in Human Colorectal Cancer and Their Regulation. *Int J Mol Sci*, 21 (13):4633.
- Pike LJ. 2003. Lipid rafts: bringing order to chaos. *J Lipid Res*, 44 (4):655-667.
- Pineles BL, Romero R, Montenegro D, Tarca AL, Han YM, Kim YM, Draghici S, Espinoza J, Kusanovic JP, Mittal P, Hassan SS, Kim CJ. 2007. Distinct subsets of microRNAs are expressed differentially in the human placentas of patients with preeclampsia. *Am J Obstet Gynecol*, 196 (3):261 e261-266.
- Pollheimer J, Knofler M. 2005. Signalling pathways regulating the invasive differentiation of human trophoblasts: a review. *Placenta*, 26 Suppl A:S21-30.
- Provansal M, Courbiere B, Agostini A, D'Ercole C, Boubli L, Bretelle F. 2010. Fertility and obstetric outcome after conservative management of placenta accreta. *Int J Gynaecol Obstet*, 109 (2):147-150.
- Qi C, Qin X, Zhou Z, Wang Y, Yang Q, Liao T. 2020. Circ_0072995 Promotes Cell Carcinogenesis via Up-Regulating miR-149-5p-Mediated SHMT2 in Breast Cancer. *Cancer Manag Res*, 12:11169-11181.

- Qiao Z, Li JF, Kou HW, Chen XR, Bao DM, Shang GW, Chen SF, Ji YH, Cheng T, Wang YS, Liu HJ. 2022. Hsa-miR-557 Inhibits Osteosarcoma Growth Through Targeting KRAS. *Frontiers in Genetics*, 12:789823.
- Rafi I, Chitty L. 2009. Cell-free fetal DNA and non-invasive prenatal diagnosis. *Br J Gen Pract*, 59 (562):e146-148.
- Rashid M, Rashid RS. 2004. Higher order repeat caesarean sections: how safe are five or more? *BJOG*, 111 (10):1090-1094.
- Read JA, Cotton DB, Miller FC. 1980. Placenta accreta: changing clinical aspects and outcome. *Obstet Gynecol*, 56 (1):31-34.
- Rekowska AK, Obuchowska K, Bartosik M, Kimber-Trojnar Z, Slodzinska M, Wierzchowska-Opoka M, Leszczynska-Gorzela B. 2023. Biomolecules Involved in Both Metastasis and Placenta Accreta Spectrum-Does the Common Pathophysiological Pathway Exist? *Cancers (Basel)*, 15 (9): 2618.
- Renaud SJ, Jeyarajah MJ. 2022. How trophoblasts fuse: an in-depth look into placental syncytiotrophoblast formation. *Cell Mol Life Sci*, 79 (8):433.
- Rezaei M, Mohammadpour-Gharehbagh A, Narooei-Nejad M, Teimoori B, Mokhtari M, Mehrabani M, Yaghmaei M, Najafi D, Salimi S. 2019. The effect of the placental DROSHA rs10719 and rs6877842 polymorphisms on PE susceptibility and mRNA expression. *J Hum Hypertens*, 33 (7):552-558.
- Richart R. 1961. Studies of placental morphogenesis. I. Radioautographic studies of human placenta utilizing tritiated thymidine. *Proc Soc Exp Biol Med*, 106:829-831.
- Rippe V, Dittberner L, Lorenz VN, Drieschner N, Nimzyk R, Sendt W, Junker K, Belge G, Bullerdiek J. 2010. The two stem cell microRNA gene clusters C19MC and miR-371-3 are activated by specific chromosomal rearrangements in a subgroup of thyroid adenomas. *PLoS One*, 5 (3):e9485.
- Ritchie W, Rasko JE, Flamant S. 2013. MicroRNA target prediction and validation. *Adv Exp Med Biol*, 774:39-53.
- Rodriguez-Rivera C, Garcia MM, Molina-Alvarez M, Gonzalez-Martin C, Goicoechea C. 2021. Clusterin: Always protecting. Synthesis, function and potential issues. *Biomedicine & Pharmacotherapy*, 134:111174-111183.
- Rolfo A, Garcia J, Todros T, Post M, Caniggia I. 2012. The double life of MULE in preeclamptic and IUGR placentae. *Cell Death Dis*, 3 (5):e305.
- Rosenberg T, Pariente G, Sergienko R, Wiznitzer A, Sheiner E. 2011. Critical analysis of risk factors and outcome of placenta previa. *Arch Gynecol Obstet*, 284 (1):47-51.
- Rudt S, Muller RH. 1993. In-Vitro Phagocytosis Assay of Nanoparticles and Microparticles by Chemiluminescence .3. Uptake of Differently Sized Surface-Modified Particles, and Its Correlation to Particle Properties and in-Vivo Distribution. *European Journal of Pharmaceutical Sciences*, 1 (1):31-39.
- Schulz J, Schilling E, Fabian C, Zenclussen AC, Stojanovska V, Claus C. 2023. Dissecting Rubella Placental Infection in an In Vitro Trophoblast Model. *Int J Mol Sci*, 24 (9): 7894.
- Schust DJ, Bonney EA, Sugimoto J, Ezashi T, Roberts RM, Choi S, Zhou J. 2021. The Immunology of Syncytialized Trophoblast. *Int J Mol Sci*, 22 (4):1767.
- Schweizer J, Bowden PE, Coulombe PA, Langbein L, Lane EB, Magin TM, Maltais L, Omary MB, Parry DA, Rogers MA, Wright MW. 2006. New consensus nomenclature for mammalian keratins. *J Cell Biol*, 174 (2):169-174.
- Shao X, Yu W, Yang Y, Wang F, Yu X, Wu H, Ma Y, Cao B, Wang YL. 2022. The mystery of the life tree: the placentas dagger. *Biol Reprod*, 107 (1):301-316.
- Shazly SA, Hortu I, Shih JC, Melekoglu R, Fan S, Ahmed FUA, Karaman E, Fatkullin I, Pinto PV, Irianti S, Tochie JN, Abdelbadie AS, Ergenoglu AM, Yenieli AO, Sagol S, Itil IM, Kang J, Huang KY, Yilmaz E, Liang Y, Aziz H, Akhter T, Ambreen A, Ates C,

- Karaman Y, Khasanov A, Larisa F, Akhmadeev N, Vatanina A, Machado AP, Montenegro N, Effendi JS, Suardi D, Pramatiarta AY, Aziz MA, Siddiq A, Ofakem I, Dohbit JS, Fahmy MS, Anan MA, and Middle East O, Gynecology Graduate Education foundation - Artificial intelligence u. 2022. Prediction of clinical outcomes in women with placenta accreta spectrum using machine learning models: an international multicenter study. *J Matern Fetal Neonatal Med*, 35 (25):6644-6653.
- Sheiner E, Shoham-Vardi I, Hallak M, Hershkowitz R, Katz M, Mazor M. 2001. Placenta previa: obstetric risk factors and pregnancy outcome. *J Matern Fetal Med*, 10 (6):414-419.
- Shiozaki A, Matsuda Y, Hayashi K, Satoh S, Saito S. 2011. Comparison of risk factors for major obstetric complications between Western countries and Japan: a case-cohort study. *The journal of obstetrics and gynaecology research*, 37 (10):1447-1454.
- Shirani F, Baghi M, Rostamian Delavar M, Shoaraye Nejati A, Eshaghiyan A, Nasr-Esfahani MH, Peymani M, Ghaedi K. 2020. Upregulation of miR-9 and miR-193b over human Th17 cell differentiation. *Mol Genet Genomic Med*, 8 (12):e1538.
- Silver RM, Landon MB, Rouse DJ, Leveno KJ, Spong CY, Thom EA, Moawad AH, Caritis SN, Harper M, Wapner RJ, Sorokin Y, Miodovnik M, Carpenter M, Peaceman AM, O'Sullivan MJ, Sibai B, Langer O, Thorp JM, Ramin SM, Mercer BM, National Institute of Child H, Human Development Maternal-Fetal Medicine Units N. 2006. Maternal morbidity associated with multiple repeat cesarean deliveries. *Obstet Gynecol*, 107 (6):1226-1232.
- Slaoui A, Talib S, Nah A, Moussaoui KE, Benzina I, Zeraiidi N, Baydada A, Kharbach A. 2019. Placenta accreta in the department of gynaecology and obstetrics in Rabat, Morocco: case series and review of the literature. *Pan Afr Med J*, 33:86.
- Smith SC, Baker PN, Symonds EM. 1997. Placental apoptosis in normal human pregnancy. *Am J Obstet Gynecol*, 177 (1):57-65.
- Sofiah S, Fung YC. 2009. Placenta accreta: clinical risk factors, accuracy of antenatal diagnosis and effect on pregnancy outcome. *Med J Malaysia*, 64 (4):298-302.
- Soleymanlou N, Jurisicova A, Wu Y, Chijiwa M, Ray JE, Detmar J, Todros T, Zamudio S, Post M, Caniggia I. 2007. Hypoxic switch in mitochondrial myeloid cell leukemia factor-1/Mtd apoptotic rheostat contributes to human trophoblast cell death in preeclampsia. *Am J Pathol*, 171 (2):496-506.
- Staun-Ram E, Goldman S, Gabarin D, Shalev E. 2004. Expression and importance of matrix metalloproteinase 2 and 9 (MMP-2 and -9) in human trophoblast invasion. *Reprod Biol Endocrinol*, 2 (1):1-13.
- Stenqvist AC, Nagaeva O, Baranov V, Mincheva-Nilsson L. 2013. Exosomes Secreted by Human Placenta Carry Functional Fas Ligand and TRAIL Molecules and Convey Apoptosis in Activated Immune Cells, Suggesting Exosome-Mediated Immune Privilege of the Fetus. *Journal of Immunology*, 191 (11):5515-5523.
- Stepien EL, Durak-Kozica M, Kaminska A, Targosz-Korecka M, Libera M, Tylko G, Opalinska A, Kapusta M, Solnica B, Georgescu A, Costa MC, Czyzewska-Buczynska A, Witkiewicz W, Malecki MT, Enguita FJ. 2018. Circulating ectosomes: Determination of angiogenic microRNAs in type 2 diabetes. *Theranostics*, 8 (14):3874-3890.
- Sturdee DW, Rushton DI. 1986. Caesarean and post-partum hysterectomy 1968-1983. *Br J Obstet Gynaecol*, 93 (3):270-274.
- Su J, Ruan S, Dai S, Mi J, Chen W, Jiang S. 2019. NF1 regulates apoptosis in ovarian cancer cells by targeting MCL1 via miR-142-5p. *Pharmacogenomics*, 20 (3):155-165.
- Sumawong V, Nondasuta A, Thanapath S, Budthimedhee V. 1966. Placenta accreta. A review of the literature and a summary of 10 cases. *Obstet Gynecol*, 27 (4):511-516.

- Sun C, Groom KM, Oyston C, Chamley LW, Clark AR, James JL. 2020. The placenta in fetal growth restriction: What is going wrong? *Placenta*, 96:10-18.
- Sun L, Xie HM, Mori MA, Alexander R, Yuan BB, Hattangadi SM, Liu QQ, Kahn CR, Lodish HF. 2011. Mir193b-365 is essential for brown fat differentiation. *Nature Cell Biology*, 13 (8):958-965.
- Szatanek R, Baj-Krzyworzeka M, Zimoch J, Lekka M, Siedlar M, Baran J. 2017. The Methods of Choice for Extracellular Vesicles (EVs) Characterization. *Int J Mol Sci*, 18 (6):1153.
- Tannetta D, Masliukaite I, Vatish M, Redman C, Sargent I. 2017. Update of syncytiotrophoblast derived extracellular vesicles in normal pregnancy and preeclampsia. *J Reprod Immunol*, 119:98-106.
- Tantbirojn P, Crum CP, Parast MM. 2008. Pathophysiology of placenta creta: the role of decidua and extravillous trophoblast. *Placenta*, 29 (7):639-645.
- Than NG, Romero R, Tarca AL, Kekesi KA, Xu Y, Xu Z, Juhasz K, Bhatti G, Leavitt RJ, Gelencser Z, Palhalmi J, Chung TH, Gyorffy BA, Orosz L, Demeter A, Szecsi A, Hunyadi-Gulyas E, Darula Z, Simor A, Eder K, Szabo S, Topping V, El-Azzamy H, LaJeunesse C, Balogh A, Szalai G, Land S, Torok O, Dong Z, Kovalszky I, Falus A, Meiri H, Draghici S, Hassan SS, Chaiworapongsa T, Krispin M, Knofler M, Erez O, Burton GJ, Kim CJ, Juhasz G, Papp Z. 2018. Integrated Systems Biology Approach Identifies Novel Maternal and Placental Pathways of Preeclampsia. *Front Immunol*, 9:1661.
- Thompson O, Otigbah C, Nnochiri A, Sumithran E, Spencer K. 2015. First trimester maternal serum biochemical markers of aneuploidy in pregnancies with abnormally invasive placentation. *BJOG*, 122 (10):1370-1376.
- Thomson DW, Dinger ME. 2016. Endogenous microRNA sponges: evidence and controversy. *Nat Rev Genet*, 17 (5):272-283.
- Thurn L, Lindqvist PG, Jakobsson M, Colmorn LB, Klungsoyr K, Bjarnadottir RI, Tapper AM, Bordahl PE, Gottvall K, Petersen KB, Krebs L, Gissler M, Langhoff-Roos J, Kallen K. 2016. Abnormally invasive placenta-prevalence, risk factors and antenatal suspicion: results from a large population-based pregnancy cohort study in the Nordic countries. *BJOG*, 123 (8):1348-1355.
- Timofeeva AV, Fedorov IS, Pirogova MM, Vasilchenko ON, Chagovets VV, Ezhova LS, Zabelina TM, Shmakov RG, Sukhikh GT. 2021. Clusterin and Its Potential Regulatory microRNAs as a Part of Secretome for the Diagnosis of Abnormally Invasive Placenta: Accreta, Increta, and Percreta Cases. *Life-Basel*, 11 (4):270.
- Tomasi TB, Jr. 1977. Structure and function of alpha-fetoprotein. *Annu Rev Med*, 28:453-465.
- Tong M, Kleffmann T, Pradhan S, Johansson CL, DeSousa J, Stone PR, James JL, Chen Q, Chamley LW. 2016. Proteomic characterization of macro-, micro- and nano-extracellular vesicles derived from the same first trimester placenta: relevance for fetomaternal communication. *Hum Reprod*, 31 (4):687-699.
- Tossetta G, Fantone S, Giannubilo SR, Ciavattini A, Senzacqua M, Frontini A, Marzioni D. 2023. HTRA1 in Placental Cell Models: A Possible Role in Preeclampsia. *Curr Issues Mol Biol*, 45 (5):3815-3828.
- Tsuda S, Nakashima A, Shima T, Saito S. 2019. New Paradigm in the Role of Regulatory T Cells During Pregnancy. *Front Immunol*, 10:573.
- Turco MY, Moffett A. 2019. Development of the human placenta. *Development*, 146 (22):dev163428.
- Tuzovic L. 2006. Complete versus incomplete placenta previa and obstetric outcome. *Int J Gynaecol Obstet*, 93 (2):110-117.
- Ukai T, Sato M, Akutsu H, Umezawa A, Mochida J. 2012. MicroRNA-199a-3p, microRNA-193b, and microRNA-320c are correlated to aging and regulate human cartilage metabolism. *J Orthop Res*, 30 (12):1915-1922.

- Umemura K, Ishioka S, Endo T, Ezaka Y, Takahashi M, Saito T. 2013. Roles of microRNA-34a in the pathogenesis of placenta accreta. *J Obstet Gynaecol Res*, 39 (1):67-74.
- Umezurike CC, Nkwocha G. 2007. Placenta accreta in Aba, south eastern, Nigeria. *Niger J Med*, 16 (3):219-222.
- UniPort. 2022. Hydrolase (KW-0378). Retrieved from <https://www.uniprot.org/keywords/KW-0378>.
- UniPort. 2022. O15511 · ARPC5_HUMAN Retrieved from <https://www.uniprot.org/uniprotkb/O15511/entry>.
- Usta IM, Hobeika EM, Musa AA, Gabriel GE, Nassar AH. 2005. Placenta previa-accreta: risk factors and complications. *Am J Obstet Gynecol*, 193 (3 Pt 2):1045-1049.
- van Beekhuizen HJ, Stefanovic V, Schwickert A, Henrich W, Fox KA, M MHG, Sentilhes L, Gronbeck L, Chantraine F, Morel O, Bertholdt C, Braun T, Rijken MJ, Duvekot JJ, International Society of Placenta Accreta Spectrum g. 2021. A multicenter observational survey of management strategies in 442 pregnancies with suspected placenta accreta spectrum. *Acta Obstet Gynecol Scand*, 100 (Suppl 1):12-20.
- Vargas A, Moreau J, Landry S, LeBellego F, Toufaily C, Rassart E, Lafond J, Barbeau B. 2009. Syncytin-2 plays an important role in the fusion of human trophoblast cells. *J Mol Biol*, 392 (2):301-318.
- Velicky P, Knofler M, Pollheimer J. 2016. Function and control of human invasive trophoblast subtypes: Intrinsic vs. maternal control. *Cell Adh Migr*, 10 (1-2):154-162.
- Verdera HC, Gitz-Francois JJ, Schiffelers RM, Vader P. 2017. Cellular uptake of extracellular vesicles is mediated by clathrin-independent endocytosis and macropinocytosis. *Journal of Controlled Release*, 266:100-108.
- Veziroglu EM, Mias GI. 2020. Characterizing Extracellular Vesicles and Their Diverse RNA Contents. *Frontiers in Genetics*, 11:700.
- Vicovac L, Jones CJ, Aplin JD. 1995. Trophoblast differentiation during formation of anchoring villi in a model of the early human placenta in vitro. *Placenta*, 16 (1):41-56.
- Wang R, Zhao J, Liu C, Li S, Liu W, Cao Q. 2023. Decreased AGGF1 facilitates the progression of placenta accreta spectrum via mediating the P53 signaling pathway under the regulation of miR-1296-5p. *Reprod Biol*, 23 (1):100735.
- Wang X, Li W, Chen Y, Zhou L. 2021. Long noncoding RNA SNHG14 affects the proliferation and apoptosis of childhood acute myeloid leukaemia cells by modulating the miR193b3p/MCL1 axis. *Mol Med Rep*, 23 (2):90.
- Wang Y, Luo J, Zhang H, Lu J. 2016. microRNAs in the Same Clusters Evolve to Coordinately Regulate Functionally Related Genes. *Mol Biol Evol*, 33 (9):2232-2247.
- Wang Z. 2011. The principles of MiRNA-masking antisense oligonucleotides technology. *Methods Mol Biol*, 676:43-49.
- Warshak CR, Ramos GA, Eskander R, Benirschke K, Saenz CC, Kelly TF, Moore TR, Resnik R. 2010. Effect of predelivery diagnosis in 99 consecutive cases of placenta accreta. *Obstet Gynecol*, 115 (1):65-69.
- Watari H. 1995. [Roles of ras genes on biological properties of human choriocarcinoma cells]. *Hokkaido Igaku Zasshi*, 70 (4):623-634.
- Wegler C, Olander M, Wisniewski JR, Lundquist P, Zettl K, Asberg A, Hjelmesaeth J, Andersson TB, Artursson P. 2020. Global variability analysis of mRNA and protein concentrations across and within human tissues. *NAR Genom Bioinform*, 2 (1):lqz010.
- Wegscheid ML, Anastasaki C, Hartigan KA, Cobb OM, Papke JB, Traber JN, Morris SM, Gutmann DH. 2021. Patient-derived iPSC-cerebral organoid modeling of the 17q11.2 microdeletion syndrome establishes CRLF3 as a critical regulator of neurogenesis. *Cell Rep*, 36 (1):109315.

- Wei X, She G, Wu T, Xue C, Cao Y. 2020. PEDV enters cells through clathrin-, caveolae-, and lipid raft-mediated endocytosis and traffics via the endo-/lysosome pathway. *Vet Res*, 51 (1):10.
- Weiniger CF, Kabiri D, Ginosar Y, Ezra Y, Shachar B, Lyell DJ. 2016. Suspected placenta accreta and cesarean hysterectomy: observational cohort utilizing an intraoperative decision strategy. *Eur J Obstet Gynecol Reprod Biol*, 198:56-61.
- Willms E, Cabanas C, Mager I, Wood MJA, Vader P. 2018. Extracellular Vesicle Heterogeneity: Subpopulations, Isolation Techniques, and Diverse Functions in Cancer Progression. *Front Immunol*, 9:738.
- Wu S, Kocherginsky M, Hibbard JU. 2005. Abnormal placentation: twenty-year analysis. *Am J Obstet Gynecol*, 192 (5):1458-1461.
- Xiao J, Yang B, Lin H, Lu Y, Luo X, Wang Z. 2007. Novel approaches for gene-specific interference via manipulating actions of microRNAs: examination on the pacemaker channel genes HCN2 and HCN4. *J Cell Physiol*, 212 (2):285-292.
- Xie J, Burt DR, Gao G. 2015. Adeno-associated virus-mediated microRNA delivery and therapeutics. *Semin Liver Dis*, 35 (1):81-88.
- Xiong T, Luo Z. 2018. The Expression of Actin-Related Protein 2/3 Complex Subunit 5 (ARPC5) Expression in Multiple Myeloma and its Prognostic Significance. *Med Sci Monit*, 24:6340-6348.
- Xu P, Ma Y, Wu H, Wang YL. 2021. Placenta-Derived MicroRNAs in the Pathophysiology of Human Pregnancy. *Front Cell Dev Biol*, 9:646326.
- Xu Z, Xiao SB, Xu P, Xie Q, Cao L, Wang D, Luo R, Zhong Y, Chen HC, Fang LR. 2011. miR-365, a Novel Negative Regulator of Interleukin-6 Gene Expression, Is Cooperatively Regulated by Sp1 and NF-kappa B. *Journal of Biological Chemistry*, 286 (24):21401-21412.
- Yanez-Mo M, Siljander PR, Andreu Z, Zavec AB, Borrás FE, Buzas EI, Buzas K, Casal E, Cappello F, Carvalho J, Colas E, Cordeiro-da Silva A, Fais S, Falcon-Perez JM, Ghobrial IM, Giebel B, Gimona M, Graner M, Gursel I, Gursel M, Heegaard NH, Hendrix A, Kierulf P, Kokubun K, Kosanovic M, Kralj-Iglic V, Kramer-Albers EM, Laitinen S, Lasser C, Lener T, Ligeti E, Line A, Lipps G, Llorente A, Lotvall J, Mancek-Keber M, Marcilla A, Mittelbrunn M, Nazarenko I, Nolte-'t Hoen EN, Nyman TA, O'Driscoll L, Oliván M, Oliveira C, Pallinger E, Del Portillo HA, Reventos J, Rigau M, Rohde E, Sammar M, Sanchez-Madrid F, Santarem N, Schallmoser K, Ostenfeld MS, Stoorvogel W, Stukelj R, Van der Grein SG, Vasconcelos MH, Wauben MH, De Wever O. 2015. Biological properties of extracellular vesicles and their physiological functions. *J Extracell Vesicles*, 4 (1):27066.
- Yang T, Li N, Hou R, Qiao C, Liu C. 2020. Development and validation of a four-microRNA signature for placenta accreta spectrum: an integrated competing endogenous RNA network analysis. *Ann Transl Med*, 8 (15):919.
- Yang X, Wang Z, Li X, Liu B, Liu M, Liu L, Chen S, Ren M, Wang Y, Yu M, Wang B, Zou J, Zhu WG, Yin Y, Gu W, Luo J. 2018. SHMT2 Desuccinylation by SIRT5 Drives Cancer Cell Proliferation. *Cancer Res*, 78 (2):372-386.
- Yang Z, Zhuang QL, Hu GF, Geng SK. 2019. MORC4 is a novel breast cancer oncogene regulated by miR-193b-3p. *Journal of Cellular Biochemistry*, 120 (3):4634-4643.
- Yao SM. 2016. MicroRNA biogenesis and their functions in regulating stem cell potency and differentiation. *Biological Procedures Online*, 18:8.
- Yi R, Qin Y, Macara IG, Cullen BR. 2003. Exportin-5 mediates the nuclear export of pre-microRNAs and short hairpin RNAs. *Genes Dev*, 17 (24):3011-3016.
- Yoo JY, Kim TH, Fazleabas AT, Palomino WA, Ahn SH, Tayade C, Schammel DP, Young SL, Jeong JW, Lessey BA. 2017. KRAS Activation and over-expression of

- SIRT1/BCL6 Contributes to the Pathogenesis of Endometriosis and Progesterone Resistance. *Sci Rep*, 7 (1):6765.
- Yu X, Wu HY, Yang Y, Wang FY, Wang YL, Shao X. 2022. Placental Development and Pregnancy-Associated Diseases. *Maternal-Fetal Medicine*, 4 (1):36-51.
- Zabel RR, Bar C, Ji J, Schultz R, Hammer M, Groten T, Schleussner E, Morales-Prieto DM, Markert UR, Favaro RR. 2021. Enrichment and characterization of extracellular vesicles from ex vivo one-sided human placenta perfusion. *Am J Reprod Immunol*, 86 (2):e13377.
- Zhang DD, Yang SQ, Hou YY, Su Y, Shi HF, Gu W. 2017a. Risk factors, outcome and management survey of placenta accreta in 153 cases: a five-year experience from a hospital of Shanghai, China. *International Journal of Clinical and Experimental Medicine*, 10 (8):12509-12516.
- Zhang H, Shykind B, Sun T. 2012. Approaches to manipulating microRNAs in neurogenesis. *Front Neurosci*, 6:196.
- Zhang J, Qin J, Su Y. 2017b. miR-193b-3p possesses anti-tumor activity in ovarian carcinoma cells by targeting p21-activated kinase 3. *Biomed Pharmacother*, 96:1275-1282.
- Zhang J, Ren R, Luo X, Fan P, Liu X, Liang S, Ma L, Yu P, Bai H. 2014. A small physiological electric field mediated responses of extravillous trophoblasts derived from HTR8/SVneo cells: involvement of activation of focal adhesion kinase signaling. *PLoS One*, 9 (3):e92252.
- Zhang J, Tao Y, Cai R, Wang Y. 2022. miR-196a-5p-Rich Extracellular Vesicles from Trophoblasts Induce M1 Polarization of Macrophages in Recurrent Miscarriage. *J Immunol Res*, 2022:6811632.
- Zhang P, Yang Q. 2021. Overexpression of SHMT2 Predicts a Poor Prognosis and Promotes Tumor Cell Growth in Bladder Cancer. *Front Genet*, 12:682856.
- Zhang SS, Kan XQ, Liu P, Yin LZ, Li QY, Xu HY. 2020. MiR-20b is implicated in preeclampsia progression via the regulation of myeloid cell leukemin-1. *Journal of Biological Regulators and Homeostatic Agents*, 34 (5):1709-1717.
- Zhang YY, Vik TA, Ryder JW, Srouf EF, Jacks T, Shannon K, Clapp DW. 1998. Nf1 regulates hematopoietic progenitor cell growth and ras signaling in response to multiple cytokines. *J Exp Med*, 187 (11):1893-1902.
- Zheng H, Shi M, Chi Z, Wang H, Wang H, Xu D. 2022. Dysregulated pseudogene BNIP3P1 inhibited cell proliferation and promoted cell apoptosis in preeclampsia by acting as a competing endogenous RNA for BNIP3. *Environ Toxicol*, 37 (5):971-982.
- Zhi D, Bai Y, Yang J, Cui S, Zhao Y, Chen H, Zhang S. 2018. A review on cationic lipids with different linkers for gene delivery. *Adv Colloid Interface Sci*, 253:117-140.
- Zhou X, Li Q, Xu J, Zhang X, Zhang H, Xiang Y, Fang C, Wang T, Xia S, Zhang Q, Xing Q, He L, Wang L, Xu M, Zhao X. 2016. The aberrantly expressed miR-193b-3p contributes to preeclampsia through regulating transforming growth factor-beta signaling. *Sci Rep*, 6:19910.
- Zhu DL, Yan HX, Yue JJ, Liu JF, Li ZB, Song JF. 2022. [Effect of inhibiting miR-204 expression on the learning and memory abilities of neonatal rats with intrauterine growth restriction and related mechanism]. *Zhongguo Dang Dai Er Ke Za Zhi*, 24 (12):1376-1383.
- Zhu JY, Pang ZJ, Yu YH. 2012. Regulation of trophoblast invasion: the role of matrix metalloproteinases. *Rev Obstet Gynecol*, 5 (3-4):e137-143.
- Zhu M, Zernicka-Goetz M. 2020. Principles of Self-Organization of the Mammalian Embryo. *Cell*, 183 (6):1467-1478.
- Zhu W, Chen X. 2023. miR-424-5p is downregulated in the placentas of patients with preeclampsia and affects trophoblast migration and invasion. *Exp Ther Med*, 25 (6):294.

Zou Z, He Z, Cai J, Huang L, Zhu H, Luo Y. 2019. Potential role of microRNA-424 in regulating ERRgamma to suppress trophoblast proliferation and invasion in fetal growth restriction. *Placenta*, 83:57-62.

APPENDIX

Table 19. Rates of placenta accreta spectrum (per 100,000 births)

Author, year of publication	Country (Period)	Population	Diagnoses	Rate per 100,000 births
(Dyer et al. 1954)	USA (1937 – 1953)	hosp	H	11,9
(Harer 1956)	USA (Not known)	hosp	C/H	9,2
(Millar 1959)	United Kingdom (1934 – 1953)	hosp	H	18,8
(Sumawong et al. 1966)	Thailand (Not known)	hosp	H	185,2
(Maqueo-Topete et al. 1968)	Mexico (1962 – 1967)	hosp	H	34,4
(Breen et al. 1977)	USA (Not known)	hosp	H	37,0
(Chew 1980)	Singapore (1971 – 1978)	hosp	H	7,2
(Read et al. 1980)	USA (1975 – 1979)	hosp	C/H	39,0
			H	24,8
(Miller et al. 1997)	USA (1985 – 1994)	hosp	H	39,8
(Makhseed and Moussa 1999)	Kuwait (1981 – 1993)	hosp	C or H, not known	9,9
(Ota et al. 1999)	Japan (1980 – 1997)	hosp	C/H	102,9
(Sheiner et al. 2001)	Israel (1990 – 1998)	hosp	C or H, not known	384,6
(Gielchinsky et al. 2002)	Israel (1990 – 2000)	hosp	C/H	899,9
(Armstrong et al. 2004)	Australia (1998 – 2002)	hosp	C/H	137,2
(Wu et al. 2005)	USA (1982 – 2002)	hosp	C/H	188,0
(Eller et al. 2009)	USA (1996 – 2008)	hosp	C/H	83,0
(Sofiah and Fung 2009)	Australia (1993 – 2005)	hosp	H	61,4
(Provansal et al. 2010)	France (1993 – 2007)	hosp	C/H	121,9
(Esh-Broder et al. 2011)	Israel (2004 – 2009)	hosp	H	166,7
(Shiozaki et al. 2011)	Japan (2001 – 2005)	pop	H	81,2
(Fitzpatrick et al. 2012)	United Kingdom (2010 – 2011)	pop	C/H	16,8
(Morlando et al. 2013)	Italy (1976 – 2008)	hosp	C/H	164,0
(Kamara et al. 2013)	Australia	hosp	C/H	106,5

	(1993 – 2008)			
(Bailit et al. 2015)	USA (2008 – 2011)	hosp	C	136.8
(Zhang et al. 2017a)	China (2004 – 2016)	hosp	C	33.5
(Mullen et al. 2019)	USA (2009 – 2014)	hosp	C/H	131.7
(Slaoui et al. 2019)	Morocco (2015 – 2016)	hosp	C/H	17.2
(Matsuzaki et al. 2021)	USA (2015 – 2017)	hosp	C or H, not known	294.4

hosp: data come from individual hospitals; pop: population-related data; C: Diagnosis was based on clinical criteria; H: Diagnosis was confirmed histologically. Updated from (Adamczyk 2017).

Table 20. Summary - Previous caesarean sections as a risk factor for placenta accrete spectrum.

Reference, Country	Population	PA – Cases (period)	Diagnosis	Previous CS as a risk factor for PAS
(FOX 1972) USA	hosp	622 (1945 – 1969)	H	✓
(Breen et al. 1977) USA	hosp	40 (Not Known)	H	✓
(Read et al. 1980) USA	hosp	22 (1975 – 1979)	C/H	✓
(Sturdee and Rushton 1986) United Kingdom	hosp	17 (1968 – 1986)	H	✓
(Makhseed and Moussa 1999) Kuwait	hosp	16 (1981 – 1993)	C/H	✓ significant correlation 2 versus 0 CS
(Miller et al. 1997) USA	hosp	62 (1985 – 1994)	H	✓ significant correlation
(Ota et al. 1999) Japan	hosp	10 (1980 – 1997)	C/H	✓
(Hung et al. 1999) Taiwan	hosp	28 (1994 – 1997)	C/H	Ø significant correlation
(Khashoggi 2003) Saudi Arabia	hosp	5 (1996 – 2000)	C or H, not known	Ø significant difference in 2 or 3 versus 4-8 CS for PA
(Wu et al. 2005) USA	hosp	111 (1982 – 2002)	C/H	significant OR ↑ for PA with 2+ CS
(Rashid and Rashid 2004) United Kingdom	hosp	5 (1994 – 2002)	H	Ø significant difference in 2 or 3 versus 4+ CS for PA

(Makoha et al. 2004) Saudi Arabia	hosp	29 (1997 – 2002)	C/H	significant OR ↑ for PA at 5 versus 3 CS and 6 versus 3 CS
(Armstrong et al. 2004) Australia	hosp	32 (1998 – 2002)	C/H	✓
(Silver et al. 2006) USA	hosp	143 (1999 – 2002)	C/H	↑ CS, ↑ relH for PA
(Daltveit et al. 2008) Norway	pop	7285 (1967 – 2003)	C or H, not known	✓ significant correlation 1st pregnancy CS and PA in 2nd pregnancy
(Kennare et al. 2007) Australia	pop	7 (1998 – 2003)	C or H, not known	✓ significant correlation 1st pregnancy CS and PA in 2nd pregnancy
(Bencaiova et al. 2007) Switzerland	hosp	31 (1999 – 2003)	C/H	∅ significant correlation
(Kwee et al. 2006) Netherlands	pop	24 (2002 – 2003)	H	↑ P for PA with 4+ CS
(Daskalakis et al. 2007) Greece	hosp	23 (1998 – 2004)	H	✓ significant correlation
(Sofiah and Fung 2009) Australia	hosp	40 (1993 – 2005)	H	✓
(Nisenblat et al. 2006) Israel	hosp	7 (2000 – 2005)	C or H, not known	significant relH ↑ for PA with 4+ CS vs. 2 CS
(Umezurike and Nkwocha 2007) Nigeria	hosp	10 (2002 – 2006)	C/H	✓
(Warshak et al. 2010) USA	hosp	99 (1990 – 2008)	H	✓
(Eshkoli et al. 2013) Israel	hosp	139 (1988 – 2011)	C	✓ significant correlation
(Fitzpatrick et al. 2012) United Kingdom	pop	134 (2010 – 2011)	C/H	significant OR ↑ for PA in 1 CS and 2+ CS
(Thurn et al. 2016) Nordic countries	hosp	205 (2009 – 2012)	C	✓ significant correlation
(Farquhar et al. 2017) Australia, New Zealand	hosp	295 (2010 – 2012)	C/H	significant OR for PA with 2+ CS
(Palova et al. 2016) Slovakia	hosp	8 (2008 – 2013)	H	✓

(Mullen et al. 2019) USA	hosp	100 (2009 – 2014)	H	✓ significant correlation
(Matsuzaki et al. 2021) USA	pop	8030 (2015 – 2017)	C	✓ significant correlation
(Iacovelli et al. 2020) Not specified	pop	Not mentioned (2018)	C or H, not known	significant OR for PA with 2 and 3 CS
(van Beekhuizen et al. 2021) International	pop	442 (2008 – 2019)	C	✓
(Matthews et al. 2022) USA	hosp	72 (2007 – 2019)	H	✓

hosp: data comes from individual hospitals; pop: population-related data; PA: Placenta accreta; C: Diagnosis was made on the basis of clinical criteria; H: Diagnosis was made histologically confirmed; CS: Caesarean section; relH: relative frequency; OR: odds ratio; P: probability; ✓: yes; Ø: no. Updated from (Adamczyk 2017).

Table 21. Summary - Placenta previa as a risk factor for placenta accreta spectrum.

Author, country	Population	PA-cases (period)	Diagnosis	PPr as a risk factor
(FOX 1972) USA	hosp	622 (1945 – 1969)	H	✓ significant correlation
(Sturdee and Rushton 1986) United Kingdom	hosp	17 (1968 – 1986)	H	✓ significant correlation
(Read et al. 1980) USA	hosp	22 (1975 – 1979)	H/C	✓ significant correlation
(Ota et al. 1999) Japan	hosp	10 (1980 – 1997)	C/H	✓ significant correlation
(Makhseed and Moussa 1999) Kuwait	hosp	16 (1981 – 1993)	C/H	✓ significant correlation
(Wu et al. 2005) USA	hosp	111 (1982 – 2002)	C/H	✓ significant correlation
(Usta et al. 2005) Lebanon	hosp	22 (1983 – 2003)	C/H	anterior or central position without significant influence.
(Lau et al. 1997) China	hosp	17 (1984 – 1994)	H	✓ significant correlation
(Miller et al. 1997) USA	hosp	62 (1985 – 1994)	H	✓ significant correlation
(Eshkoli et al. 2013) Israel	hosp	139 (1988 – 2011)	C	✓ significant correlation
(Rosenberg et al. 2011) Israel	pop	2424 (1988 – 2009)	Not known	✓ significant correlation

(Warshak et al. 2010) USA	hosp	99 (1990 – 2008)	H	✓ significant correlation
(Sheiner et al. 2001) Israel	hosp	302 (1990 – 1998)	Not known	✓ significant correlation
(Tuzovic 2006) Croatia	hosp	14 (1992 – 2001)	C/H	significant ↑ OR in PPr total than PPr partial/marginal; ∅ significant difference between the anterior and posterior position
(Sofiah and Fung 2009) Australia	hosp	40 (1993 – 2005)	H	✓ significant correlation
(Hung et al. 1999) Taiwan	hosp	28 (1994 – 1997)	C/H	✓ significant correlation
(Bahar et al. 2009) Saudi Arabia	hosp	306 PPrA (1996 – 2005)	C/H	significant ↑ OR in PPr complete/partial than PPr marginal
(Bencaiova et al. 2007) Switzerland	hosp	31 (1999 – 2003)	C/H	✓ significant correlation
(van Beekhuizen et al. 2021) IS-PAS	hosp	442 (2008 – 2019)	C	✓ significant correlation
(Weiniger et al. 2016) Israel	hosp	99 2002 – 2012	C/H	✓ significant correlation
(Fitzpatrick et al. 2012) United Kingdom	pop	134 (2010 – 2011)	C/H	✓ significant correlation
(Mullen et al. 2019) USA	hosp	100 (2009 – 2014)	C	✓ significant correlation
(Bassetty et al. 2021) India	hosp	21 (2013 – 2018)	C	✓ significant correlation
(Matsuzaki et al. 2021) USA	hosp	8030 (2015 – 2017)	C	✓ significant correlation
(El Gelany et al. 2019) Egypt	Hosp	102 (2017 – 2018)	C/H	✓ significant correlation

hosp: data come from individual hospitals; pop: population-related data; C: Diagnosis was based on clinical criteria; H: Diagnosis was confirmed histologically; PA: Placenta accreta; PPrA: Placenta previa accreta; PPr: Placenta previa; OR: Odds Ratio; ✓: yes; IS-PAS: International Society of Placenta Accreta Spectrum. Updated from (Adamczyk 2017).

List of figures

Figure 1. The early phases of human placental development.....	2
Figure 2. A human placental trophoblast cells differentiation.	6
Figure 3. The incidence of placenta accreta spectrum.....	9
Figure 4. miRNA biogenesis and modification of its activity by miRNA mimics and miRNA inhibitors oligonucleotides.....	13
Figure 5. Various types and biogenesis pathways of extracellular vesicles (EVs).	24
Figure 6. The pathways involved in extracellular vesicles (EVs) uptake by target cells.	25
Figure 7. Diagram depicting the enrichment of small extracellular vesicles (sEVs) and large extracellular vesicles (IEVs) by serial ultracentrifugation	46
Figure 8. miR-193b-3p expression and localization in the villous tree of human placentas.....	52
Figure 9. miR-193b-3p localization in the decidual layer human placenta.....	52
Figure 10. miR-193b-3p expression in cells.....	53
Figure 11. Forskolin treatment of BeWo cells induces syncytialization markers expression without altering miR-193b-3p expression.	54
Figure 12. Influence of miR-193b-3p on syncytialization markers in BeWo cells treated with forskolin for 48 h.....	55
Figure 13. Effects of miR-193b-3p on BeWo cells syncytialization.....	56
Figure 14. miR-193b-3p reduces JEG-3 cell migration	57
Figure 15. The influence of miR-193b-3p on JEG-3 cell proliferation and apoptosis	59
Figure 16. Characterization of JEG-3 EVs fractions.....	60
Figure 17. Uptake of JEG-3 EVs by Jurkat T cells.	63
Figure 18. The influence of miR-193b-3p enriched JEG-3 EVs on miR-193b-3p expression in Jurkat T cells.....	64
Figure 19. miR-193b-3p enriched JEG-3 EVs reduce Jurkat T cells proliferation	66
Figure 20. Graphical representation of quantitative proteomics data from JEG-3 cells transfected with or without miR-193b-3p-inhibitor.....	68
Figure 21. Validation of proteomics data for identification of potential miR-193b-3p targets.....	72
Figure 22. Potential targets of miR-193b-3p and their effects on cellular processes	90

List of tables

Table 1. Overview of keratins expressed in different trophoblast types	9
Table 2. Risk factors for PAS.....	10
Table 3. Summary of miRNAs dysregulated in PAS	19
Table 4. Studies involving miR-193b-3p	21
Table 5. List of equipment	28
Table 6. List of materials.....	29
Table 7. List of Chemicals	30
Table 8. List of kits.....	32
Table 9. List of buffers and solutions.....	33
Table 10. List of probes.....	33
Table 11. List of antibodies	33
Table 12. List of TaqMan™ miRNA Primers	34
Table 13. List of miRNA sequence	34
Table 14. List of TaqMan™ Gene expression assays.....	35
Table 15. List of medium and buffers used for cell culture	36
Table 16. List of cell lines	36
Table 17. List of software.....	37
Table 18. Significantly changed proteins in miR-193b-3p-inhibitor transfected JEG-3 cells in comparison to non-transfected cells	66
Table 19. Rates of placenta accreta spectrum (per 100,000 births).....	112
Table 20. Summary - Previous caesarean sections as a risk factor for placenta accrete spectrum.....	113
Table 21. Summary - Placenta previa as a risk factor for placenta accreta spectrum.	115

ACKNOWLEDGEMENT

First and foremost, all praises to almighty Allah, whose mercy and blessings enabled me to successfully complete my work. I would like to express my sincere gratitude to my advisor, Dr. Rodolfo Favaro, for his motivation, guidance, patience, and continuous support. I truly learned a great deal of knowledge during my discussions with him. His guidance has helped me throughout the entire duration of research. I would like to extend additional thanks to Prof. Udo Markert for his guidance and advice during my PhD time. I would also like to thank my second supervisor, Prof. Aria Baniahmed, for his support, prompt responses and assistance with any problem I encountered during my study.

I owe profound gratitude to the Deutscher Akademischer Austauschdienst (DAAD) for the financial support of my PhD study. My special thanks go to ST33 section of DAAD including Mr. Mostafa Fathy, Mrs. Claudia Garbers, and Mr. Philipp Effertz for their invaluable help and unwavering support throughout the challenging phases of my PhD.

I would like to further thank Dr. Andre Schmidt and Dr. Mario Müller for their assistance with the proteomics part of my study. Thank you for the knowledge, fruitful discussion and for joyful moments.

Many thanks to the following respected people who provided their specialized equipment to help me conduct some of my experiments: PD Dr. Martin Westerman and Mr. Frank Steiniger, Dr. Elisabeth Preussger, Dr. Daniela Pelzel, Prof. Dr Christian Huebner, and Dr. Federico Ribaldo. Additionally, I want to express my gratitude to all of my colleagues at the Placenta laboratory for the enjoyable times we shared.

I am highly obliged to Prof. Jutta Hübner, Dr. Gunda Huskobla, Dr. Hanna Kauhous, Prof Thorsten Heinzl, and Prof. Uwe Cantner for their generous assistance during my PhD. Special thanks in this regard to Dr. Hendrik Huthoff for his valuable advice, insightful discussions, and thesis corrections.

Last but not the least; I extend my heartfelt thanks to my beloved husband, parents, siblings, friends, and my kids (Sara and Mohammed) for their prayers, continuous encouragement, and never-ending support. The accomplishment of this work would not have been possible without all of them. Thank you!

Ehrenwörtliche Erklärung

Hiermit erkläre ich, dass mir die Promotionsordnung der Medizinischen Fakultät der Friedrich-Schiller-Universität bekannt ist,

ich die Dissertation selbst angefertigt habe und alle von mir benutzten Hilfsmittel, persönlichen Mitteilungen und Quellen in meiner Arbeit angegeben sind,

mich folgende Personen bei der Auswahl und Auswertung des Materials sowie bei der Herstellung des Manuskripts unterstützt haben: Prof. Dr. Udo Markert und Dr. Rodolfo Favaro

die Hilfe eines Promotionsberaters nicht in Anspruch genommen wurde und dass Dritte weder unmittelbar noch mittelbar geldwerte Leistungen von mir für Arbeiten erhalten haben, die im Zusammenhang mit dem Inhalt der vorgelegten Dissertation stehen,

dass ich die Dissertation noch nicht als Prüfungsarbeit für eine staatliche oder andere wissenschaftliche Prüfung eingereicht habe und

dass ich die gleiche, eine in wesentlichen Teilen ähnliche oder eine andere Abhandlung nicht bei einer anderen Hochschule als Dissertation eingereicht habe.

Jena, 17.07.2024

Heba M. A. Skaik (El-Shorafa)